Remote Sensing Series 72

Irene Garonna

Large-scale Dynamics of Land Surface Phenology and its Climatic Constraints

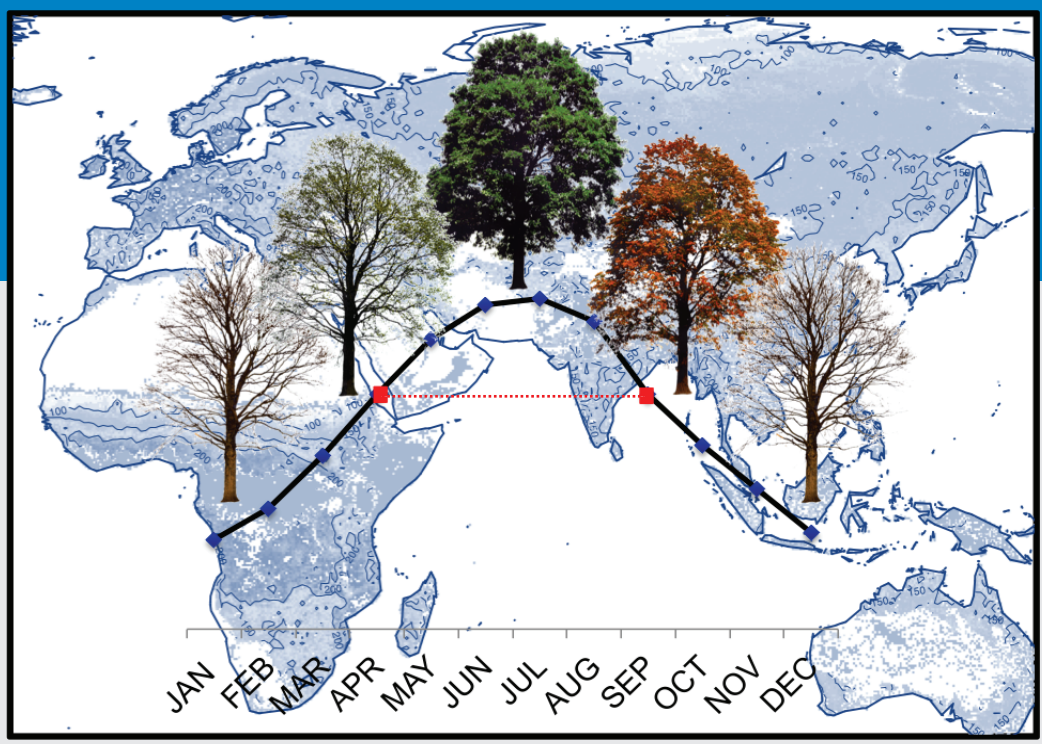

Remote Sensing Laboratories
Department of Geography
University of Zurich, 2016

Remote Sensing Series 72

Irene Garonna

Large-scale Dynamics of Land Surface Phenology and its Climatic Constraints

Remote Sensing Laboratories
Department of Geography
University of Zurich, 2016

Front page: image collage of two illustrations contained in the thesis. Background: global map of average growing season length (with modified colours). Foreground: illustration of sample NDVI annual profile and the derived growing season length.

Garonna, Irene

Large-scale dynamics of land surface phenology and its climatic constraints.

Remote Sensing Series, Vol. 72
Remote Sensing Laboratories, Department of Geography, University of Zurich
Switzerland, 2016

ISBN: 978-3-906894-01-0

This work was approved as a PhD thesis by the Faculty of Science of the University of Zurich in the fall semester 2016. Doctorate committee: Prof. Dr. Michael E. Schaepman (chair), Dr. Rogier de Jong (dissertation supervisor), Prof. Dr. Bernhard Schmid.

LARGE-SCALE DYNAMICS OF LAND SURFACE PHENOLOGY AND ITS CLIMATIC CONSTRAINTS

Dissertation
zur
Erlangung der naturwissenschaftlichen Doktorwürde
(Dr. sc. nat.)
vorgelegt der
Mathematisch-naturwissenschaftlichen Fakultät
der
Universität Zürich

von
Irene Garonna
aus
Italien

Promotionskomitee
Prof. Dr. Michael E. Schaepman (Vorsitz)
Prof. Dr. Bernhard Schmid
Dr. Rogier de Jong (Leitung der Dissertation)

Zürich, 2016

Abstract

Vegetation phenology – the timing of seasonal activity of plants – is a widely used indicator of global change. At the ecosystem level, phenology modulates atmosphere-biosphere exchanges of energy, carbon and water and is thus a central constituent of Terrestrial Biosphere Models (TBMs). Satellite Remote Sensing (RS) offers the ability to retrospectively derive information on Land Surface Phenology (LSP) from existing records of vegetation activity at a variety of scales.

This thesis presents a global assessment of large-scale trends in LSP for the last 3 decades and in combination with climatic constraints to plant growth. To achieve this, an algorithm was first developed to extract yearly estimates for Start-, End- and Length of the Growing Season (respectively SOS, EOS and GSL) from the longest record of vegetation activity currently available at global scale, from 1982 to 2012. This methodology was tested over Europe and then applied at global scale, resulting in a comprehensive assessment of LSP variability for the last 3 decades. This assessment builds on previous literature to quantify GSL trends for the past 30 years and to evaluate the relative contribution of SOS and EOS to overall GSL change. Throughout the thesis, two LSP derivation methods are compared and environmental stratifications are used to identify and interpret LSP changes. Then, this thesis examines the relative importance of three modelled climatic constraints to plant growth (photoperiod, evaporative demand and minimum temperature) on SOS and EOS over the same time period.

This thesis provides a consistent record of large-scale LSP estimates for 1982-2012, suitable for global studies. Results confirm a global average lengthening of the RS-derived growing season over 1982-2012, at an average rate of 0.22-0.34 days/year (depending on the metric chosen). Findings reveal a strong contribution of EOS change towards GSL trends and highlight the importance of studying leaf senescence processes, until recently overlooked by both field and LSP studies. Significant GSL trends were found over 13-19% of global land surfaces, with considerable variation both within and between environmental zones. Approximately 1/3 of areas with significant GSL trends were located within the boreal/alpine biome, which emerges as a key LSP change area and where climatic constraints appear to have eased over the same period.

This thesis identifies differences in the climatic constraints underlying phenology at SOS and EOS, that are often not represented in TBMs. Furthermore results demonstrate significant shifts in the relative importance of climatic constraints in the temperate and boreal biomes, ranging from 1 to 8% during the study period. A widespread decrease in the influence of minimum temperature at both SOS and EOS was found in both biomes, leading to spatially heterogeneous increases in the relative importance of moisture and photoperiod constraints. Findings reveal an increasing influence of the moisture constraint on LSP in most boreal and temperate environmental zones, with the strongest increases for EOS and over temperate zones.

This thesis discusses various implications of these findings for improving the representation of phenology in TBMs and, considering the strengths and weaknesses associated with this approach, and lays out number of research directions. These range from technical improvements to investigating the consequences of phenological shifts for global primary productivity and for species distributions at large scales.

In conclusion, by providing global phenological information since 1982, this thesis contributes to quantifying large-scale spatial variability in phenology in an original way and to advancing the characterization of its climatic constraints. Hence, this thesis stands in support of LSP as an invaluable complement to traditional phenological studies, in particular given the pressing issue of global change.

Zusammenfassung

Vegetationsphänologie, der Zeitpunkt der saisonalen Entwicklung von Pflanzen, ist ein häufig verwendeter Indikator weltweiter Veränderungen. Auf Ökosystemebene verändern phänologische Prozesse den Energie-, Kohlenstoff- und Wasseraustausch zwischen Atmosphäre und Biosphäre und sind entsprechend zentrale Bestandteile Terrestrischer Biosphärenmodelle (TBM). Satellitengestützte Fernerkundung (*Remote Sensing*, RS) ermöglicht es, mittels bestehender Aufnahmen der Vegetationsaktivität auf unterschiedlichen Skalen rückblickend Informationen zur Phänologie der Landoberfläche (*Land Surface Phenology*, LSP) zu erhalten.

Die vorliegende Arbeit behandelt die globale Analyse grossskaliger Trends der LSP über die letzten drei Jahrzehnte in Kombination mit den klimatischen Einschränkungen des Pfanzenwachstums. Im Rahmen der Analyse wurde ein Algorithmus entwickelt, um den Beginn, das Ende sowie die Dauer der Wachstumsperiode der Vegetation (*Start-*, *End-* und *Length of Growing Season*, *SOS*, *EOS* und *GSL*) zu bestimmen. Zurückgegriffen wurde dabei auf den längsten verfügbaren globalen Datensatz zur Vegetationsaktivität, von 1982 bis 2012. Diese Methode wurde zuerst für Europa getestet und dann weltweit angewendet, was eine umfassende Beschreibung der Variabilität der LSP in den letzten drei Jahrzehnte ermöglichte. Besagte Analyse baut auf vorangehender Literatur auf, um GSL-Trends über die letzten 30 Jahre zu quantifizieren und den relativen Anteil von SOS und EOS zur Variabilität der GSL zu bestimmen. Im weiteren Verlaufe dieser Arbeit wurden zwei LSP-Ableitungsmethoden verglichen; ferner wurde eine Gliederung nach Umweltbedingungen zur Identifikation und Interpretation von Änderungen der LSP verwendet. Abschliessend wurde die relative Bedeutung dreier modellierter klimatischer Einschränkungen des Pflanzenwachstums (Photoperiode, Sättigungsdampfdruckdefizit und Mindesttemperatur) auf SOS und EOS über den gleichen Zeitraum untersucht.

Als Produkt der vorliegenden Arbeit resultierte eine konsistente Datenreihe der grossskaligen LSP-Entwicklung für die Jahre 1982 bis 2012, welche für globale Studien geeignet ist. Resultate bestätigen im globalen Mittel eine Verlängerung der durch RS abgeleiteten Wachstumsperiode über den genannten Zeitraum, mit einer durchschnittlichen Rate von 0.22 bis 0.34 Tagen pro Jahr (je nach verwendeter

Methode). Da Veränderungen von EOS einen wichtigen Anteil an Trends der GSL haben, ist es besonders wichtig Blattalterungsprozesse zu untersuchen, was bis vor Kurzen nicht nur in Feldstudien sondern auch in Untersuchungen zur LSP vernachlässigt wurde. Signifikante GSL-Trends betrafen 13 bis 19% der globalen Landflächen, mit beträchtlicher Variabilität sowohl innerhalb als auch zwischen verschiedenen Biomen. Da ungefähr ein Drittel der Fläche mit signifikantem Trend im borealen/alpinen Biom auftrat, nimmt es eine Schlüsselrolle ein. In diesem Biom scheinen die klimatische Einschränkungen über den untersuchten Zeitraum abgenommen zu haben.

Weiterhin wurden verschiedene klimatische Einschränkungen der Phänologie während SOS und EOS untersucht, die in TBMs oft vernachlässigt werden. Die Ergebnisse zeigen signifikante Verschiebungen der relativen Bedeutung von klimatischen Einschränkungen in den gemässigten und borealen Biomen von 1 bis 8% in der untersuchten Zeitspanne. In beiden Biomen wurde ein weit verbreiteter Rückgang des Einflusses der Minimaltemperatur sowohl auf SOS als auch auf EOS festgestellt. Dadurch gewannen regional entweder die Feuchtigkeit oder die Länge der Photoperiode in diesen Biomen an Bedeutung. Die Ergebnisse deuten somit auf einen wachsenden Einfluss der Wasserverfügbarkeit auf LSP in den meisten borealen und gemässigten Zonen hin, mit dem stärksten Anstieg für EOS und in der gemässigten Klimazone.

In dieser Arbeit werden einige Folgen dieser Ergebnisse für die Einbindung der Phänologie in TBMs erläutert. Zusammen mit diesen Einflussmöglichkeiten werden die Stärken und Schwächen des verfolgten Ansatzes diskutiert und eine Reihe von zukünftigen Forschungsfeldern vorgeschlagen. Schlussendlich stellt diese Arbeit globale Phänologiedaten seit 1982 zur Verfügung und leistet einen besonderen Beitrag zur Quantifizierung der grossräumigen Variabilität der Phänologie. wurde auch die Charakterisierung der klimatischen Einschränkungen verbessert. Somit untermauert die vorliegende Arbeit die LSP als Komponente von unschätzbarem Wert zur Ergänzung von traditionellen phänologischen Studien, insbesondere im Hinblick auf den fortschreitenden globalen Wandel.

Table of contents

List of Abbreviations

ANOVA	Analysis of Variance
AVHRR	Advanced Very High Resolution Radiometer
CM	Cold & Mesic environmental zone
CV	Coefficient of Variation
DGVM	Dynamic Global Vegetation Model
DOY	Day of Year
ECMWF	European Centre for Medium-Range Weather Forecast
EnKF	Ensemble Kalman Filter
EOS	End Of Season
EVI	Enhanced Vegetation Index
fAPAR	fraction of Absorbed Photosynthetically Active Radiation
FET	Fit Error Tolerance
FFT	Fast Fourier Transform
FGCZ	Functional Genomics Center Zurich
FLAE	First-Last Author Emphasis
GEnS	Global Environmental Stratification
GEO-BON	Group on Earth Observation Biodiversity Observation Network
GIMMS	Global Inventory Monitoring and Modeling Systems
GOME	Global Ozone Monitoring Experiment
GPM	Global Phenological Monitoring
GPP	Gross Primary Productivity
GS	Growing Season
GSI	Growing Season Index
GSL	Growing Season Length
HANTS	Harmonic Analysis of NDVI Time Series
IGBP	International Geosphere Biosphere Programme
IIASA	International Institute for Applied Systems Analysis
IPCC	Intergovernmental Panel on Climate Change
IPG	International Phenological Gardens
LAI	Leaf Area Index
LANMAP	European Landscape Classification
LSP	Land Surface Phenology
MERIS	Medium Resolution Imaging Spectrometer
MI	Max-Increase method
MODIS	Moderate Resolution Imaging Spectroradiometer
MP	Midpoint-Pixel method
MVC	Maximum Value Compositing
NASA	National Aeronautics and Space Administration

NDVI	Normalized Difference Vegetation Index
NEP	Net Ecosystem Productivity
NH	Northern Hemisphere
NIR	Near InfraRed reflectance
NOAA	National Oceanic and Atmospheric Administration
NPP	Net Primary Productivity
PFT	Plant Functional Type
Photo	Photoperiod
RED	reflectance in the visible RED band
RQ	Research Question
RS	Remote Sensing
SH	Southern Hemisphere
SiF	Sun-induced Fluorescence
SOS	Start Of Season
SPOT	Satellite Pour l'Observation de la Terre
TAT	Throw-Away Threshold
TBM	Terrestrial Biosphere Model
TMin	Minimum Temperature
URPP-GCB	University Research Priority Programme Global Change and Biodiversity
VI	Vegetation Index
VPD	Vapour Pressure Deficit

Chapter

1

Introduction

1.1 Plant phenology: a science for global change

Plant phenology is the study of the timing of recurring events in the life cycle of plants and animals as influenced by the environment (Leith 1974). While most phenological studies in animals focus on timing of breeding or migration, plant phenology typically studies the timing of observable phases of plant life cycles – such as flowering, fruiting or leaf development, coloration and fall (Menzel 2006). The timing of seasonal development of plant leaves has vast implications across ecological scales, going from individual to community to ecosystem levels (Morisette *et al.* 2009; Forrest & Miller-Rushing 2010; Wilczek *et al.* 2010). The timing of life history events in relation to seasonal conditions is critical for the survival and reproductive success of any individual plant or population. At community level, phenological variation within and between species shapes competitive interactions and is therefore key for maintaining species co-existence (Cleland *et al.* 2007; Richardson *et al.* 2013). At ecosystem level, plant phenology also influences ecosystem functioning by altering both the physical properties of the land surface (e.g. albedo, surface roughness) and the physiological activity of the canopy (e.g. through photosynthesis and carbon sequestration) (Richardson *et al.* 2013).

The connection between plant phenology and climate is particularly interesting, because plant phenology both responds to and influences the climate system (Morisette *et al.* 2009). Indeed, phenology generates various feedbacks to the climate system, such as those summarized in Figure 1.1 and reviewed in Peñuelas *et al.* (2009) and Richardson *et al.* (2013). Because of its role in modulating carbon and water cycles, phenology is a key process within Terrestrial Biosphere Models (TBMs) (Zhao *et al.* 2013; Fisher *et al.* 2014). For instance, the accurate representation of phenology within a model is important for characterizing how much carbon is taken out of the atmosphere by the biosphere on seasonal and annual timescales (Fisher *et al.* 2014).

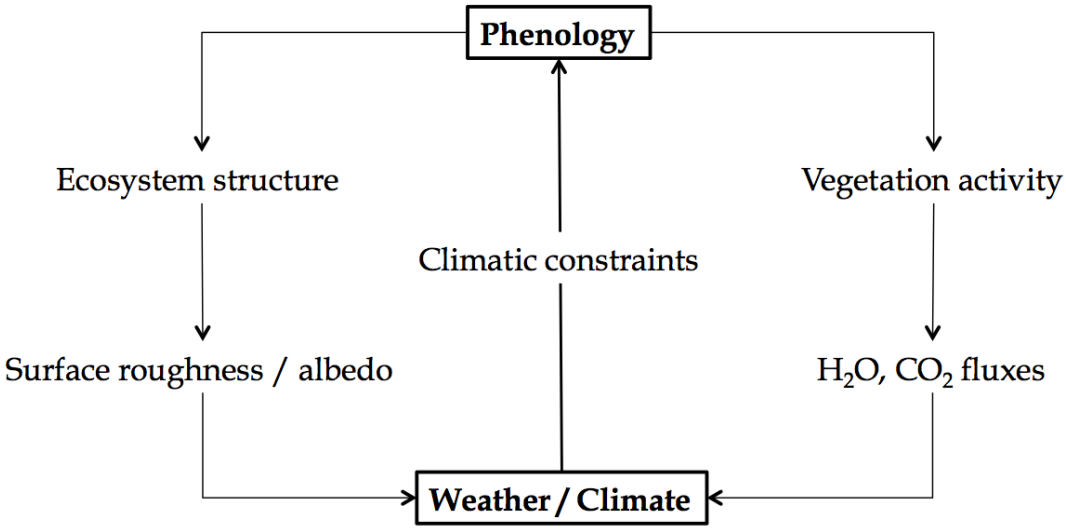

Figure 1.1 Illustration of some of the key feedback mechanisms between vegetation phenology and the climate system [modified after Richardson *et al.* (2013)]. Climatic constraints are climatic resources or conditions necessary for plant growth, such as the availability of moisture, light and temperature (Field *et al.* 1995) and are described further in Section 1.1.3.

1.1.1 Emergence of a science for global change

Human interest into the seasonal rhythms of plant development is long-standing, with examples of systematic observation of life cycle phases of plants as old as 705AD for cherry flowering observations in Japan (Menzel 2002). In the Western world, many phenological records started as the past time activity of naturalists such as Robert Marsham in England since 1736 (Marsham 1789), Henry David Thoreau in the United States (Whitfield 2001) or – closer to home – Marc-Louis Rigaud-Martin in Geneva, Switzerland (Figure 1.2). Phenology emerged as a scientific discipline in the late 19th century, together with its appellation, which was first coined by Belgian botanist Charles Morren in 1853 (Puppi 2007) and stems from the Greek word *phaino* (meaning "to appear").

a) Robert Marsham's *Indications of Spring* observations for both plants and animals as published in 1789 in Norfolk, England (Marsham 1789).

b) Recorded bud break date for the conker horse chestnut trees in Geneva, Switzerland. This record is maintained since 1808 and updated regularly by the Federal Office of Meteorology and Climatology (MeteoSwiss 2016). The red line represents the 20-year average.

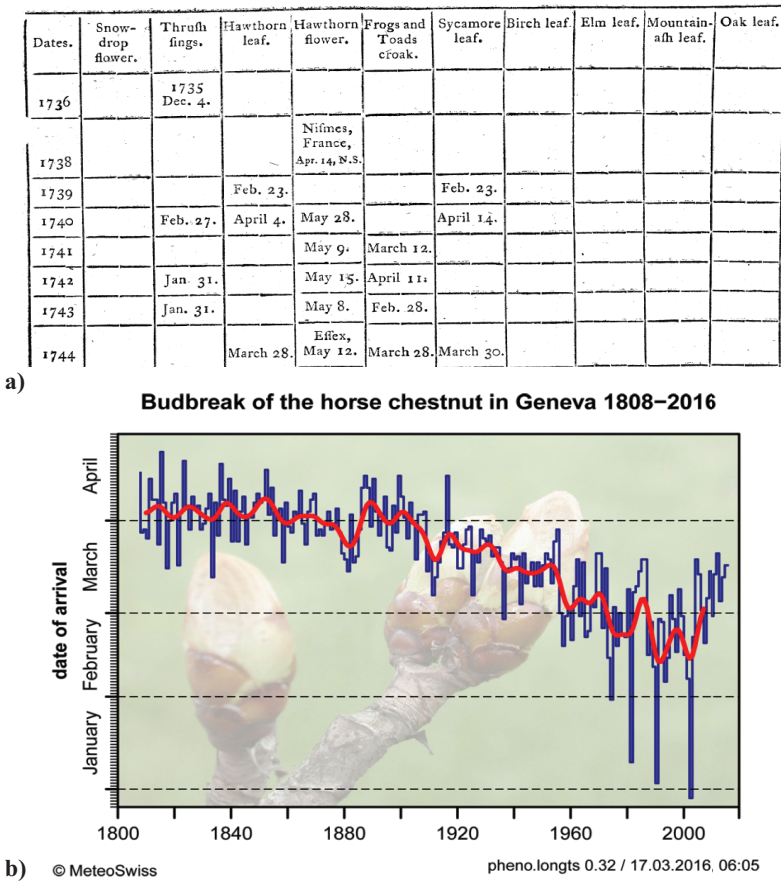

a)

XIII. *Indications of Spring, obs*

Dates.	Snow-drop flower.	Thrush sings.	Hawthorn leaf.	Hawthorn flower.	Frogs and Toads croak.	Sycamore leaf.	Birch leaf.	Elm leaf.	Mountain-ash leaf.	Oak leaf.
1736		1735 Dec. 4.								
1738				Nifmes, France, Apr. 14, N.S.						
1739			Feb. 23.			Feb. 23.				
1740		Feb. 27.	April 4.	May 28.		April 14.				
1741				May 9.	March 12.					
1742		Jan. 31.		May 15.	April 11.					
1743		Jan. 31.		May 8.	Feb. 28.					
1744			March 28.	Eſſex, May 12.	March 28.	March 30.				

b)

Figure 1.2 Two examples of historical phenological records.

Over the last decades, phenology has gained increasing attention by the global change community for a number of reasons (Menzel 2002; Noormets 2009). Firstly, the sensitivity of phenology to meteorological and climatic variations makes it a useful tool for monitoring climate and reconstructing past conditions (Cleland *et al.* 2007). For instance, records such as the century-long cherry tree blossoming dates in Japan since the 9th Century (Aono & Kazui 2008) or grapevine harvesting archives in France since the 14th Century (Chuine *et al.* 2004) have been used to trace back past climate variability. Secondly, phenology has been described as "perhaps the simplest process in which to track changes in the ecology of species in response to climate change" by the Intergovernmental Panel on Climate Change (IPCC) Assessment Report 4 (Rosenzweig *et al.* 2007). Plant phenology is indeed easy to observe, sensitive to

environmental variation, scalable from leaf to globe and linked to many aspects of ecosystems – making it an indicator of plant response to climate and other environmental change (Cleland *et al.* 2007; Schwartz 2013). Moreover, seasonal shifts are easily understandable to the broader public – adding to the value of this indicator for climate change communication to the public and policy makers (IPCC 2007). Because of this phenology has been widely used as a compelling evidence of the impact of climate change on species and ecosystems (Bradley *et al.* 1999; Menzel & Fabian 1999), but also as a potential Essential Biodiversity Variable (EBV) i.e. a variable central to the monitoring, reporting and management of global biodiversity change (Pereira *et al.* 2013; Skidmore *et al.* 2015).

Traditional phenological monitoring consists of observational records of which plants have reached a given life cycle stage (e.g. budburst, flowering, fruiting) and the associated timing (Badeck *et al.* 2004; Cleland *et al.* 2007; Gu *et al.* 2010). In order to facilitate phenological studies for global change research, several monitoring initiatives have been set up, such as the national phenology observation programs in the United States[1], Japan[2], Sweden[3], the Netherlands[4] as well as citizen-science phenology networks (e.g. Project Budburst[5]). Typically these programs are partnerships between national agencies, non-governmental organizations, botanical gardens or research institutions (Schwartz *et al.* 2012). The collection and dissemination of these data have been used to address research questions up to regional scale (Whitfield 2001). Nonetheless, using these data is not without challenges: firstly, these multi-distributor datasets often present uneven sampling design, frequency and/or spatial distribution of observations (Gerst *et al.* 2015). Secondly, quantifying phenological states is not straightforward: for instance, definitions of what constitutes leaf-out usually varies

[1] USA National Phenology Network
[2] Phenological Eyes Network [http://pen.agbi.tsukuba.ac.jp/index.html]
[3] Swedish National Phenology Network [http://www.slu.se/en/collaborative-centres-and-projects/swedish-national-phenology-network/]
[4] Dutch Phenological Network – Nature's Calendar [https://www.wageningenur.nl/en/show/Natures-Calendar-The-Dutch-phenological-network.htm]
[5] Project Budburst [http://budburst.org/]

from study to study (Polgar & Primack 2011). Moreover, the observations remain subjective and are not absolute measures. For instance, the common estimation of when 50% of leaves – both on the tree and on the ground – have autumn colouring, is no easy task (Menzel 2002). The quality of the data itself is thus dependent on both the skill and the effort put in by the person making the observation (Menzel 2002). This means that even within databases with common practices or taken from the same observer, the inaccuracies are difficult to estimate and are likely to vary in both space and time. Together, these elements complicate the task to compile observational data for large-scale comparisons (Menzel 2002).

In recent years, phenology networks such as the International Phenological Gardens (IPG) in Europe and the Global Phenological Monitoring (GPM) Programme are placing great effort in standardizing observation practices, harmonizing data management and limiting the subjective component of the data gathering to safeguard the usefulness of each data series (Whitfield 2001; Chmielewski *et al.* 2013). This effort is still in development and constantly being improved, with considerable work from researchers, funding agencies and volunteers.

1.1.2 Observational evidence for phenological shifts

The existence of phenological records dating back more than one hundred years have allowed the identification of phenological trends particularly in Europe (Menzel *et al.* 2006a), where most data is concentrated. A large body of literature has documented directional shifts in the phenology of both animal and plant species, in relation to global climate change (Walther *et al.* 2002; Cleland *et al.* 2007). Different meta-analyses have attempted to quantify these phenological responses across broad taxonomic groups and using large-scale ground observational data. Among these, Root *et al.* (2003) indicated a temperature-related shift in the phenology over 80% of the 143 species studied, encompassing invertebrates, amphibians, birds as well as plants (Root *et al.* 2003). Interestingly, tree species presented the slowest change rates in this study, though highly significant. Most studies focusing on vegetation phenology have

concentrated on spring-related events such as leaf-out or flowering (Table 1.1), which present substantial variation both within and among species, as well as a high sensitivity to temperature (Polgar & Primack 2011). The general conclusions are the documentation of directional changes in the onset of spring across the world in many species and across taxa, that cannot be attributed solely to normal year-to-year variation and thus have been linked to climate change (Walther *et al.* 2002; Parmesan 2007; Polgar & Primack 2011). Table 1.1 illustrates some of these studies, presenting a widespread advance of spring over the last 30 years – albeit with disparate estimates in the magnitude of change reported (Table 1.1).

Table 1.1 Examples of spring advancement results derived from meta-analyses of observational data. Another extensive review can be found as part of IPCC Assessment Report 4, Section 1.3.5.1 on Phenology (IPCC 2007).

Study	Taxa	Time period	Number of species	Geographical scale	Spring change reported (in days decade^{-1})
Root *et al.* (2003)	Numerous animal and plant species	Past 50 years	1468	Global	- 5.1
Parmesan and Yohe (2003)			1700+	Global	- 2.3
Parmesan (2007)			203	Northern Hemisphere	- 2.8
Fitter & Fitter (2002)	Various plant species	Past 50 years	385	Great Britain	-4.5
Cayan *et al.* (2001)	Lilac and honeysuckle	Past 40-50 years	2+	Western United States	-2 to -3.8
Menzel (2000)	Various plant species	1959–1996	16	Europe	- 2.1
Schwartz & Reiter (2000)	Lilac species	1959-1993	2+	North America	-1.4 to -1.7
Menzel & Fabian (1999)	Numerous tree species	Past 30 years	-	Europe	-2

1.1.3 Factors controlling plant phenology

Understanding the factors that control plant phenology is at the crux of building a predictive science, with many potential applications. Phenological dynamics of a given plant is the result of interplay between environmental and genetic factors. Species are under pressure to match their phenology to favourable environmental conditions and positive biotic interactions to increase their fitness and reproductive success (Pau *et al.* 2011). Thus, plants have evolved the ability to use environmental cues indicating the season and consequent resource availability. These effects of evolution within a plant community manifest themselves as genetic predispositions for earlier growth or for a species' sensitivity to environmental conditions (Forrest & Miller-Rushing 2010). This genetic component – thoroughly reviewed by Wilczek *et al.* (2010) – combined with both the availability of resources and the limitations imposed by competition (Chuine 2010; Zhao *et al.* 2013), are central to controlling a given plant's phenological patterns.

For most species, the genes and environmental cues involved in activating leaf out or senescence remain largely unknown (Polgar & Primack 2011). However, three main climatic factors have been identified as primary drivers for canopy greenness at large scales and have been shown to affect plant phenology in a variety of ways, namely temperature, photoperiod (day length) and water availability (Churkina & Running 1998; Botta *et al.* 2000; Nemani *et al.* 2003) (Figure 1.3). Indeed, temperature is considered as the main control of plant development (Menzel 2006) and the link between warm temperatures in the spring and leaf-out timing has been widely studied (Polgar & Primack 2011). It is generally accepted that the high variability of temperature in spring has induced the evolution of safeguards in some species (Morison & Morecroft 2008). For instance, chilling requirements in the winter indicate that winter has passed, thus preventing the plant from breaking dormancy too early (Körner & Basler 2010). Similarly, photoperiod is a reliable indicator of time of year given the regular seasonal change in photoperiod at a given location (outside of the equator) (Morison & Morecroft 2008) and is known to regulate the leaf-out of some

species (Forrest & Miller-Rushing 2010). Finally, moisture availability has been shown to drive phenological patterns in many tropical and arid areas (Forrest & Miller-Rushing 2010). Though it is unclear whether moisture or precipitation are themselves cues in life history cycles of some plants, it is clear that this parameter influences the growing season duration in many areas (Zhang *et al.* 2009) Some desert species germinate in response to drought (Kimball *et al.* 2010), and both rain and drought have been suggested as germination or flowering promoters among tropical forest species (Brearley *et al.* 2007; O'Brien *et al.* 2013).

Together with edaphic and nutrient requirements, these so-called "climatic growth constraints" interact to limit vegetation activity to varying degrees in different parts of the world (Rathcke & Lacey 1985; Nemani *et al.* 2003) and have been shown to explain large-scale spatial and temporal variations in canopy phenology (Churkina & Running 1998; Menzel 2002). Following the work of Churkina & Running (1998) and Nemani *et al.* (2003), Jolly *et al.* (2005) built the first generalized model allowing to predict canopy phenology without a priori knowledge of vegetation and based solely these three climatic growth constraints (Figure 1.3).

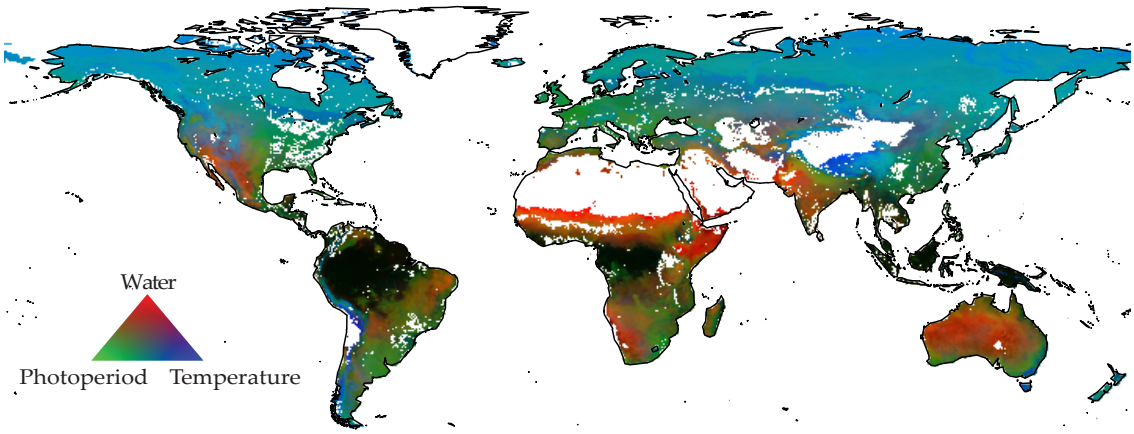

Figure 1.3 Geographic distribution of potential climatic constraints to phenology, as modelled using weather data (ECMWF ERA-Interim) for the years 1982-2012. The colours represent the relative importance of each of the constraints in limiting plant development through the year and their combination expresses co-limitations in most areas of the world [data from Stöckli *et al.* (2011)].

1.2 Remote sensing for advancing phenological knowledge

Remote Sensing (RS) is a key resource in the study of vegetation dynamics and has been used extensively both to investigate inter-annual changes in vegetation functional characteristics such as primary productivity (Running *et al.* 2004) and in terms of intra-annual dynamics of vegetation activity (White *et al.* 2009a; Primack & Miller-Rushing 2011).

Remote sensing phenology provides a number of advantages, such as: (i) the possibility to derive wall-to-wall phenological information i.e. a complete spatial sampling (Schimel *et al.* 2013); (ii) the ability to retrospectively derive phenology from existing satellite datasets (Reed *et al.* 2003); (iii) the potential for global monitoring (Cleland *et al.* 2007). A number of approaches have been used to derive metrics from time series of Vegetation Indices (VIs) to provide information about vegetation activity over large areas, in a systematic and continuous way. The technological and methodological advancements within RS have thus opened a new avenue for phenological research, called Land Surface Phenology (LSP) and defined as "the study of seasonal patterns of vegetated land surfaces as observed from remote sensing" (Friedl *et al.* 2006).

1.2.1 Times series of vegetation activity

VIs are combinations of multiple spectral values used to infer the amount of vegetation within a pixel (Campbell & Wynne 2011). Since the 1980s, a myriad of VIs have been put forward, among which are the Normalized Difference Vegetation Index (NDVI), the Enhanced Vegetation Index (EVI), vegetation cover percentage or fraction of Absorbed Photosynthetically Active Radiation (fAPAR). Since then, many LSP studies have used VI time series to derive information about the annual timing of vegetation growth, senescence, and dormancy, at resolutions ranging from moderate (250-m) to coarse (25-km) (Friedl *et al.* 2006; White *et al.* 2009a). Although VIs are the

main source of LSP information, the possibility of using passive microwave data (which is insensitive to atmospheric data contamination but still sensitive to vegetation biomass) as well as other types of data to complement such LSP analyses has also been explored (Jones *et al.* 2011; Alemu & Henebry 2013).

The work presented in this thesis focuses mostly on two indices – the NDVI (Rouse *et al.* 1974) and the Leaf Area Index (LAI). These two indices are the most commonly used for vegetation dynamics and thus have the strong advantage of comparison with other studies (Yengoh *et al.* 2015). They also provide a continuous description of phenological development continuously, rather than only phenological 'first' events such as in traditional phenological observations.

On one hand, NDVI is a unitless measure ranging from -1 to +1, with positive values corresponding to vegetated zones. The rationale behind NDVI is that photosynthesizing leaves absorb the portion of the electromagnetic spectrum that drives photosynthesis (particularly in the visible red band), but reflect strongly radiation in the Near InfraRed (NIR) part of the spectrum in order to avoid over-heating the plant and denaturing its proteins (Jensen 2009). The NDVI takes advantage of these reflectance characteristics (Figure 1.4) and is calculated as follows:

$$NDVI = (NIR - RED) / (NIR + RED) \quad (1.1)$$

Where NIR is reflectance in the NIR and RED is reflectance in the visible red band. NDVI is linearly correlated to fAPAR (Neigh *et al.* 2008) and has a positive relationship with canopy density or vigour. Thus, it is commonly used as a proxy for vegetation activity, whereby the higher the index, the greater the chlorophyll content (and thus the photosynthetic capacity) of the target.

The longest time series available at global scale is based on the Advanced Very High Resolution Radiometer (AVHRR) sensor on board various National Oceanic and Atmospheric Administration (NOAA) satellites. The so-called $NDVI_{3g}$ dataset assembles data from these into one continuous and non-stationary time series, available globally at coarse resolution. Extensive work has been undertaken regarding data quality screening, geometric correction, between-sensor calibrations and geometric, atmospheric and solar zenith corrections to produce these data (more

details and references can be found in Chapter 2), and numerous studies support its use for the study of vegetation dynamics at large scale (Yengoh *et al.* 2015; Marshall *et al.* 2016).

On the other hand, the Leaf Area Index (LAI) is defined as the leaf area unit per unit ground area and is usually expressed in m^2/m^2 (Mason & Reading 2005). Contrarily to NDVI, which qualitatively assesses vegetation density and is a spectral index, LAI is a derived biophysical variable quantifying the amount of vegetation present on the ground (Jones & Vaughan 2010). LAI may be estimated from NDVI, but the two are not directly proportional to each other, because a given change in LAI has less effect on radiation interception at high canopy densities (Figure 1.5).

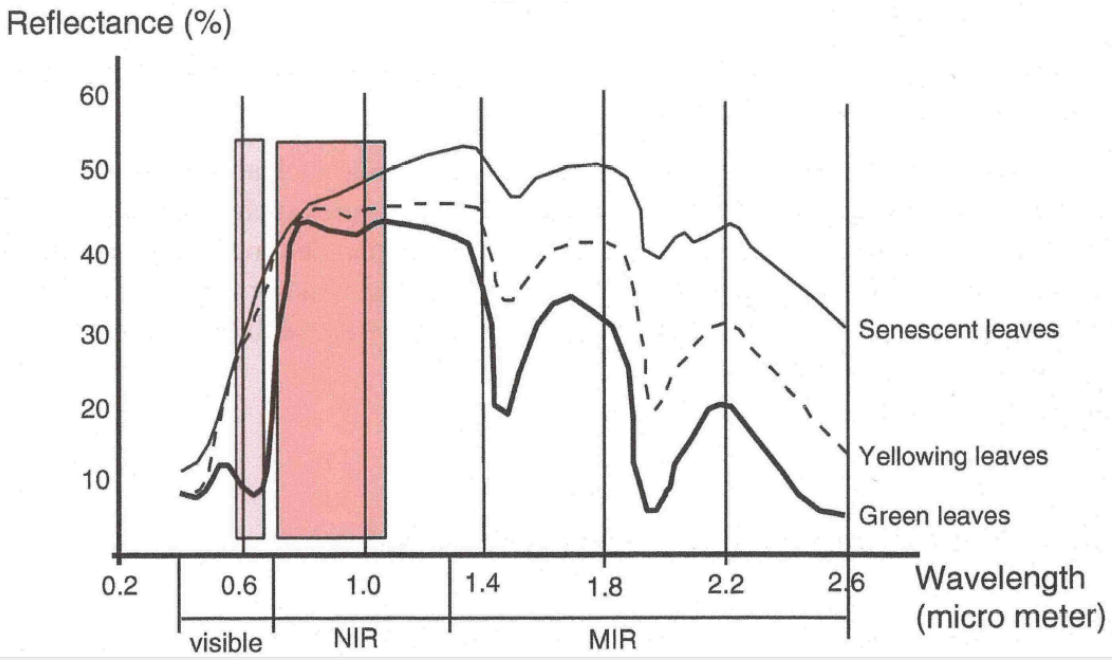

Figure 1.4 Typical spectral reflectance curves for vegetation at three stages of development. The RED and NIR spectral bands of the NOAA AVHRR sensor are represented by the red rectangles. [Reproduced with permission from (Yengoh *et al.* 2015), p. 10].

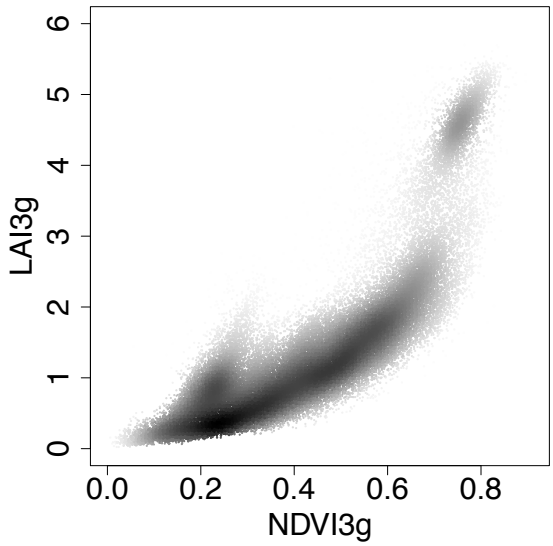

Figure 1.5 Relationship between LAI_{3g} and $NDVI_{3g}$ datasets at global scale, for an example year (2002). Data sources: LAI_{3g} (Zhu *et al.* 2013); $NDVI_{3g}$ (Pinzon & Tucker 2014).

1.2.2 Land Surface Phenology (LSP) metrics

Most LSP studies derive one or a number of metrics from VI time series, typically following smoothing of the annual VI curve. LSP metrics represent species-averaged information over large and diverse areas, most commonly at landscape-scale. This allows counter-balancing some of the limitations posed by observational records, for instance with the possibility to have a synoptic view or to integrate across taxa.

Figure 1.6 and Table 1.2 illustrate some of the types of metrics found in LSP literature. These include biomass-related metrics (e.g. integrals or amplitudes), seasonality-related (e.g. green up rate) as well as metrics defining the timing of phenological stages of the vegetation, as for instance the Start-, End- and Length of the Growing Season (SOS, EOS and GSL respectively) (Revermann *et al.* 2016).

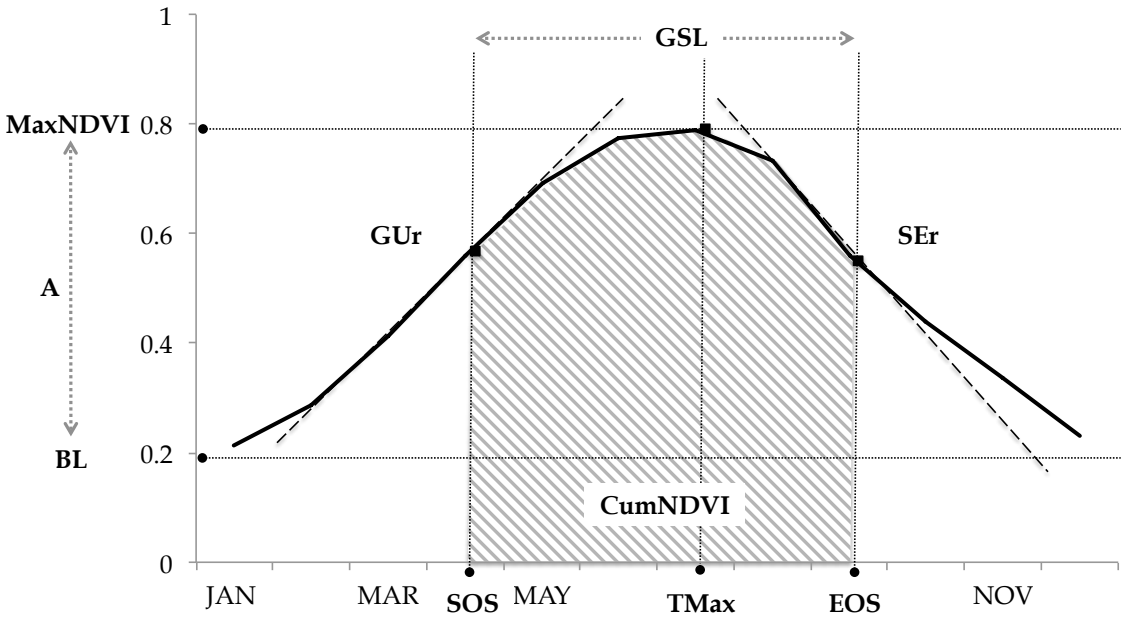

Figure 1.6 Examples of metrics found in LSP literature, for an example NDVI annual profile.

A variety of approaches exist for defining each metric, including fixed or variable thresholds, inflection points or moving averages (more details in Chapter 3). An inter-comparison of 10 different methods for deriving SOS across North America found large differences between them, with average estimates varying up to ± 60 days (White *et al.* 2009b), thus highlighting the importance of cautiously selecting LSP metric derivation methodology.

Table 1.2 RS definitions of some common LSP metrics found in the literature.

Metric	Abbreviation	Remote Sensing retrieval
Growing Season Length	GSL	Number of days between SOS and EOS
Start of GS	SOS	Time of onset greenness
End of GS	EOS	Time of end of greenness
Maximum of the GS	MaxNDVI	Value of peak vegetation index
Time of GS maximum	TMax	Time of peak vegetation index
Length of GS	GSL	Duration of greenness
Indicative of GS productivity	CumNDVI	Integrated NDVI
Base Level	BL	Minimum NDVI
Amplitude	A	MaxNDVI - BL
Green-Up rate	GUr	Annual NDVI increase rate
Senescence rate	SEr	Annual NDVI decrease rate

It is important to note that no direct correspondence may be assumed between observed vegetation phenology and satellite-derived variables (White *et al.* 2009a) and that their ecological interpretation remains a topic of investigation (Badeck *et al.* 2004; White & Nemani 2006; Cleland *et al.* 2007). Table 1.3 summarizes some key differences between land surface and vegetation phenolog*ies*. Indeed, although LSP is related to vegetation phenology via the absorption and reflectance of photosynthetically active radiation, LSP is derived through pixel values, and as such may represent a mixture of land covers in an area-averaged fashion.

Nevertheless, LSP remains a key biological indicator of terrestrial ecosystems' responses to environmental variations (Zhao *et al.* 2012), and one that helps to characterize land surface fluxes of energy, carbon and water (Friedl *et al.* 2006). Particularly within the context of global change research, LSP metrics provide a useful connection between the study of plant physiology and that of ecosystem-wide processes (Liang & Schwartz 2009; Zhao *et al.* 2012).

Table 1.3 Examples of differences in ground and RS-derived phenological metrics.

Feature	Ground pheno-metric	RS pheno-metric
Scale	Point	Pixel
Species	Single	Multi
Temporal range	May be long (over 50 years)	Max 30 years (VI data)
Spatial variability derivation	Difficult	Possible
Example	Bud burst date	Time of maximum annual green-up

1.3 Key challenges in phenology for global change research

Monitoring phenology in the context of global change does not come without challenges. In particular, four key aspects were put forward as research needs by different review articles (Cleland *et al.* 2007; Morisette *et al.* 2009; Pau *et al.* 2011). These challenges will be taken into particular consideration throughout the thesis.

1.3.1 Getting a global picture

Answering questions about the effect of global change on phenology requires the availability of extensive and reliable phenological data. The aim is to cover a breadth in space, time and range of species in order to be able to draw large-scale conclusions. Within the large body of research dedicated to phenological shifts and their link to climate, there is a bias in the availability of results towards the Northern Hemisphere and particularly to Europe and North America (Menzel 2000; Defila & Clot 2001; Parmesan 2007). This makes it hard to provide a global assessment. The same is true for LSP studies, which have mostly focused on Northern Hemisphere temperate mid-latitudes. There is therefore a need for both data and studies focusing on the global scale (Menzel 2002; Cleland *et al.* 2007; Fu *et al.* 2014). As global scale phenological networks do not yet exist (Schwartz 1998), LSP appears as an important source of information for getting a global picture.

1.3.2 Filling research gaps

Most phenological studies have focused on spring events and their advance in association with spring warming (Parmesan & Yohe 2003; Root *et al.* 2003; Parmesan 2007; Poloczanska *et al.* 2013). The climate signal of spring events is fairly well understood, given that nearly all spring changes in plants correlate with temperatures of previous months (IPCC 2007). However, autumn processes – such as fruit ripening

or leaf senescence – have been comparatively overlooked and remain presently under-studied (Gallinat *et al.* 2015; Parmesan & Hanley 2015).

Previous studies on autumn phenology generally focused on few species or very limited in scale (Liu *et al.* 2016). Among the few large-scale studies focusing on autumn timing, a large meta-analysis of autumn events in Europe found leaf senescence to be delayed with climate warming across Europe (Menzel *et al.* 2006b), though Walther *et al.* (2002) found shifts in autumn to be generally less pronounced and more heterogeneous than those of spring. More recent findings from a remote sensing study suggest that extended growing seasons across Northern temperate forests may be equally attributed to spring advancement and autumn delay (Jeong *et al.* 2011). Hence, there is general agreement that more attention should be placed on autumn phenology to compensate past 'neglect'.

1.3.3 Bridging the scale mismatch

There is a need to reconcile the mismatch between the scale at which phenological observations are taken (typically at plant or plot level, for one or a small number of species) and the large-scale view of global models, which are not capable of capturing species level detail (White *et al.* 1997).

The strong inter- and intra-species variation in phenology found through field studies (Parmesan & Hanley 2015) makes existing field observations not representative across species or vegetation types present at the landscape scale. This complicates the important task of obtaining large-scale phenological data for global monitoring and for model validation, which appears as a challenge.

1.3.4 Understanding the relative importance of climatic constraints

Despite the importance of phenology for modulating biogeochemical cycles, it is widely acknowledged that this parameter is poorly represented in many TBMs (Kucharik *et al.* 2006; Migliavacca *et al.* 2012; Richardson *et al.* 2012). A phenology

model comparison within 14 TBMs found that almost all models failed to track the phenology, leading to overestimation of gross ecosystem photosynthesis and forecasts of carbon and water cycling (Richardson *et al.* 2012). Currently, approximately one third of TBMs prescribe leaf onset/offset dates using remote sensing, thus assuming no variation from year to year (Schwalm *et al.* 2010; Huntzinger *et al.* 2012; Schaefer *et al.* 2012; Fisher *et al.* 2014). When leaf phenology parameters are not prescribed in TBMs, most models use mostly temperature-based parameterizations, including thresholds or accumulations, to model leaf onset and loss (Fisher *et al.* 2014; Delpierre *et al.* 2016).

This is (at least partly) due to the many uncertainties remaining about what factors drive leaf onset and senescence at large scales (Zhao *et al.* 2013). In particular, despite the links established between climatic and phenological trends (e.g. warming and spring advance (Myneni *et al.* 1997; Keenan 2015)), there is uncertainty on what the relative roles of seasonal changes in temperature, moisture or photoperiod are in influencing phenology (Körner & Basler 2010; Parmesan & Hanley 2015). For instance, warming and drought may have opposing effects on leaf senescence timing, and therefore the impact of climate change depends on the relative importance of each factor in different regions (Estiarte & Peñuelas 2015). Steps forward in this direction are therefore key for improving model representation of phenology and estimating climate change impacts.

1.4 Thesis aims

Previous sections of this Chapter put forward that phenology is a key topic within global change research, with important challenges in need of facing. Whilst phenological observations and experiments are done mostly at the plant or plot level, the pressing issue of global change and the large-scale view of global models call for much larger scales of observations. As climatic changes are projected to accelerate over the coming century (IPCC 2013), there is a need to understand phenological responses and dynamics at large scale (Morisette *et al.* 2009).

The broad aim of this research is to provide a comprehensive large-scale assessment of past LSP dynamics at global scale in combination with climatic constraints. More precisely, given the research needs outlined in Section 1.3 and the opportunities offered by RS data availability, the goals of this research are the following:

- Provide consistent estimates of LSP trends at a scale suitable for global studies.
- Assess the relative contribution of spring and autumn shifts to growing season length changes.
- Examine the relative importance of climatic constraints on LSP and its dynamics through time.

The study period of 1982-2012 is defined by the present availability of satellite data records from which LSP can be derived.

1.4.1 Research Questions (RQs) and hypotheses

Three research questions may be formulated as follows:

RQ1: Can changes in Growing Season Length (GSL) be detected at global scale using VI records, and what do these records of unveil about large-scale phenological shifts?

RQ2: What is the contribution of spring and autumn shifts to overall GSL changes and is there evidence for differing controls underlying spring and autumn phenology at large scale?

RQ3: What climatic constraints underlie LSP variability, and how does their relative importance vary during this period?

The general hypotheses are:

I. that growth constraints have eased over the past 3 decades, resulting in longer growing seasons;
II. that LSP varies differentially in different environmental zones, given the variety of human and environmental pressures that interact on land surfaces;
III. that start and end of season phenology vary differentially because they have differing climatic controls; and
IV. that variation in LSP has repercussions on the relative importance of climatic constraints in many regions.

1.4.2 Structure of the thesis

Chapter 1 provides a background to the thesis and introduces its goals and research questions.

Chapter 2 describes the development of an algorithm to estimate Start-, End- and Length- of the Growing Season (SOS, EOS and GSL, respectively) metrics from the 30 year-long global $NDVI_{3g}$ record. This Chapter also establishes a consistent evaluation of symmetry between SOS and EOS trends. Hypotheses I, II and III are evaluated in this Chapter for a well-studied and data-rich area that is in particular demand of continental-wide monitoring schemes (Pan-Europe).

Chapter 3 builds on the previous methodology to provide a comprehensive assessment of LSP variability at global scale. The previously developed algorithm is adapted to a global assessment, which identifies hotspots of change worldwide, tests for shifts in GSL trends, and assesses the SOS/EOS trend asymmetry at global scale. With this Chapter we present NDVI3g-derived LSP dynamics and discuss in context to the existing literature. Hypotheses I, II and III are also tested in this Chapter at global scale.

Chapter 4 examines the implications of the LSP variability found in previous Chapters on climatic drivers of SOS and EOS independently. We assess the relative importance of three climatic constraints of phenology for SOS and EOS for the last three decades and examine discusses the representation of phenology in TBMs. This Chapter tests Hypotheses III and IV by examining the effects of LSP variability on climatic constraint distribution at SOS and EOS as well as the differences in climatic constraints that may underlie these two phenological processes.

Finally, Chapter 5 discusses the main findings of the thesis and provides general conclusions as well as an outlook on possible research directions.

Chapter

2

Contribution of autumn phenology to changes in satellite-derived growing season length estimates across Europe

Garonna, I., De Jong, R., De Wit, A.J.W.,

Mücher, C.A., Schmid, B. and Schaepman, M.E.

This chapter is based on the peer-reviewed article:

Global Change Biology, 2014 (20), 3457-3470

DOI: 10.1111/gcb.12625

and has been modified to list all cited references in the Bibliography chapter.

Abstract

Land Surface Phenology (LSP) is the most direct representation of intra-annual dynamics of vegetated land surfaces as observed from satellite imagery. LSP plays a key role in characterizing land-surface fluxes, and is central to accurately parameterizing terrestrial biosphere–atmosphere interactions, as well as climate models. In this paper we present an evaluation of Pan-European LSP and its changes over the past 30 years, using the longest continuous record of Normalized Difference Vegetation Index (NDVI) available to date in combination with a landscape-based aggregation scheme. We used indicators of Start-Of-Season, End-Of-Season and Growing Season Length (SOS, EOS and GSL, respectively) for the period 1982–2011 to test for temporal trends in activity of terrestrial vegetation and their spatial distribution. We aggregated pixels into ecologically representative spatial units using the European Landscape Classification (LANMAP) and assessed the relative contribution of spring and autumn phenology.

GSL increased significantly by 1.8–2.4 days/decade over 18–30% of the land area of Europe, depending on methodology. This trend varied extensively within and between climatic zones and landscape classes. The areas of greatest growing-season lengthening were the Continental and Boreal zones, with hotspots concentrated in southern Fennoscandia, Western Russia and pockets of continental Europe. For the Atlantic and Steppic zones, we found an average shortening of the growing season with hotspots in Western France, the Po valley, and around the Caspian Sea. In many zones, changes in the NDVI-derived end-of-season contributed more to the GSL trend than changes in spring green-up, resulting in asymmetric trends. This underlines the importance of investigating senescence and its underlying processes more closely as a driver of LSP and global change.

Authors' contributions (alphabetical order): IG, RdJ, MES designed the study and developed the methodology. IG, RdJ, CAM collected the data. IG, RdJ, AdW performed the analysis. All authors wrote the manuscript.

2.1 Introduction

As anthropogenic pressure on ecosystems is increasingly documented, so is the understanding that its impact is likely to intensify over the coming years (IPCC 2007; Rockström *et al.* 2009; Running 2012; IPCC 2013). Monitoring vegetation dynamics constitutes a crucial effort for environmental management (Zhou *et al.* 2001; Reed *et al.* 2003), and the advances in quality and availability of remote sensing products have proven very fruitful in observing vegetation activity at various scales (Zhou *et al.* 2001; Zhang *et al.* 2003; Running *et al.* 2004; Turner Ii *et al.* 2007; Zeng *et al.* 2013). The Normalized Difference Vegetation Index (NDVI) is the most commonly used proximate indicator for vegetation activity (Rouse *et al.* 1974; Tucker 1979). It has been used among other purposes to describe seasonal dynamics of vegetation activity (Reed *et al.* 1994; Julien & Sobrino 2009) and for assessing inter-annual trends in these seasonal dynamics, in particular greening and browning trends at various scales (Myneni *et al.* 1997; Zhou *et al.* 2001; de Jong *et al.* 2011).

In the field of Land Surface Phenology (LSP), remote sensing methods are used to study seasonal patterns of vegetated land surfaces (de Beurs & Henebry 2005; Friedl *et al.* 2006; Julien & Sobrino 2009). In contrast to plant phenology, LSP does not aim to describe the physiological cycle of individual plants, but rather to assess vegetation activity over the growing season at the ecosystem level (Stöckli & Vidale 2004). LSP provides key variables in terrestrial biosphere and climate change models, because green vegetation cover regulates land surface fluxes through albedo, CO_2 assimilation and evapotranspiration (Arora & Boer 2005; Richardson *et al.* 2012; Richardson *et al.* 2013). Furthermore, vegetation seasonality can be used as an important habitat descriptor .

The fact that Europe is undergoing major environmental change is widely recognized (Menzel & Fabian 1999; Metzger *et al.* 2008; EEA 2012; IPCC 2013). There is therefore a need to provide integrative assessments of the state and trends shaping the

European environment (Hazeu *et al.* 2011). However, the heterogeneity of ecologically meaningful areas within this region makes it difficult to understand the impact and vulnerability of this region to global climate change (Metzger *et al.* 2006). Europe's climatic spectrum allows it to encompass a considerable variety of biomes (Meeus 1995; Mücher *et al.* 2010; Bailey 2014). Also, the long history of human presence and different types of land-use management helped to shape Europe's complex landscape and vegetation mosaic (Meeus 1995), which in turn may significantly feed back on regional climatic change (Foley *et al.*, 2003). Aggregating pixels of the terrestrial surface into relatively homogeneous vegetation types facilitates the understanding of changes in such a complex region and provides the basis for assessment and monitoring programs at the European scale (Metzger *et al.* 2005; Mücher *et al.* 2010).

As one of various environmental classification methods, the European Landscape Classification LANMAP (Mücher *et al.* 2010) uses a systematic, quantitative and objective approach to incorporate land cover/land use, climate, geomorphology and soil characteristics in a single map (Hazeu *et al.* 2011). Thus LANMAP constitutes a more complete categorization of the European environment than would a land cover/land use classification alone. Landscapes reflect the combination of abiotic, biotic and anthropogenic processes that are needed for the analysis of environmental and ecological data at the European scale (Mücher *et al.* 2010).

In this paper we evaluate NDVI-derived growing season temporal trends and their spatial pattern across all of Europe over the past 30 years, using a landscape-based aggregation scheme. Various previous studies have reported shifts in European growing seasons both from field (Menzel 2000; Ahas *et al.* 2002; Menzel *et al.* 2006) and from remote sensing data (Stöckli & Vidale 2004; Julien & Sobrino 2009; Hamunyela *et al.* 2013). However, the reported trends in Growing Season Length (GSL) vary considerably, depending on the methodology used, the temporal and spatial extent and the data resolution. Moreover, most studies have focused on an advancement of spring events (through green-up and Start-Of-Season, SOS) and only few have tested for a climatically-induced prolongation (or advancement) of the End-Of-Season (EOS)

(Jeong *et al.* 2011; Høgda *et al.* 2013). The timing and rate of autumn senescence have been found to vary across the canopy even more than those of spring development (Richardson *et al.* 2009), making this process potentially harder to track than green-up. Here, we provide a comprehensive LSP analysis over all of Europe by assessing long-term trends in LSP metrics. We put focus on the relative contribution of SOS and EOS dynamics, since both may have different ecological implications and a different set of underlying drivers.

Given the temperature increases that have shaped the last 3 decades, we hypothesize that growth constraints have generally eased in Europe over the past 30 years, resulting in longer GSL. Going into more detail and towards attribution of these changes, our second hypothesis is that GSL trends varied between Europe's heterogeneous ecological zones and between spring and autumn, because of differing controlling factors to vegetation dynamics as well as the variety of human pressures in Europe.

2.2 Data and Methods

In our approach, we extracted LSP metrics (i.e. SOS, EOS and GSL) from the longest continuous NDVI record available to date, and analysed the spatial and temporal variation in these LSP metrics per landscape unit. The time series were smoothed to remove biased observations and LSP metrics were extracted using a maximum-increase and a midpoint method. The LSP metrics were used to detect change and spring-autumn symmetry.

2.2.1 Time series of vegetation activity

We used the latest release of the Global Inventory Monitoring and Modeling Systems (GIMMS) NDVI dataset, produced from Advanced Very High Resolution

Radiometer (AVHRR) data (Pinzon *et al.* 2005; Tucker *et al.* 2005; Pinzon & Tucker 2014). This dataset is more commonly referred to as $NDVI_{3g}$, with the suffix 3g referring to the 3rd generation processing applied to correct for orbital drift effects, calibration, viewing geometry, stratospheric volcanic aerosols and other errors unrelated to vegetation change (Pinzon *et al.* 2005; Tucker *et al.* 2005; Sobrino *et al.* 2008). $NDVI_{3g}$ contains global NDVI observations at ca. 8-km spatial resolution, derived from AVHRR channels 1 and 2 — corresponding to red (0.58 to 0.68 μm) and infrared wavelengths (0.73 to 1.1 μm), respectively. The dataset spans from July 1981 to December 2011 and has a bi-monthly temporal resolution. Each 15-day data value is the result of Maximum Value Compositing (MVC; Holben (1986)), a process aiming to minimize the influence of atmospheric contamination (e.g. from aerosols and clouds). This technique assumes that NDVI undergoes smooth variations throughout the year (Sellers *et al.* 1996) and that atmospheric disturbance is responsible for sharp temporary drops in values, creating time series outliers (Holben 1986). We extracted data for all European land pixels from all complete years of GIMMS $NDVI_{3g}$ (i.e. 1982–2011), and stacked them by calendar year (January to December).

2.2.2 European Landscape Classification

The latest version (v3) of LANMAP (Mücher *et al.* 2010) was used to classify landscapes for the LSP analysis. This classification is available at a scale of ~1:2M and covers all of Europe: it extends from west to east covering the area between the Atlantic coast and the Ural Mountains. More precisely, the region stretches from Iceland (North-West) to Nova Zembla (North-East) and from Gibraltar (South-West) to Azerbaijan (South-East). This area covers about 11 million km^2 and represents around 220 000 $NDVI_{3g}$ pixels. Four key types of data were used to delineate landscape units: climate, altitude, parent material (geological information) and land cover/land use. The resulting hierarchical map includes four levels from the highest (Level 1) dividing Pan-Europe into eight climatic zones to the lowest (Level 4) dividing Europe into 350 landscape classes (Mücher *et al.* 2010). Within LANMAP, landscapes are defined as

"ecological meaningful units where many processes and components interact" (Mücher *et al.* 2010). This classification therefore creates a more ecologically significant stratification than would land use/land cover alone. Also, the use of a landscape classification as opposed to more 'conventional' land cover classifications (such as GLOBCOVER or similar) is in line with European environmental reporting efforts. An illustration of LANMAP is presented in Figure 2A.1 (as Supporting Information).

The LANMAP classification system was re-projected and rasterized, using a centre-pixel approach, to match the 8-km grid of the $NDVI_{3g}$ dataset. Binary masks were created for Level 1 and Level 4 classes (climatic zones and landscape classes, respectively). After extracting LSP metrics on a pixel-by-pixel basis for the whole region, these LANMAP classes were used to aggregate pixels into ecologically meaningful classes, and thus better interpret results.

2.2.3 Harmonic analysis

We used harmonic analysis to model yearly NDVI profiles as smooth curves, which can be used for extracting of phenological metrics. The Harmonic Analysis of NDVI Time Series (HANTS) algorithm (version 1.3, Fast Fourier implementation (FFT)) (Roerink *et al.* 2000; Roerink *et al.* 2003; de Wit & Su 2005) has been shown to effectively represent the intra-annual variability of GIMMS NDVI data, particularly in regions outside the tropics and the high latitudes (de Jong *et al.* 2011). HANTS describes the seasonal pattern in NDVI through low-frequency sine functions, which can be used to analytically derive LSP metrics.

A variety of smoothing algorithms have been used in the field of LSP (for a review see de Beurs & Henebry (2010)) but there is no consistently superior performing method for global applications (Reed *et al.* 2003; Atkinson *et al.* 2012). We choose HANTS based on its capacity to analytically represent the growing season and to be widely applicable for the extraction of phenological metrics (White *et al.* 2009). A detailed description of the HANTS parameterization is given in Table 2A.1.

2.2.4 Deriving the LSP indices: SOS, EOS and GSL

Our choice of two LSP indicators was based on the comprehensive study of White et al. (2009), acknowledging the wide variety of LSP metrics described in the literature (Reed *et al.* 1994; Reed *et al.* 2003; White *et al.* 2009; de Beurs & Henebry 2010). In their inter-comparison and validation of 10 NDVI-derived Start-Of-Season (SOS) metrics, White et al. demonstrated a strong variability of average SOS date estimates, reaching differences as high as ± 60 days between individual methods. However, they also put forward two indicators — Midpoint $_{pixel}$ and Max-increase (corresponding to HANTS-FFT in their study) — as best matches to both measured and modelled phenological observations. We therefore considered these two as the most appropriate for use in our study, and refer to them as MP (Midpoint $_{pixel}$) and MI (Max-increase).

We interpolated the HANTS-smoothed $NDVI_{3g}$ to a daily frequency, using a spline function (Forsythe *et al.* 1977). Then we used both LSP derivation methods to extract SOS for each NDVI annual profile. MP is a local threshold method, whereby the SOS is defined as the day-of-year at which the NDVI reaches half its annual amplitude. For its implementation, we first translated each pixel's annual NDVI profile to a ratio, based on its annual range:

$$NDVI_{ratio} = \frac{NDVI - NDVI_{min}}{NDVI_{max} - NDVI_{\min}} \qquad (2.1)$$

We then extracted each SOS as the first day of year at which $NDVI_{ratio}$ is greater than the midpoint, i.e. when $NDVI_{ratio} > 0.5$, as shown in Figure 1a. The MI algorithm, on the other hand, defines SOS as the date of maximum increase in NDVI i.e. as the maximum of the first derivative, located between the maximum annual NDVI value and its first preceding inflection point (Figure 2.1b). The EOS, for both methods, is defined as the first day (after SOS) with an NDVI value lower than or equal to the NDVI value at SOS for that given year. SOS and EOS are always expressed in Day-Of-Year (DOY), and the Growing Season Length (GSL) was then calculated as the number of days between SOS and EOS.

For some pixels, the growing season may straddle the end of the calendar year. This is common in southern Europe, where the growing season may occur during winter. Deriving LSP metrics from such profiles necessitated a specific approach, since both MP and MI algorithms were constrained to the calendar year. We thus identified all pixels for which the SOS date was found to be within the first GIMMS scene of the calendar year. For each of these cases, the NDVI profile for the following year was appended to the time series (as shown in Figure 2.1c), and both LSP metric retrieval algorithms were repeated. Two types of 'irregular' profiles were considered potentially unstable in our method, and were therefore discarded from our analysis: firstly, pixels for which there is no distinct seasonality (e.g. in arid areas); secondly, pixels with double (or more) growing seasons. The first type was defined as pixels for which the annual NDVI range is lower or equal to 0.1 for more than 10 (out of the 30) years. The latter were identified using a flagging algorithm that scanned the distribution of consecutive DOYs considered within the growing season (presented in the Supporting Information section and Figure 2A.3).

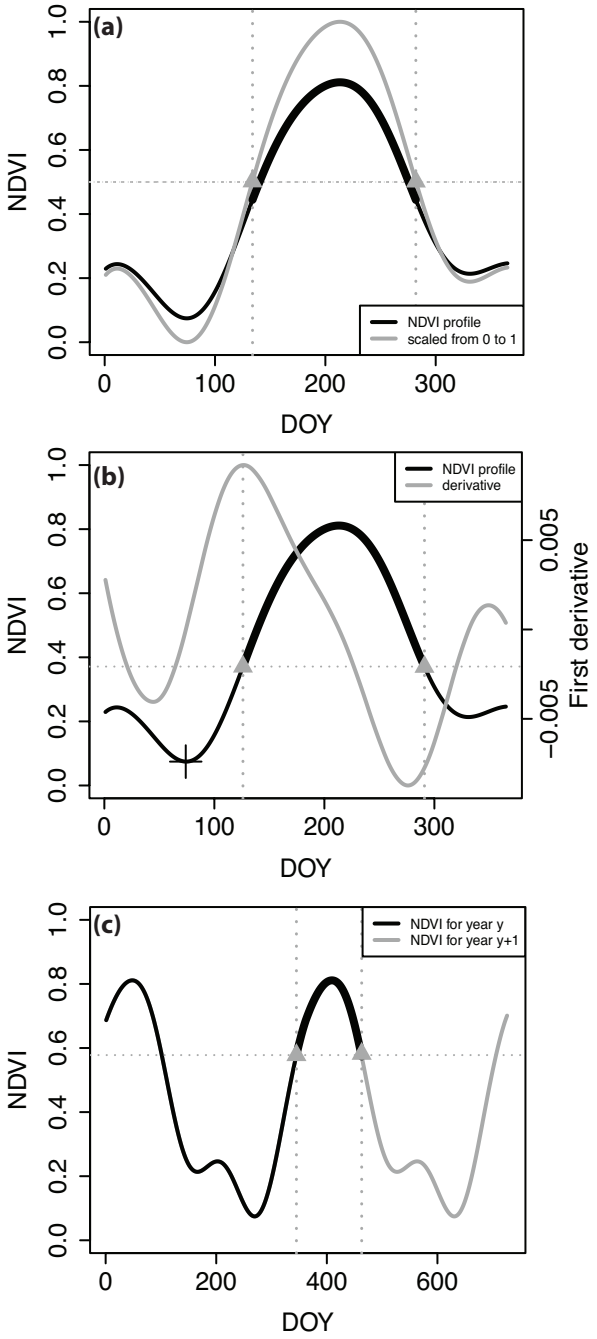

Figure 2.1 Illustration of MP (a) and MI (b) methods, as well as a case of growing season straddling two calendar years (c). The black bold line highlights the growing season as extracted from our algorithm. The grey triangles represent SOS and EOS dates, respectively. In (b), the black square refers to the NDVI annual maximum, and the cross refers to the first inflection point preceding SOS.

2.2.5 Quantification of change and trend symmetry

Linear regression analysis was used to detect trends in LSP metrics. We quantified trends using the slope of the regression line representing the LSP variation over time. The fitted slopes were tested for significance using ANalysis Of VAriance (ANOVA) with a significance level (α) of 0.05. The Coefficient of Variation (CV) was calculated across years for each pixel and then averaged by landscape class, as a measure of inter-annual variation in GSL. Only pixels for which trends significantly differed from zero were considered in our results. All LSP metrics were derived and analysed for trends using the statistics software R (http://www.r-project.org/, version 3.0.1.).

In order to quantify the relative contribution of trends in SOS and EOS to the overall GSL changes observed, we calculated the C-index as follows:

$$C = -1 + \frac{2*abs(\Delta_{SOS})}{abs(\Delta_{SOS})+abs(\Delta_{EOS})} \qquad (2.2)$$

for which Δ_{SOS} and Δ_{EOS} are the rate of change of SOS and EOS (respectively) and are expressed in days/decade. The C-index has no unit and varies from –1 to 1. A negative C value means that the change in GSL is mostly attributable to a shift in EOS, whereas a C value close to 1 means that SOS shifts dominate in the overall GSL change. In this respect, we evaluate the symmetry of EOS and SOS shifts over the time period. Figure 2.2 illustrates examples of symmetric and asymmetric trends using, as an example, the case of both EOS and SOS contributing to an overall lengthening of the growing season.

Example	Illustration	C-value	Symmetric trends
1)	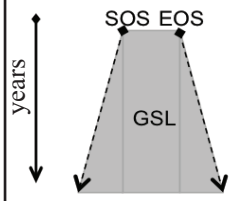	C = 0	Yes
2)	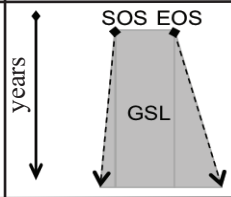	C < 0	No
3)	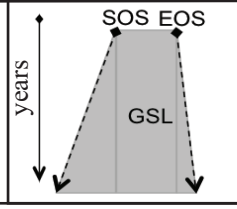	C > 0	No

Figure 2.2 Illustration of MP (a) and MI (b) methods, as well as a case of growing season straddling.

2.3 Results

The LSP extraction method was successful for 97% of the total number of pixels; the remaining 3% — amounting to around 16 000 pixels — were discarded because of their low annual NDVI range (about 8000 pixels) or the presence of multiple growing seasons during a calendar year (8000 additional pixels). The latter were mostly located in the Mediterranean zone (as illustrated in Figure 2A.2), covering over 31% of its total extent.

2.3.1 Characterization of Pan-European LSP using 30 years of NDVI data

Figure 2.3 presents the average phenological profiles with their average SOS and EOS dates for the eight Pan-European climatic zones. The Boreal and Alpine zones have the highest seasonal variation in NDVI, with differences between winter and

summer NDVI greater than 0.6 points. The Mediterranean zone, on the other hand, has the smallest NDVI range, of only approximately 0.15 NDVI points. The Alpine, Boreal, Arctic and but also the Steppic and Anatolian zones are all characterized by very low winter NDVI values ($NDVI_{winter} \leq 0.2$), whereas profiles for the Continental, Atlantic and Mediterranean zones are higher through the whole year. The intra-annual NDVI profiles for the Arctic, Alpine and Boreal zones present a shape that is rather symmetrical around the annual maximum, whereas the others (namely the Anatolian, Steppic and Continental zones) have a slower autumn decline than spring increase in NDVI (Figure 2.3).

Figure 2.4 illustrates differences in SOS, EOS and GSL between climatic zones and between the two methods used to derive LSP indices. There was generally good agreement between the methods regarding average and relative GSL values for most climatic zones. However, the MI method led to consistently smaller estimates of GSL than the MP method. Generally, EOS values varied more between the two methods than did SOS values, which were relatively stable between the two methods for all climatic zones. The highest average GSL values were found for the Atlantic and Continental zones and the lowest are for the Arctic and Anatolian zones. Over the whole 30-year period, the average GSL in Pan-Europe is approximately 159 ± 30 days i.e. about 5.5 months.

Figure 2.5 presents the average GSL and its CV for each landscape class (LANMAP Level 4). GSL declined with latitude from > 180 days in southern and central Europe to < 120 days in northern Europe. Both LSP derivation methods yielded the highest average GLS values in Germany, France, the Balkans, and the UK. Values derived by the MI method had a higher CV in most areas but the largest CVs were found by both methods in the Mediterranean and Atlantic zones and in the west of the Caspian Sea (Figure 2.5b). These high CV are linked to particularly high inter-annual variability in GSL in these areas rather than to high spatial variability in GSL within climatic zones or geographic areas.

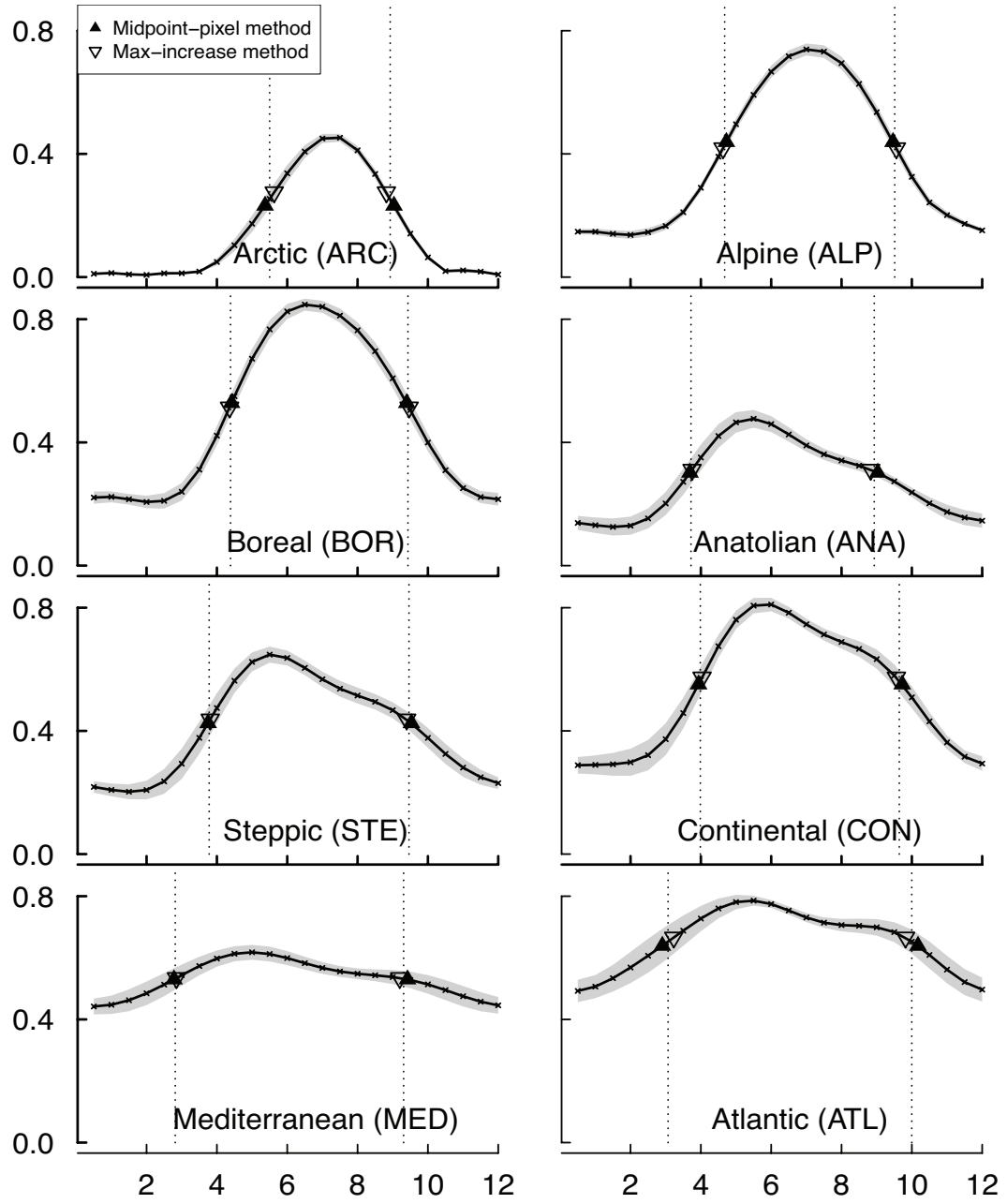

Figure 2.3 NDVI average annual profile, with SOS and EOS for the eight LANMAP-derived climatic zones of Europe. The time series (solid lines and crosses) are plotted with their standard deviations (shaded). SOS and EOS are solid and empty triangles as derived by the MP or MI methods, respectively.

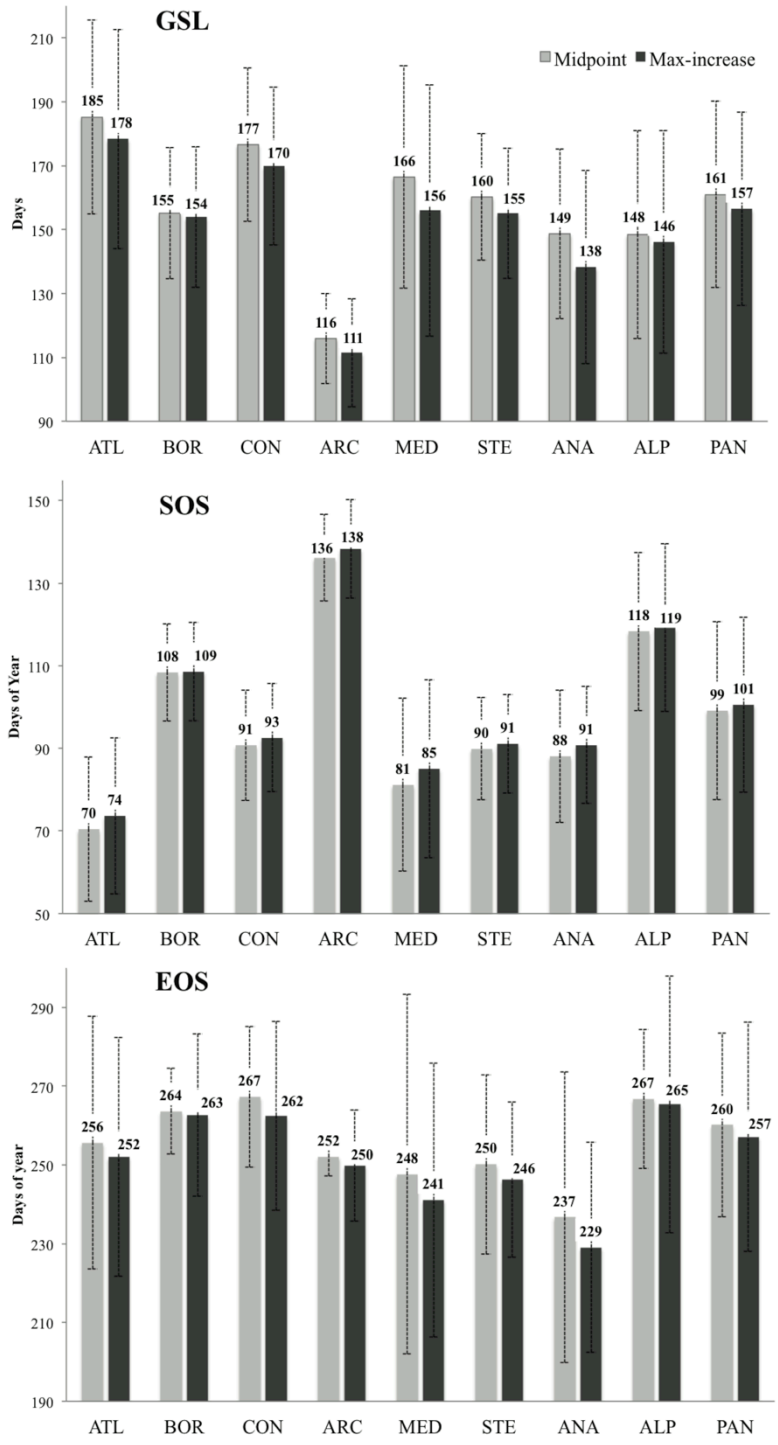

Figure 2.4 Average GSL (top, in days), SOS and EOS (middle and bottom, in day-of-year) from 1982–2011 in eight climatic zones (LANMAP Level 1) and for all of Europe (PAN) derived by MP and MI methods. MP results are in light grey, MI in dark grey.

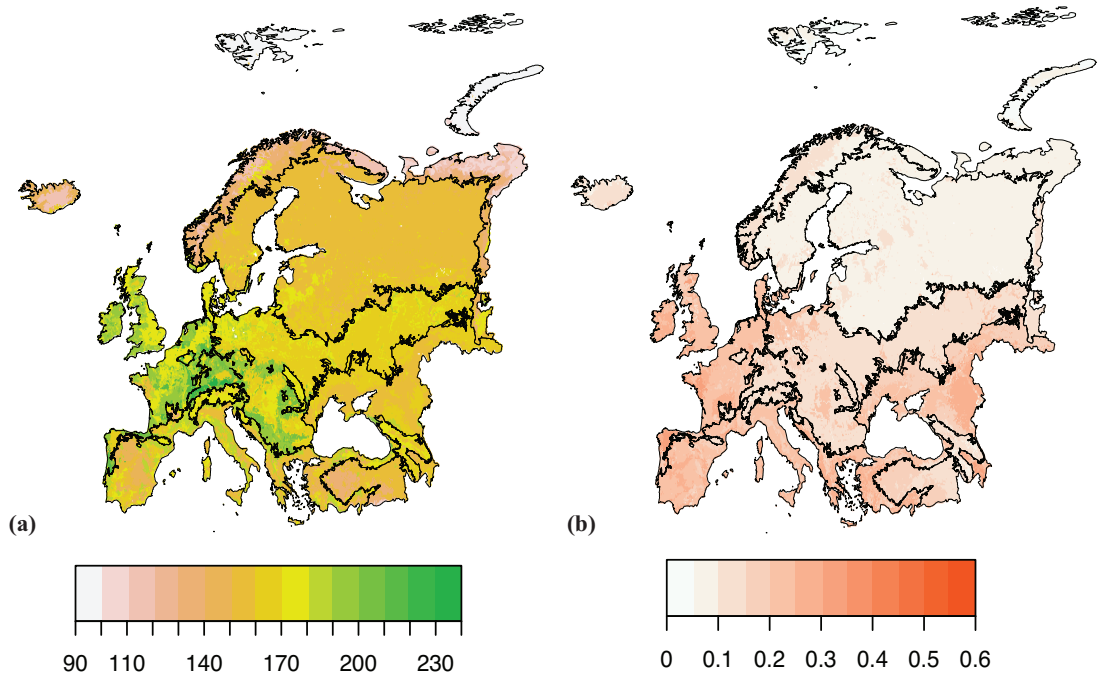

Figure 2.5 Mean GSL (a, in days) and CV (b, no unit) by landscape class, as derived from MP. LANMAP Level 1 zones borders are drawn in black. The corresponding figure for MI is in the Supporting Information section (Figure S4).

2.3.2 Inter-annual trends in Growing Season Length

We found significant trends (α=0.05) in NDVI3g-derived GSL over 18–30% of the Pan-European region (Table 2.1). Consistent with our hypothesis, both LSP derivation methods revealed an average GSL increase for the Continental, Boreal and Alpine zones (Figure 2.6). In particular, significant trends covered up to 46% and 32% of the total area of the Boreal and Continental climatic zones, respectively. For the whole of Europe, an average lengthening between 1.8–2.4 days per decade was recorded (MI method for the first, MP for the latter estimate). However, in contrast to our first hypothesis, significant GSL decreases over the past 30 years occurred in the Steppic and Atlantic climatic zones. For the Mediterranean and Anatolian zones, the two derivation methods yielded opposite inter-annual trends indicating inconsistent temporal trends in GSL over the 30-year observation period. These were also zones for which most pixels had to be either discarded or did not show a significant linear trend

over the years: only about 14–17% pixels in the Anatolian and about 7–11% in the Mediterranean zones showed significant linear trends (Table 2.1).

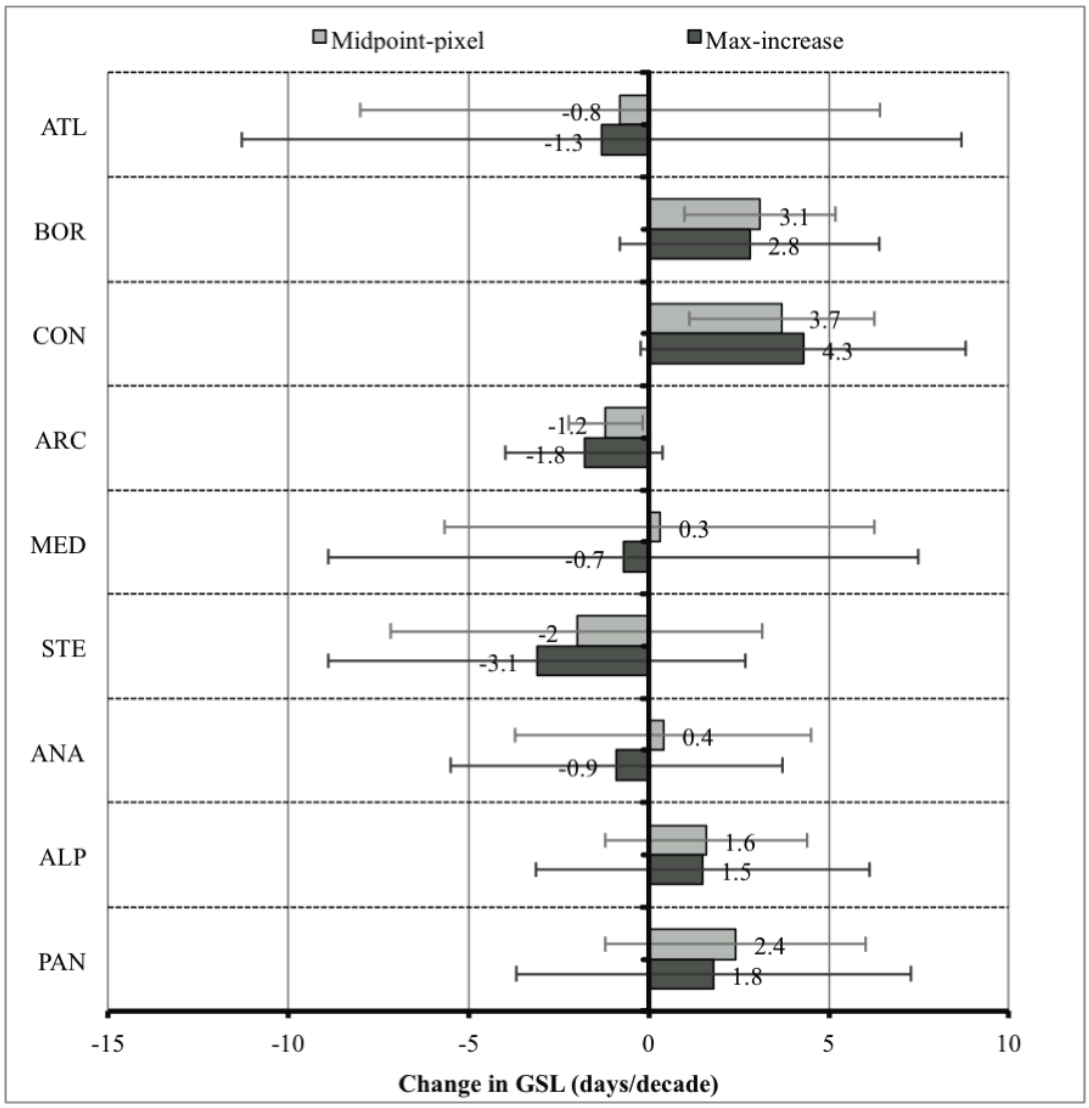

Figure 2.6 Average GSL change (in days/decade) and its standard deviation (error bars) for each climatic zone. Only pixels with trends significant at 5% were considered.

Table 2.1 Percentage of significant trends found in each LANMAP Level 1 zone.

Zone	% of pixels with significant GSL change	
	MP	**MI**
Atlantic	18	12
Boreal	46	26
Continental	32	16
Arctic	5	4
Mediterranean	11	7
Steppic	17	19
Anatolian	17	14
Alpine	16	12
Pan-Europe	30	18

Although the Boreal and Continental climatic zones showed a relatively uniform increase in GSL over the 30-years observation period (Figure 2.7a), considerable within-zone variation was found across most of Pan-Europe. The variation between landscape classes was greatest in the Atlantic, Mediterranean and Steppic climatic zones (Figure 2.7a). Looking at the spatial distribution of the significant trends that are responsible for the above-described average trends, we see that positive changes were concentrated in Southern Fennoscandia, in Western Russia, and in pockets of continental Europe (Figure 2.7b). Negative changes, on the other hand, were mostly concentrated in Western France, the Po valley in Italy and around the Caspian Sea. Among all the significant trends found (covering 18–30% of the study area depending on the LSP metric used), 69–85% were positive (for MI and MP methods, respectively). This means that 12–24% of the land surface area of Europe was characterized by increasing GSL from 1982–2011 whereas only 4–5% by decreasing GSL.

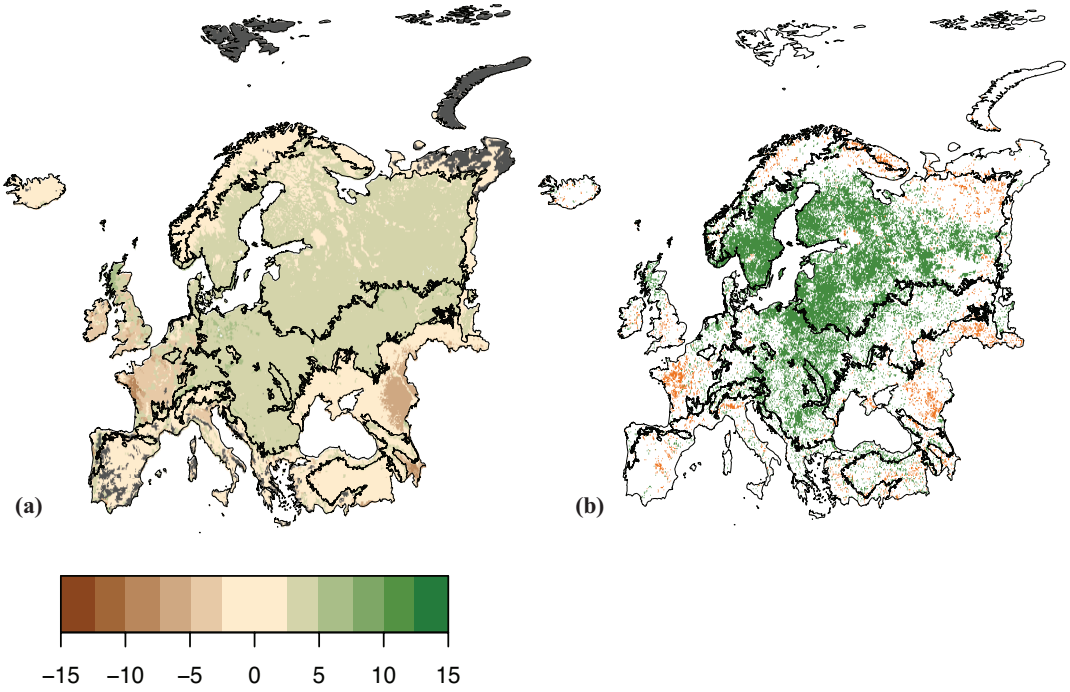

Figure 2.7 Average inter-annual linear trends in GSL (in days/decade) using the MP method, averaged by landscape class (a) and on a per-pixel basis (b). In (b), pixels with overall lengthening of the growing season are represented in green, pixels with overall shortening of the growing season are in orange. The corresponding figure as derived by the MI method is presented in the Supporting Information section (Figure S5).

Increases in GSL decline across Europe from the west to the east (Figure 2.8a) and are largest in mid-latitudes (Figure 2.8b). For the latter the MI method yielded more scattered values than did the MP method, reflecting the higher variability of results using the first of the two methods.

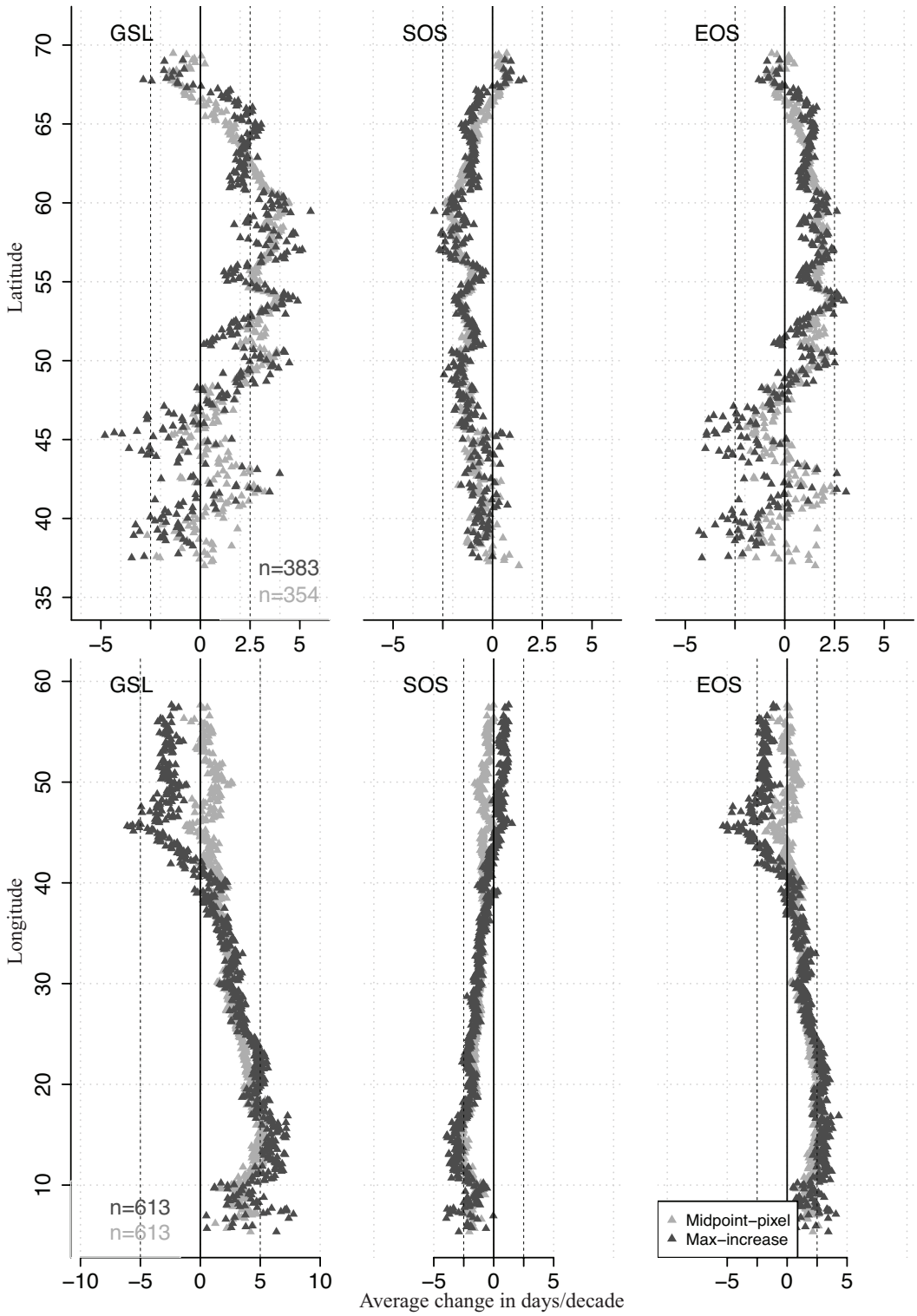

Figure 2.8 Variation in inter-annual change (days/decade) in GSL, SOS and EOS across latitude (top) and longitude (bottom) in Europe. Light and dark light grey colours represent results using the MP and MI methods, respectively.

2.3.3 Trends in green-up and senescence dates

Figure 2.9 shows the intra- and inter-annual variations in the $NDVI_{3g}$ data. For Europe in general (Figure 2.9a) the two methods to derive LSP indicators give very similar results although the SOS dates are consistently earlier with the MP than with the MI method. In the regional plots (Figure 2.9b), the contour lines indicate the high inter-annual variability in NDVI values for the Mediterranean, Anatolian, Steppic and Atlantic zones. Figure 9 and Table 2 also provide information on the attribution of a general GSL trend to changes in SOS, EOS, or both. For three zones in particular, the C-Index values are negative, indicating that EOS trends tend to be greater than SOS ones: these are the Continental, Mediterranean and Steppic zones. Also, EOS trends are more often significant than SOS ones (Table 2.2), as seen for the Anatolian, Atlantic and Steppic zones. More precisely, the strongest absolute values of the C-index are found in regions with an overall shortening growing season, namely the Steppic and Mediterranean zones. In all other zones, C-values are close to 0 or differing in sign depending on method; indicating an approximately equal contribution of SOS and EOS to the overall growing season trend identified.

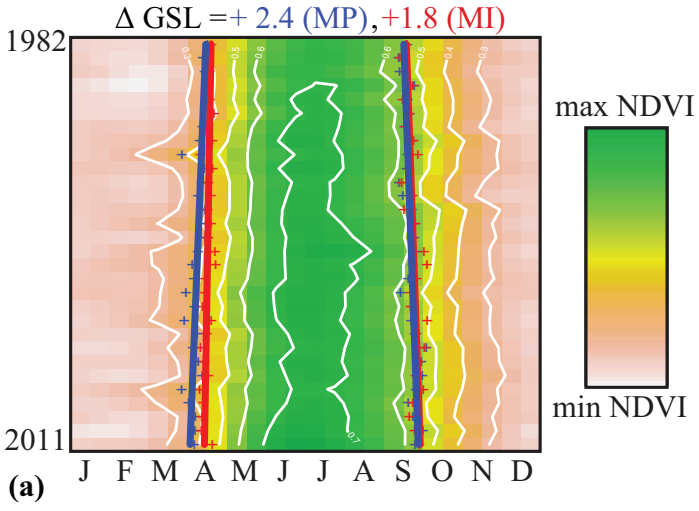

Figure 2.9 Inter-annual and seasonal variability in NDVI (a) for Pan-Europe, and (b) for each climatic zone individually. Blue and red markers indicate SOS and EOS as derived from the MP and MI methods, respectively. Solid lines represent trends significant at 5% level whereas dashed lines are not significant.

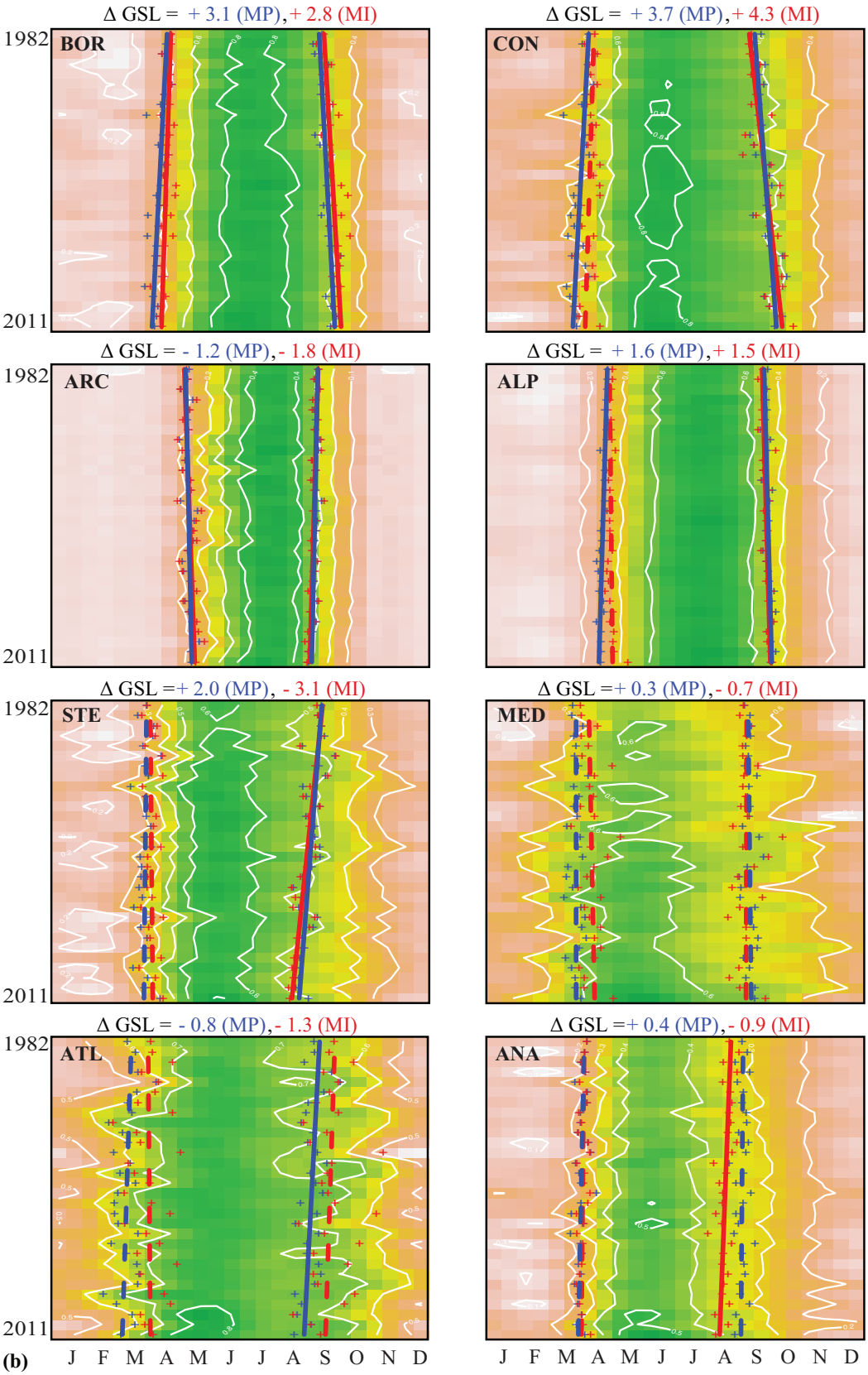

Figure 2.9 (continued)

Table 2.2 Trends in SOS and EOS (in days/decade) and C index value for each climatic zone. For all climatic zones, the first row indicates results from the MP method and the second row shows results from MI. Stars indicate statistical significance.

Climatic zone	Δ SOS	Δ EOS	C- Index
ATL	-1	-1.8 **	-0.3
	-0.8	-2.1	-0.4
BOR	-1.5 ***	+1.6 ***	0
	-1.3 ***	+1.4 ***	0
CON	-1.6 ***	+2.2 ***	-0.2
	-1.9 *	+2.4 ***	-0.1
ARC	+0.6 **	-0.6 ***	0
	+1 **	-0.8 ***	0.1
MED	-0.1	+0.2	-0.3
	-0.2	-0.9	-0.6
STE	-0.4	-2.4 ***	-0.7
	-0.1	-3.2 ***	-0.9
ANA	-0.7 *	-0.3	0.4
	-0.6	-1.5 ***	-0.4
ALP	-0.8 ***	+0.8 ***	0
	-0.8	+0.7 ***	-0.1
PAN	-1.3 ***	+1.1 ***	0.1
	-1.1 **	+0.7 ***	0.2

2.4 Discussion

After comparing results as derived from MP and MI methods, a number of conclusions on Pan-European LSP and on the trends over the past 30 years can be drawn, as discussed in detail below.

2.4.1 LSP metrics comparison

Based on the findings of White *et al.* (2009), some level of difference between LSP indicators was anticipated, and should be acknowledged. Firstly, for most climatic

zones the MI method gives a later SOS date than MP (Figures 2.3 and 2.5). This was expected, since White *et al.* (2009) found MI to be "consistently late in SOS estimation". Secondly, the MI method shows a larger year-to-year variation in SOS, and thus in EOS, estimates (Figure 2.5b). The conservative (i.e. late) SOS date estimates result in a reduced range of variation and small variations are thus easily over-emphasized. Also, by focusing on the slope of the NDVI profile, the MI method is more prone to variations in seasonal shape, compared to MP, thus leading to fewer pixels displaying significant trends (Table 2.1). Thirdly, Southern landscapes show the greatest divergence in average GSL between methods (Figure 2.4), and these latitudes (albeit for North America) were already identified as areas of high variability between LSP metrics (White *et al.* 2009). They highlighted the Mediterranean climatic zone of North America as the one where the ability of satellite methods to retrieve SOS is lowest. This is confirmed in our European study, where we find that this zone has the highest between method variability, both in terms of average GSL and the trends found, as well as highest inter-annual variation in derived GSL (highest CV in Figure 2.5) and lowest NDVI annual range (Figure 2.3). For this climatic zone, it is important to bear in mind that over 7000 pixels (i.e. more than 31% of the zone) were discarded based on the presence of two (or more) growing seasons within a single year. As shown in Figure 2A.2, excluded pixels covered large parts of Spain and Portugal. There the LSP characteristics are only partly representative of the Mediterranean zone, and particular caution must be used in their interpretation.

Despite these differences, the MP and MI methods show a generally good agreement in both the type and the magnitude of LSP changes observed (Figure 2.7 and S2.4). Although the overall number of pixels with significant trends is much lower for the MI method (Table 2.1), the distribution of the trends and the relative LSP average change per climatic zone are very similar between the two methods (Figure 2.7 and S2.4). This provides further confidence in the trends derived, and which we discuss hereafter.

2.4.2 LANMAP-dependent growing season trends

In our results, 18–30% of the total study area displayed statistically significant change in GSL. When only significant trends were considered, over 60% demonstrated a lengthening of the growing season. As hypothesized, we found an average lengthening of the growing season in Europe of 18–24 days/decade for 1982–2011. These results appear to be consistent with previous studies based on ground observations (Menzel & Fabian 1999; Ciais *et al.* 2008) and remote sensing data (Stöckli & Vidale 2004; Jeong *et al.* 2011; Eastman *et al.* 2013). Stöckli and Vidale (2004) found an average lengthening of 9.6 days/decade for the a narrower 'European domain' for 1982-2001; (Julien *et al.* 2006) highlighted Scandinavia and Western Russia as areas with significant increase in NDVI amplitude in the period 1982-1999; and a study focusing on Fennoscandia concluded that Southern areas present the greatest SOS advance of the area (Høgda *et al.* 2013). However, it is important to note that our areas of strongest growing season lengthening do not correspond to the areas highlighted by Eastman *et al.* (2013), who also used $NDVI_{3g}$. This may be explained by the fact that these zones are particularly high Leaf Area Index (LAI) areas, where – despite a significantly longer growing season – NDVI may saturate and therefore not increase the annual amplitude sought by Eastman et al. in their analysis of Fourier components.

The trends observed are spatially variable and differ considerably between both climatic zones and landscape classes, and are therefore in agreement with our second hypothesis. The Boreal and Continental climatic zones appear to have undergone the greatest average lengthening of the growing season in the last 30 years. In these zones, vegetation growth is mainly limited by photoperiod and temperature (Nemani *et al.* 2003). Various studies have reported shifts towards more favourable conditions for plant growth particularly in boreal regions, for instance by a decline in snow cover duration in the boreal forest (Goetz *et al.* 2005; Eastman *et al.* 2013), or through a 50% increase in seasonal amplitude of CO_2 observations at high latitudes since 1960 (Graven *et al.* 2013). More favourable conditions may lead to an expanded growing season, meaning a longer carbon uptake period (Metzger *et al.* 2008), and increased biomass

formation. This was put forward by Menzel & Fabian (1999), who observed a European growing season lengthening of 10.8 days from 1960-1990s, based on ground phenological observations. These areas of lengthening are mostly concentrated in Southern Fennoscandia, Western Russia and within pockets of continental Europe.

Relating to our second hypothesis, it should be noted that some areas within Pan-Europe show considerable decrease in GSL. Areas of shortening of the growing season are concentrated in Western France, the Po region in Italy and around the Caspian Sea. An average shortening of the growing season is also present over 4–5% of the Arctic zone. However, this region being most prone to HANTS-induced artefacts (de Jong *et al.* 2011), we do not discuss it here. The Mediterranean and Anatolian zones show unclear patterns – with results being strongly dependent on the method used. Southern Europe – where seasonal changes in moisture availability limit vegetation activity – is believed to be shifting towards increasingly arid and warm conditions (Julien *et al.* 2006). Moreover climate change models have indicated that the summer drought that is characteristic of Mediterranean ecosystems is likely to increase in duration and intensity with intensifying climate change (IPCC 2007; Richardson *et al.* 2013). Such a scenario is likely to translate to an earlier onset of spring that is offset by an earlier and longer-lasting summer drought period (decreasing vegetation activity).

With each pixel representing ca. 64 km^2 surface area, most European pixels represent multiple land covers, which complicates the possibility of validating derived LSP metrics with ground phenological data. The latter are mostly species-centric, whereas our LSP data represent multiple land covers in an area-averaged fashion. Moreover, although LSP is related to plant phenology via the absorption and reflectance of photosynthetically active radiation, this parameter also includes the confounding effects of soil, snow and atmosphere (Kathuroju *et al.* 2007) as well as potential non-climatic factors influencing the land surface, such as anthropogenic disturbance or fires (White *et al.* 2009). These render LSP values, particularly at this coarse scale, not directly comparable to field-derived vegetation phenology data (Badeck *et al.* 2004). Smaller-scale or land-cover specific studies have found LSP metrics

and ground-observation trends to be comparable (Hamunyela *et al.*, 2013) but at a Pan-European scale, comparison with field-derived phenological trends using ground data remains difficult.

Disentangling drivers of LSP metric change – which may be either climatic, anthropogenic or both (Evans & Geerken 2004; Yin *et al.* 2012; de Jong *et al.* 2013) – also requires further research. For instance, land abandonment in the post-Communist Eastern Europe has been widely documented in the literature (Kuemmerle *et al.* 2009), and the Po plain of Italy is known to have undergone rapid socio-economic transformations in the last 30 years (Marchetti 2002). The Fennoscandian lowlands and southern France are strongly agricultural, and therefore the shortening of the growing season observed may be linked to warming-induced shortening of the growing season (Lobell *et al.* 2011) as well as to agricultural practices. Indeed, in cultivated areas, earlier harvesting may lead to a shortening trend in our NDVI-derived growing seasons. However, the attribution of trends to their corresponding drivers remains beyond the scope of this paper.

2.4.3 Asymmetry in SOS and EOS trends

Our results show an equal or stronger association of the GSL trends with EOS delay/advance, than with SOS ones (Table 2.2). This asymmetry in SOS vs. EOS trends is an important finding because autumn trends are generally not as well documented as spring ones in the literature (Jeong *et al.* 2011; Richardson *et al.* 2013). In Figures 2.6 and 2.9, for example, we see that EOS trends dominate the GSL trends: we generally find 'delayed' autumn for those zones with overall lengthening, and advance in autumn date for those zones with an average shortening of the vegetation period. Also, EOS trends are generally stronger (deviate more from 0) than SOS trends for most climatic zones (Figure 2.6). These results highlight the importance of including EOS in LSP studies. Furthermore, two recent LSP studies (one for Northern temperate forests and another focusing on the Appalachian) have concluded that the extended length of season found since 1982 – a process initially attributed mainly to an earlier start-of-

season –may have shifted, in recent years, to a considerable delay in end-of-season (Jeong *et al.* 2011; Zhao *et al.* 2012).

In Europe, these advanced EOS dates may be simply linked to areas of land use change, or to the increasing importance of limiting factors to plant growth at the end of the season. For instance, one limit could be insufficient water availability at the end of the growing season. These hypotheses remain to be tested in future studies.

2.5 Conclusions and Outlook

In this landscape-based assessment of LSP trends from 1982 to 2011, the $NDVI_{3g}$ dataset provides us with the opportunity to document intra-annual dynamics of European LSP with an unprecedented timespan, adding almost 10 years to the so far longest European LSP study (Stöckli & Vidale 2004). Despite some marked differences, the two LSP derivation algorithms used gave various consistent results – which we summarize hereafter.

- We observe significant trends in $NDVI_{3g}$-derived growing season length over 18–30% of terrestrial Pan-Europe. These trends vary extensively both within and amongst climatic zones and landscape classes, but overall demonstrate an average lengthening of the growing season in Pan-Europe – which we quantify at 1.8–2.4 days per decade on average.
- The Continental and Boreal climatic zones have experienced significant lengthening of the NDVI-derived growing season – with hotspots in southern Fennoscandia, Western Russia and pockets of continental Europe. On the other hand, considerable shortening of the growing season was found in Western France, the Po valley in Italy and around the Caspian Sea. Although associations between these trends and land use/land cover change or shifting environmental conditions are suggested, further study and a finer spatial resolution are needed to discern the drivers of the trends observed.
- Despite more attention having been placed on SOS trends in previous studies, we find equal or stronger contribution of EOS to the overall GSL found throughout

Europe. These results highlight the importance for future LSP studies to concentrate just as much on the process of senescence as to annual green-up.

As pointed out in other studies (Atzberger *et al.* 2013; Zeng *et al.* 2013), there is a need for cross-sensor inter-calibration as a consistency check of the trends found. However, AVHRR has much broader bands than both MODIS and SPOT sensors. This fact, along with the strong differences in both spatial and temporal resolutions, means that we expect sensor choice to have considerable effect on the results found. This is indeed the case in the recent comparison by Atzberger *et al.* (2013) who found only moderately good agreement between GIMMS and MODIS over the 2002-2011 period. Finally, it would be useful to explore the consequences of the observed LSP trends on species distributions at large spatial scales. Indeed, changes in vegetation activity and phenology – as observed from NDVI – can be used to make inferences about habitat conditions, species survival, migration and composition at large scales (Pettorelli *et al.* 2005; Coops *et al.* 2013).

Acknowledgements

The contributions of MS and BS are supported by the University of Zurich Research Priority Program on 'Global Change and Biodiversity' (URPP GCB). We thank Jim Tucker and the NASA GIMMS team for providing the $NDVI_{3g}$ data for this analysis. We thank Richard Fuchs for indicating useful references relating to land cover change in Europe. We also thank the reviewers for the useful comments and feedback on the manuscript. Authors sequence is listed following the FLAE approach (doi: 10.1371/journal.pbio.0050018).

Supporting Information

2A.1 The European Landscape Map (LANMAP)

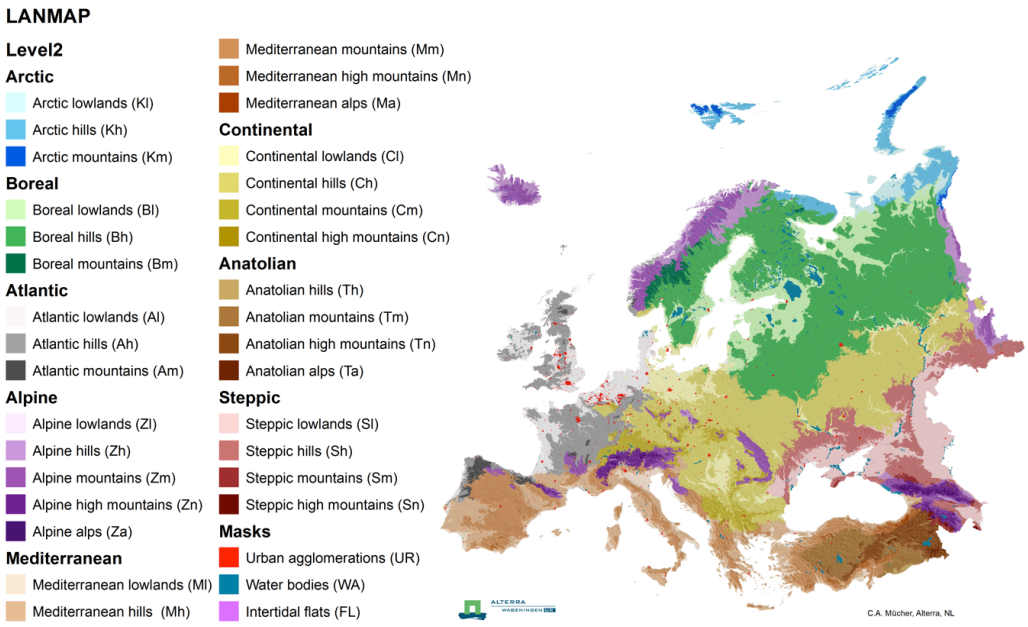

Figure 2A.1 LANMAP Level 2 classes. [Reproduced with permission from Mücher *et al.* (2010)].

2A.2 HANTS algorithm description

The HANTS algorithm (version 1.3) was implemented using IDL and ENVI software (Exelis, versions 8.3 and 5.1 respectively). An underlying assumption behind the use of this algorithm is that mathematical functions can effectively represent phenological development (Moody & Johnson 2001; White *et al.* 2009). The algorithm operates iteratively: after applying a Fast Fourier Transform (FFT), the inverse transform is used to create a supposed 'noise-free' NDVI series. The difference between the latter and the original time series is then computed. The Fit-Error-Tolerance (FET) is the absolute acceptable deviation of an NDVI value from the fitted curve, and is defined by the user. Any NDVI value for which this difference is greater than the FET is replaced with the filtered value. This operation is repeated until the difference between the two curves is lower than the threshold, for all points, or until the

maximum number of iterations (iMax) is reached. A Throw-Away-Threshold (TAT) defines the maximum number of NDVI observations that can be discarded in the fitting process.

Table 2A.1: Parameters used for the HANTS algorithm implementation

Parameter	Value
Number of yearly data points	24
Fourier frequencies	0,1,2,3
Fit Error Tolerance (FET)	0.1
Max. number of iterations (iMax)	6
Throw-Away Threshold (TAT)	10

2A.3 Multiple growing seasons mask

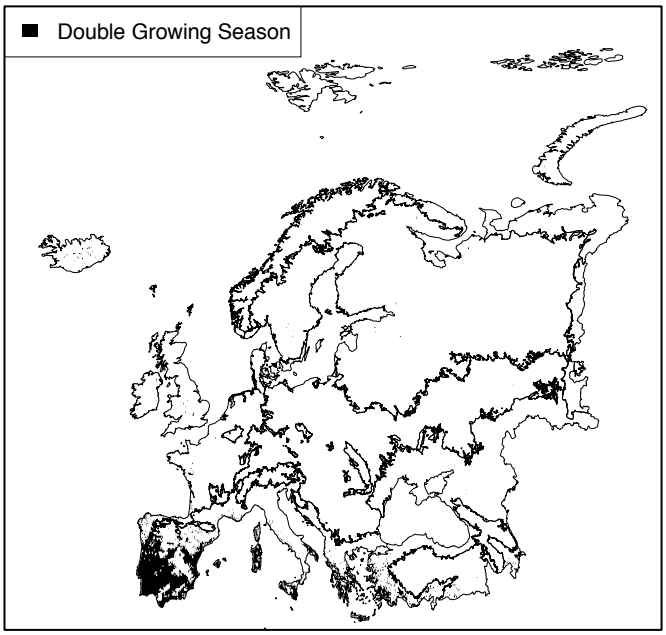

Figure 2A.2: Discarded pixels due to the presence of two (or more) growing seasons within a year. Black borders delineate LANMAP climatic zones.

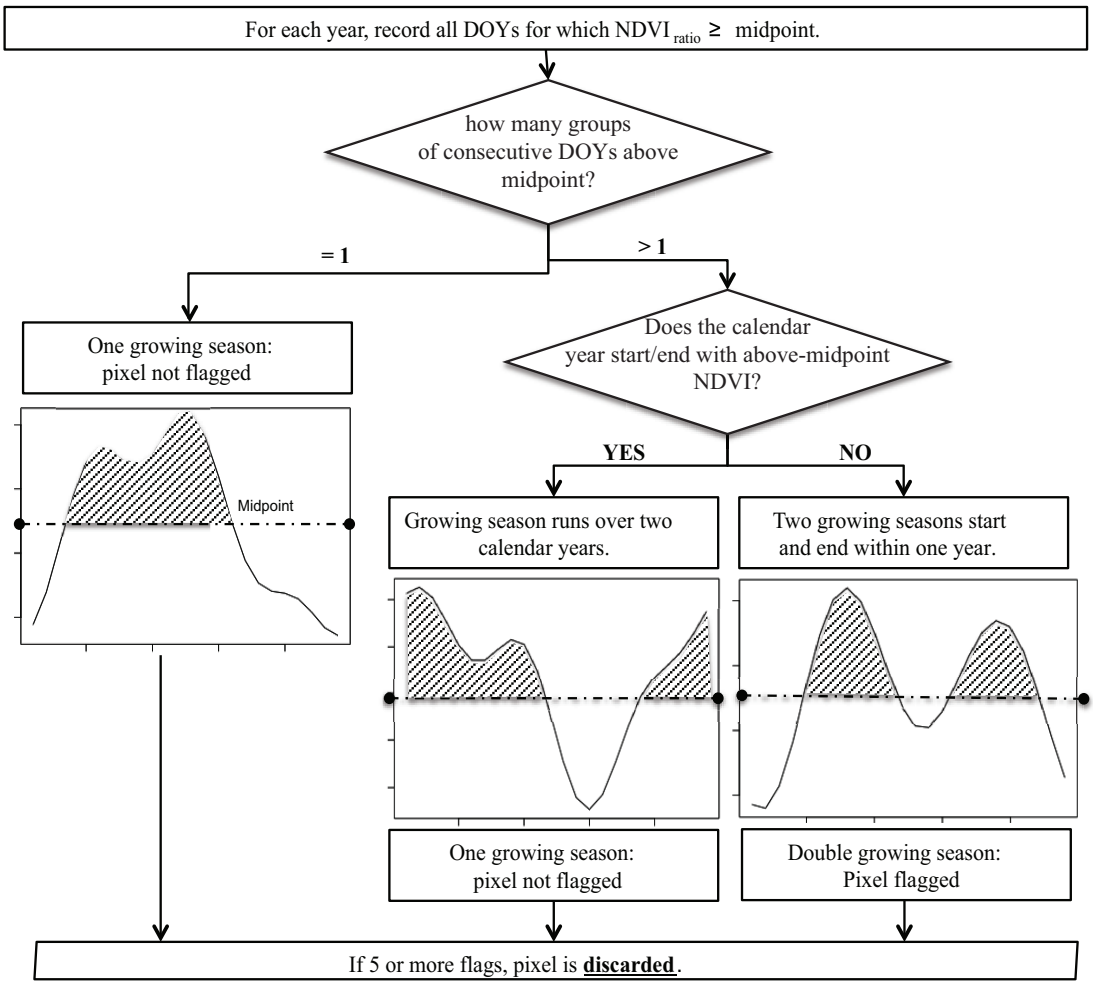

Figure 2A.3: Illustration of double growing season mask.

During LSP metric retrieval from the data, annual profiles fulfilling the following two criteria were flagged: 1) presence of more than one group of consecutive DOY above the midpoint; 2) the calendar year starts or ends with above-midpoint $NDVI_{ratio}$. For any given pixels, if 5 or more years (out of the 30) presented such a flag, then the pixel was considered to have more than one growing season, and was therefore discarded from further analysis.

2A.4 Results from Max-increase method

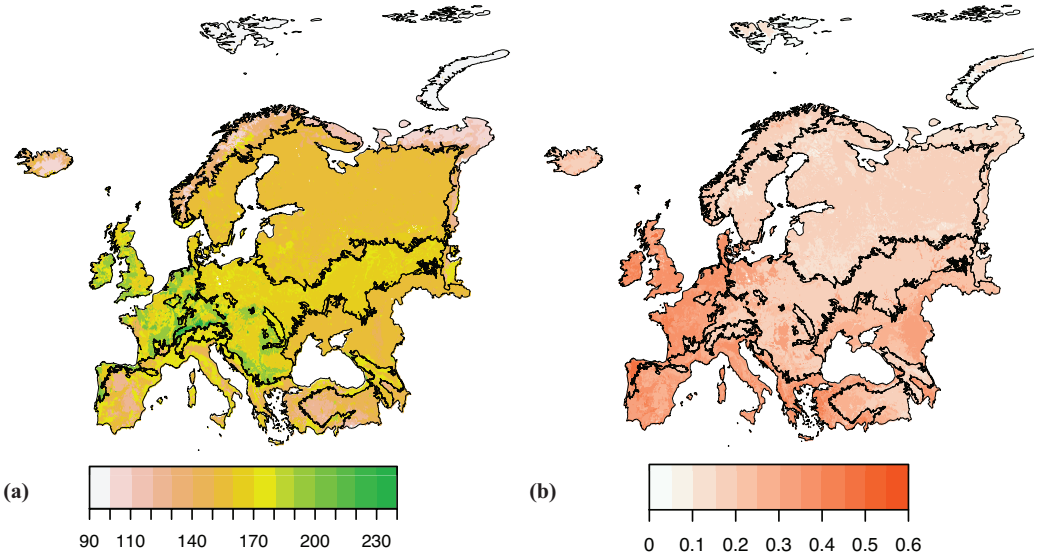

Figure S2.4: Mean GSL (a, in days) and CV (b, no unit) by landscape class, as derived from the Max-increase method. LANMAP Level 1 zone borders are drawn in black.

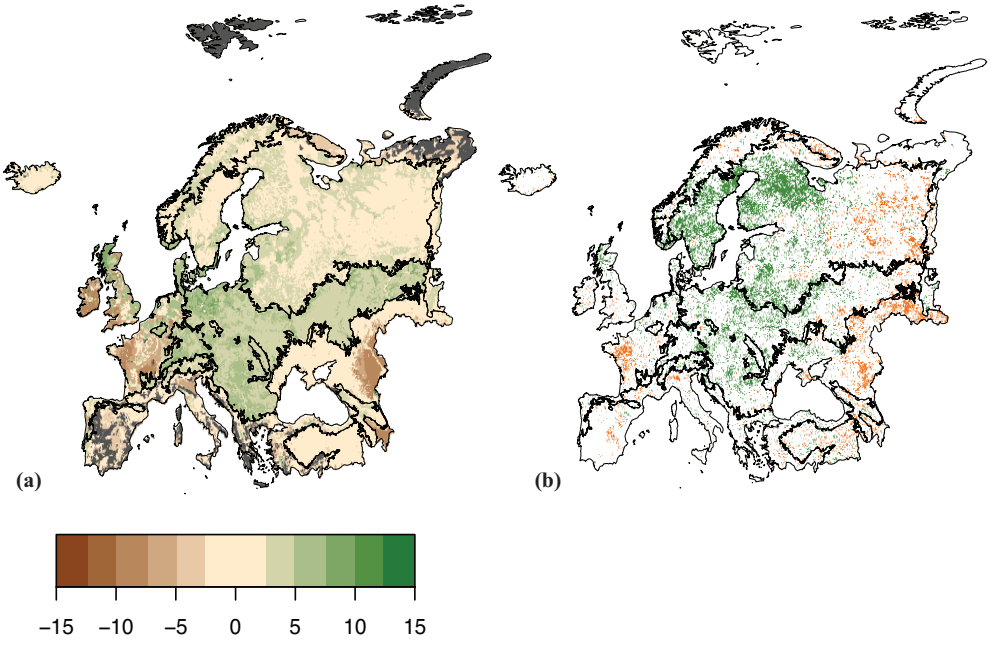

Figure S2.5: Average (linear) change in GSL (in days/decade) using the Max-increase method, averaged by landscape class (a) and on a per-pixel basis (b). In (b), pixels with overall lengthening of the growing season are represented in green; pixels with overall shortening of the growing season are represented in orange.

Chapter

3

Variability and evolution of global land surface phenology over the past three decades (1982-2012)

Garonna, I., De Jong, R. and Schaepman, M.E.

This chapter is based on the peer-reviewed article:

Global Change Biology, 2016 (22), 1456-1468

DOI: 10.1111/gcb.1316

and has been modified to list all cited references in the Bibliography chapter.

Abstract

Monitoring Land Surface Phenology (LSP) is important for understanding both the responses and feedbacks of ecosystems to the climate system, and for representing these accurately in terrestrial biosphere models. Moreover, by shedding light on phenological trends at a variety of scales, LSP has the potential to fill the gap between traditional phenological (field) observations and the large-scale view of global models. In this study, we review and evaluate the variability and evolution of satellite-derived Growing Season Length (GSL) globally and over the past three decades. We used the longest continuous record of NDVI data available to date at global scale to derive LSP metrics consistently over all vegetated land areas and for the period 1982-2012. We tested GSL, Start- and End-Of Season metrics (SOS and EOS, respectively) for linear trends as well as for significant trend shifts over the study period. We evaluated trends using global environmental stratification information in place of commonly used land cover maps to avoid circular findings.

Our results confirmed an average lengthening of the growing season globally during 1982-2012 – averaging 0.22-0.34 days/year, but with spatially heterogeneous trends. 13-19% of global land areas displayed significant GSL change, and over 30% of trends occurred in the boreal/alpine biome of the Northern Hemisphere, which showed diverging GSL evolution over the past 3 decades. Within this biome, the "Cold and Mesic" environmental zone appeared as an LSP change hotspot. We also examined the relative contribution of SOS and EOS to the overall changes, finding that EOS trends were generally stronger and more prevalent than SOS trends. These findings constitute a step towards the identification of large-scale phenological drivers of vegetated land surfaces, necessary for improving phenological representation in terrestrial biosphere models.

Authors' contributions (alphabetical order): IG, RdJ, MES designed the study and developed the methodology. IG, RdJ collected the data and performed the analysis. All authors wrote the manuscript.

3.1 Introduction

Monitoring vegetation phenology is not only important to understand the response of vegetation to a changing climate, but also to determine the feedback mechanisms that vegetation response may generate on the climate itself (Cleland *et al.* 2007; Morisette *et al.* 2009; Peñuelas *et al.* 2009). For instance, the timing and duration of vegetation activity throughout a year are central to the understanding of the variability and distribution of the terrestrial carbon sink, and the recent increase in land carbon uptake has been linked to vegetation phenology changes, in addition to CO_2 and land management effects (Schimel *et al.* 2001; Sitch *et al.* 2015).

Aside from this key role vegetation phenology plays in the carbon cycle, it is also important for modulating the intra-annual dynamics of albedo, surface roughness and water fluxes (among others). Thus, vegetation phenology is recognized as a fundamental process of biosphere-atmosphere interactions within coupled climate models (Richardson *et al.* 2013). However, accurately representing phenology in terrestrial biosphere models remains a challenge (Richardson *et al.* 2012) for a number of reasons, amongst which are the wide inter-specific and spatial variations in phenological changes that exist at plant level (Ibañez *et al.* 2010), and our limited knowledge of the physical processes that initiate leaf onset and senescence (Arora & Boer 2005). Thus, there is a need to improve our understanding of the seasonality of vegetation activity at large scales (Richardson *et al.* 2012). Large-scale phenological data may allow us to quantify the phenological responses to climate and vice versa, and thus provides the potential to bridge the gap between plant-level and modelled phenological research (Morisette *et al.* 2009).

The existing records of satellite-derived Vegetation Indices (VIs) provide an opportunity to retrospectively derive information about the phenology of vegetated land surfaces – and have given rise to the field of Land Surface Phenology (LSP; Reed *et al.* (2003)). In recent years, LSP research has increased considerably: for instance, the

number of yearly publications on LSP increased ten-fold in 10 years (2004-2014) (*Scopus*, October 2015, data not shown). Methodologies of varying complexity have been put forward to derive LSP descriptors such as Start-, End- and Length of the Growing Season (SOS, EOS and GSL, respectively) from VI time series, and commonly used approaches include threshold-based, derivative-based, and model-fitting methods (for a survey of methods, see Reed *et al.* (1994) and de Beurs & Henebry (2010)). The range of methodologies used contributes to the variation in trends reported, and the variation in LSP indicators and remote-sensing datasets used constitutes a challenge to comparing different studies.

Figure 3.1 presents reported estimates of long-term change (10 years or more) in SOS, EOS and GSL in large-scale (at least continental) latitudinal LSP studies. Generally the direction of large-scale LSP change is in agreement between studies: results generally point to a lengthening of the growing season associated with both SOS advance and EOS delay, but quantitative estimates related to large-scale trends vary considerably between studies (Figure 3.1). In particular, there is inter-decadal variation in the trends found and several recent studies have revealed the important contribution of changing senescence to overall GSL trends (Jeong *et al.* 2011; Zhao *et al.* 2012; Zhu *et al.* 2012; Garonna *et al.* 2014). Previous large-scale studies have also mostly considered the Northern Hemisphere (as illustrated in Figure 3.1), despite contrasting indications about productivity trends in the Southern Hemisphere (SH) for the last decade (Zhao & Running 2010) and despite the most commonly used sensor (AVHRR) having a global reach. In sum, the spatial and temporal coverage of existing large-scale LSP studies remains imbalanced, and the need for comprehensive global analyses of long-term changes in the seasonal patterns of VIs has already been recognized (Buitenwerf *et al.* 2015).

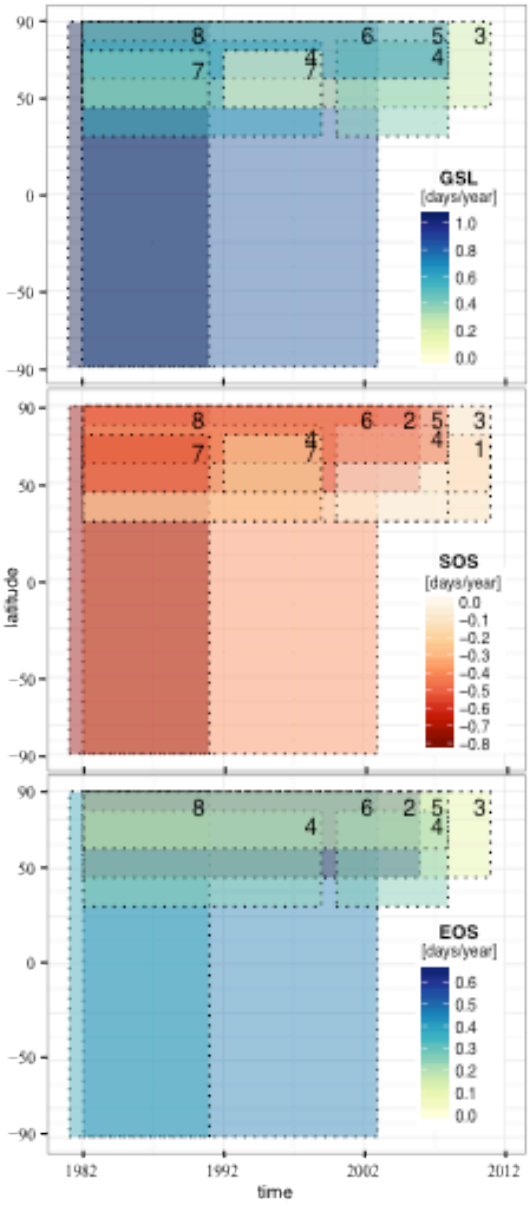

Figure 3.1 Summary illustration of trend estimates in GSL, SOS and EOS (from top to bottom, respectively) as reported in latitudinal large-scale and long-term LSP studies. The scope of each study is represented by a rectangle within the temporal and spatial scope of the present study (1982-2012, global). Each rectangle delineates the time period and latitudinal extent considered by the study, and is coloured corresponding to the trend reported. NB: The list of studies represented is not exhaustive. We selected the examples closest to a global extent, which considered at least 10 years of data and which explicitly reported quantitative estimates for LSP change. Figure 3A.1 includes results from the present study. Key: 1: Wang *et al.* (2015); 2: Jeganathan *et al.* (2014); 3: Barichivich *et al.* (2013); 4: Jeong *et al.* (2011); 5: Zeng *et al.* (2011); 6: Julien & Sobrino (2009); 7: Tucker *et al.* (2001); 8: Myneni *et al.* (1997).

In this paper, we evaluate the evolution and variability of Growing Season Length (GSL) over the past 30 years at global scale, based on an analysis of the most extensive (both in time and space) VI time series available to date. Our characterization of LSP trends of the last 30 years adds a decade to the most extensive global study in Figure 3.1 (Julien & Sobrino 2009) and pursues two main objectives: (1) identify specific bioclimatic zones where LSP change has occurred; (2) evaluate the relative contribution of Start- and End- of Season (SOS and EOS, respectively) to the overall changes. Taking into consideration the available literature on the topic, our analysis seeks to provide consistent and comprehensive estimates of large-scale LSP trends over the last 3 decades, suitable for global studies.

3.2 Data and methods

Two common descriptors of SOS, EOS and GSL were used to extract LSP metrics on annual and per-pixel bases. We examined the temporal variation of these metrics through the period 1982-2012 and interpreted existing trends using an independent global environmental stratification. This methodology is based on previous work at regional scale (Garonna *et al.* 2014), which was further developed as described in the following sections.

3.2.1 Time series of vegetation activity

The $NDVI_{3g}$ dataset is the longest continuous time series of vegetation activity presently available at global scale (Tucker *et al.* 2005; Pinzon & Tucker 2014). Two data points per month are provided at a 0.0833 degree spatial resolution. The estimated overall uncertainty is ±0.005 NDVI units throughout the AVHRR continuum (Pinzon & Tucker 2014) and negligible in comparison to the minimum annual variation we imposed in our analysis (0.1 NDVI units). This latest version ($NDVI_{3g}$) was developed

with the aim of providing a continuous and non-stationary global data record throughout the AVHRR timespan, which are particularly suitable for trend analysis (Zeng *et al.* 2013; Pinzon & Tucker 2014). $NDVI_{3g}$ has been recalibrated to improve data quality at Northern latitudes (Pinzon & Tucker 2014).

Within the $NDVI_{3g}$ record, less than 0.01% of land pixels contain values flagged as 'missing data' within their time series. Data points flagged as 'possible snow', very common at northern high latitudes, were retrieved by Pinzon & Tucker (2014) either from the average seasonal profile or from spline interpolation. We considered these values as part of the LSP seasonality of snow-affected data, and therefore did not remove them from our time series. To correct for cloud interference, however, we used each year of $NDVI_{3g}$ data (1981-2012) as input for the Harmonic Analysis of NDVI Time Series (HANTS) algorithm (version 1.3, Fast Fourier implementation (Roerink *et al.* 2000; Roerink *et al.* 2003; de Wit & Su 2005), which produces a smooth yearly curve using both Fourier analysis and an iterative flagging of outliers within the time series. We parameterized HANTS following Garonna *et al.* (2014). For the HANTS implementation as well as for all following steps, we considered calendar years (January to December) for Northern Hemisphere (NH) pixels and July-to-June NDVI time series for Southern Hemisphere (SH) pixels.

3.2.2 Extraction of LSP metrics

We used two commonly used definitions for SOS and EOS following White *et al.* (2009) and Garonna *et al.* (2014), which we call $Midpoint_{pixel}$ and Max-Increase methods (MP and MI, respectively). The MP method uses a relative threshold to define SOS: namely, SOS is the day-of-year at which the NDVI reaches half its annual amplitude in an upward direction. The MI method defines SOS as the day of maximum increase in NDVI in the year. For both MP and MI, the EOS is defined as the first day (after SOS) with an NDVI value lower or equal to the NDVI at SOS for that year. SOS and EOS are expressed in Day-Of-Year (DOY) and the GSL is the number of days between SOS and EOS within a year.

Table 3.1: Summary of quality flags used in the LSP retrieval algorithm.

Flag type	Description	Consequence
Two or more growing seasons within a year	This flag is based on the number of consecutive days of the year with an NDVI above the midpoint. For a detailed description see Garonna *et al.* (2014)	LSP metric discarded from further analysis
No distinct seasonality	Annual NDVI range of 0.1 or less	
Little/no vegetation	30-year mean NDVI is 0.1 or less	
Growing season straddling the year end	When SOS and/or EOS occur within the first/last 15 days of the year	The following year of NDVI data is considered before restarting the LSP retrieval process

We adopted the algorithm used in Garonna *et al.* (2014) and added flags in order to better account for irregularities in the growing season and to identify various cases that required special attention. Each of these flags is summarized and described in Table 3.1. Each pixel having more than 15 flagged metrics (i.e. 50% of the total available years) was discarded from further analysis.

3.2.3 Analysis of temporal variability

For each pixel, we examined trends for GSL, SOS and EOS using linear regression, and tested the significance of a non-zero slope using a t-test. Only statistically significant trends at 5% level were considered in our results. In order to shed light on multi-decadal changes in LSP, we analysed the variability in the trends in global average GSL using a 10-year moving window. In order to compare our global trend estimates with previous global studies, we further tested for significance and extent of significant trends over the 1982-1991 and 1982-2003 periods.

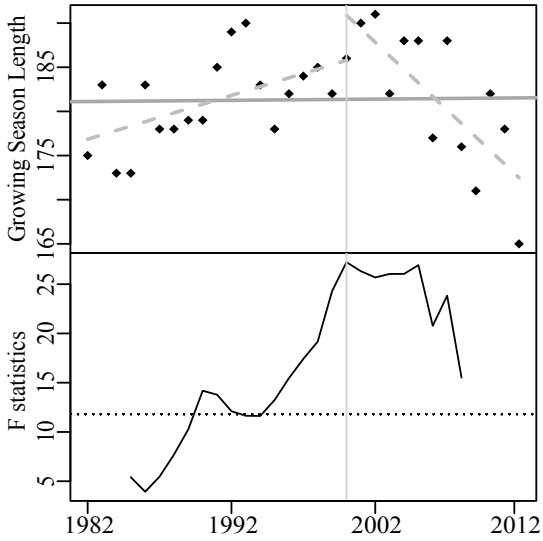

Figure 3.2 The top graph presents a sample GSL time series for 1982-2012, of a single pixel in Alaska (60.91° N, 157.58° W). The solid grey line represents the trend line under the assumption of monotonicity, whereas the dashed grey line detects a structural change in the linear regression in the year 2000. The bottom graph presents the F statistics for this time series, crossing the significant boundary line (dotted) and reaching a maximum in the year 2000.

For each GSL time series, we tested for the presence of a trend shift in the 31-year long time series by means of an F-test, which considers a potential single-shift of unknown timing in the time series (Andrews & Ploberger 1994; Hansen 2002; Andrews 2003; Zeileis *et al.* 2003). This method – illustrated in Figure 3.2 – uses an iterative procedure that minimizes the residual sum of squares to estimate the optimal break position within a specified data window. In our case, we assigned minimum segment length of 5 years before/after a breakpoint (corresponding to approximately 15% of the total time period), following suggestions of previous studies (Bai & Perron 2003; Verbesselt *et al.* 2010; de Jong *et al.* 2012). Although time series may contain more than one significant trend shift, the F-test identifies only the most relevant shift in the time series (where it exists). Where evidence for structural change in the regression coefficients was found, its timing was dated using the method of Zeileis *et al.* (2003).

3.2.4 Environmental stratification

We used the Global Environmental Stratification (GEnS) to stratify our results (Metzger *et al.* 2013b). This high-resolution bioclimate map of the Earth is available through the Group on Earth Observation (GEO) portal (http://www.geoportal.org). GEnS classifies all land areas in 125 strata, 18 environmental zones (GEnZ) and 7 biomes using multivariate statistical clustering (Metzger *et al.* 2013a; Metzger *et al.* 2013b). Its native resolution is 30 arcsec (approximately 1km^2 at the equator) in the Winkel Tripel projection (Metzger *et al.* 2013b). We rasterized and resampled GEnS to match the $NDVI_{3g}$ spatial resolution using a maximum area criterion (Verburg *et al.* 2011). In other words, the class covering the largest area within a pixel determined the pixel class attribution. An implication of this aggregation method is that the overall representation of less prevalent classes is further reduced in the resampled data (Verburg *et al.* 2011).

Examining the spatial distribution of the trends found, we considered a "hotspot" of LSP change any GEnS climatic zone with the highest proportion of significant GSL trends within it, as well as a good between-methods agreement both in terms of this proportion and in the average change estimates found (absolute difference < 0.1 days/year). To evaluate the area covered by the LSP changes found, we re-projected our results as well as the GEnS stratification to the equal-area MODIS Sinusoidal projection.

3.3 Results

3.3.1 GSL climatology for 1982-2012

Our algorithm successfully captured SOS, EOS and GSL metrics from 71% of all land pixels available at GIMMS $NDVI_{3g}$ resolution (approximately 2 x 10^6 pixels in total), thus providing annual LSP metrics for most vegetated land areas. The remaining i.e. discarded areas were the following: pixels presenting no distinct NDVI seasonality

and/or little vegetation cover represented 14% of all land pixels (in white in Figure 3.3); and pixels flagged as having two or more growing seasons during a year covered 15% of land pixels (in grey in Figure 3.3). The latter covered parts of the Amazon and central African forested areas, as well as most of Ethiopia and Somalia, Northern India, North-Eastern China, Northern Argentina and central United States.

Most of the NH presented both low Coefficient of Variation (CV) values (< 0.2) and a high proportion (>80%) of successful LSP metric extracted for each pixel from the 31 year-long $NDVI_{3g}$ time series (Figure 3.3) – indicating that the LSP metrics extracted were consistent in these regions. This was particularly true for roughly all areas > 40°N. Conversely, drylands and tropical biomes generally presented a low proportion of non-flagged observations as well as high year-to-year variability in GSL estimates (i.e. high CV values in Figure 3.3) and we considered these areas with particular caution in the interpretation of our results.

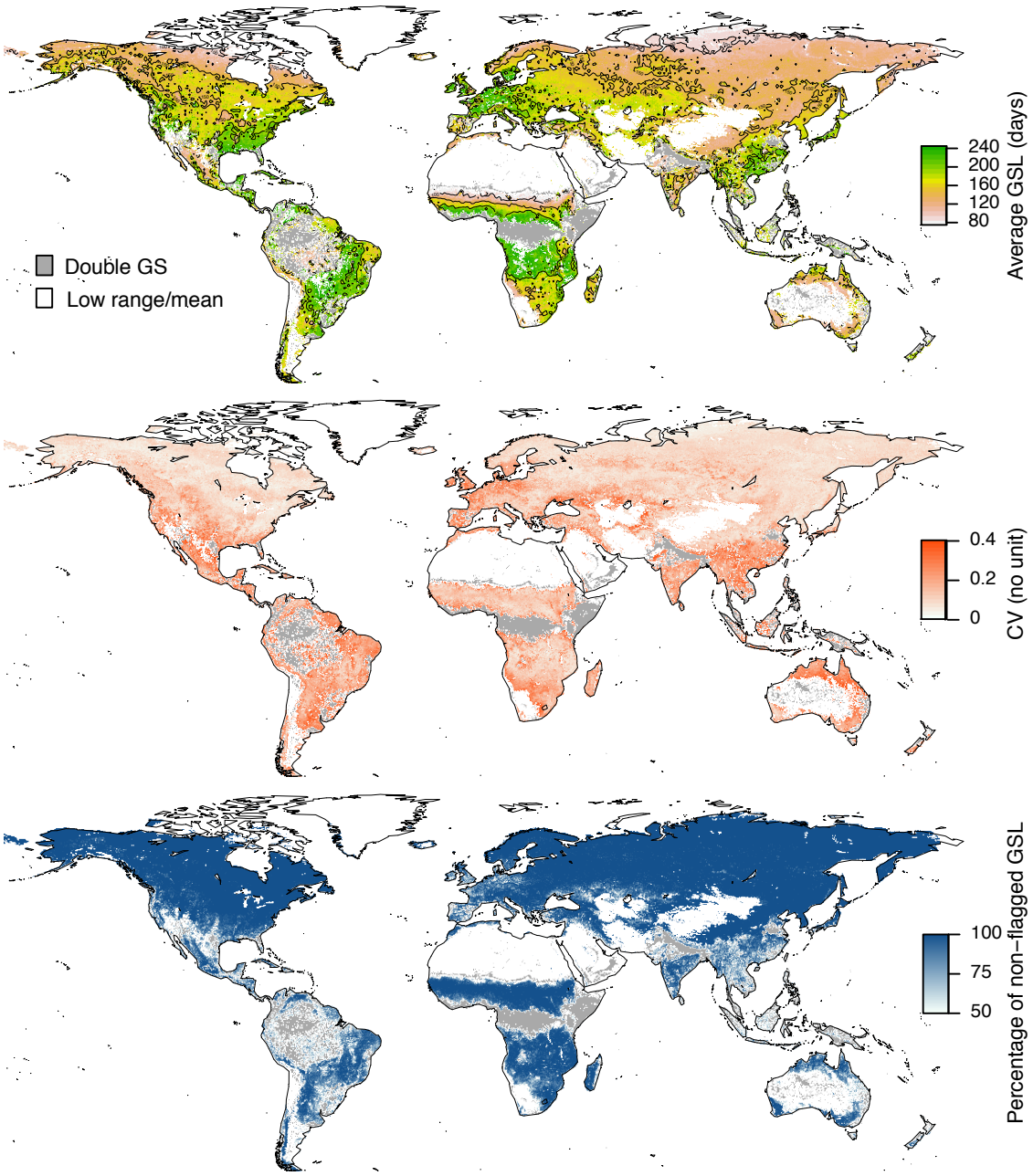

Figure 3.3 Average (top, in days), Coefficient of Variation (middle, no unit) and proportion (bottom, in %) of GSL metrics successfully extracted over 1982-2012, using the MP method. White areas represent pixels flagged as having low NDVI annual range or long-term average; grey represents pixels flagged as displaying two or more growing seasons during single years. For the top panel, contour lines represent thresholds of 100, 150 and 200 days.

3.3.2 Trends in Growing Season Length (GSL) for 1982-2012

We found significant trends (α = 5%) in GSL over 13-19% of global land areas (as derived from MI and MP, respectively). The majority of areas presenting significant trends (63% for MP and 54% for MI) exhibited a lengthening of the growing season. Globally, our results indicate an average global lengthening of 0.34-0.22 days/year (according to MP and MI, respectively). Table 3.2 presents average estimates and extent of trends over the 1981-1991 period (following the Myneni *et al.* 1997 study) and over 1982-2003 period (as the Julien & Sobrino 2009 study), as well as over 1982-2012 (entire $NDVI_{3g}$ time series). We found good agreement between our $NDVI_{3g}$-derived trends and these two global studies listed in Figure 3.1. Differences in change estimate between time periods considered indicated a pattern of decreasing magnitude in GS lengthening with increasing timespan of the study. Conversely, the total area affected by GSL change approximately doubled when considering 1982-2012 as compared to the first decade only (Table 3.2).

Results from our structural change test suggested the vast majority of significant GSL trends are monotonic. Only 3% of all pixels with significant GSL change presented evidence of structural change: these were located mostly in Eastern Siberia and Northern Canada, where the most frequent timing of the estimated shifts in GSL were the early 2000s and the 1990s, respectively. However, analysing the variability in the trends of global average GSL using a 10-year moving time window, we observe a lower and even reversed trend in the 2000s, both using the MP and MI metrics.

Table 3.2: GSL trend estimates relative to two previous studies at global scale.

Time period	Average GSL trend (days per year)		Area covered by trends (in % of global land areas, MP/MI methods)
	Reported in previous study	This study (MP / MI methods)	
1981-1991	+1.09 (Myneni et al., 1997)	+1.13 / +1.01*	8 / 7
1982-2003	+0.8 (Julien & Sobrino, 2009)	+0.61 / +0.67	14 / 10
1982-2012	-	+0.22 / +0.34	13 / 19

*= the closest available time period was used i.e. 1982-1991.

GSL trends varied greatly with environmental zone (Figures 3.4 and 3.5). GS lengthening was found within the "Cold and Mesic" and "Cool, Temperate and Dry" zones spanning across boreal Eurasian and North America, as well as in a large part of the "Extremely Hot and Xeric" zone, particularly in the Sudano-Sahelian region and in large parts of India (Figure 3.4). On the other hand, GS shortening was found mostly in the "Extremely Cold and Mesic" zone across N. America and Siberia. Finally, shortening was also found in small strata in central Asia as well as in Northern Argentina, Southern Australia and North-Eastern China. Figure 3.5 presents both the average change estimates found per environmental zone (as derived from both methods), as well as the zonal distribution of the GSL trends found. We found greater disparity between methods in dry areas i.e. all zones qualified as "arid", "xeric" or "dry" and "extremely hot" areas, as opposed to "wet", "moist" and "mesic" zones which tended to have closer trend estimations. The MI method led to fewer significant trends overall, as well as higher trend averages per zone (Figure 3.5).

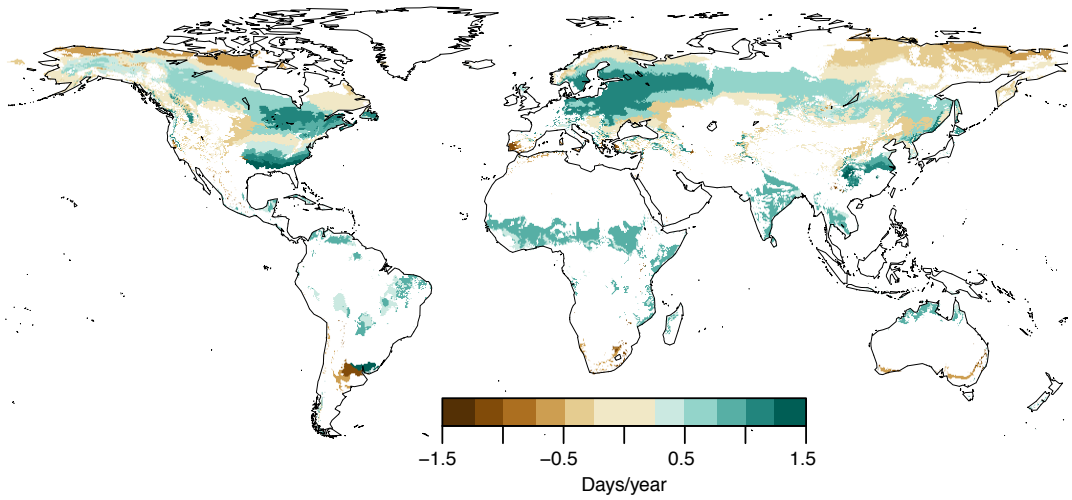

Figure 3.4 Average linear trends in GSL (in days/year) using the MP method, averaged by environmental stratum. Only significant trends (α = 5%) are considered. Environmental strata for which less than 20% of the area displayed significant trends are left white. The corresponding map as derived from the MI method is presented in Figure 3A.2 in the SI section. Also, the per-pixel distribution of GS lengthening and shortening is presented in Figure 3A.3.

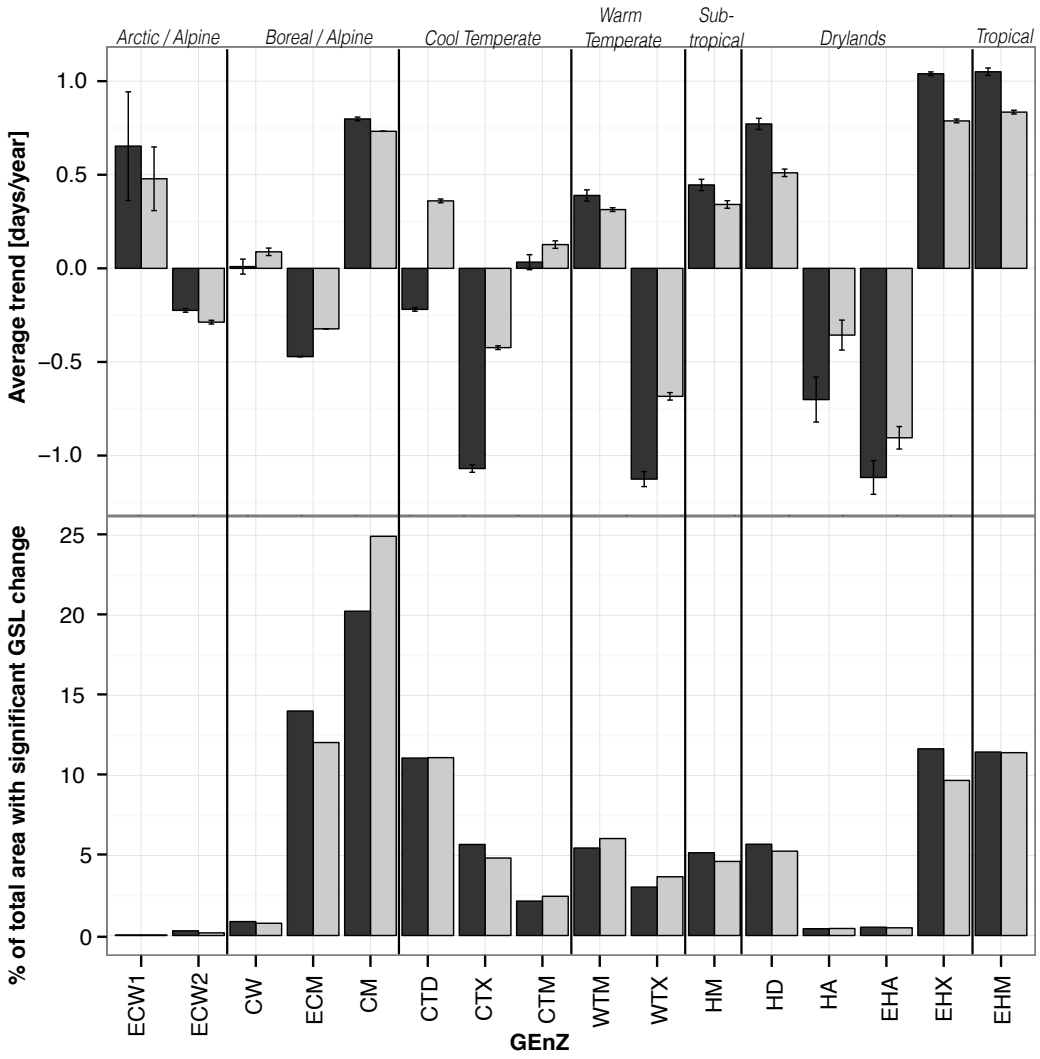

Figure 3.5 Average GSL trend and standard error (in days/year, top) and distribution of significant (α = 5%) GSL trends (in % of total area, bottom panel) by Global ENvironmental Zone (GEnZ), as derived by the MP and MI methods (in light and dark grey colour, respectively). Biome names are indicated at the top. Zones are abbreviated as follows: ECW1: "Extremely Cold And Wet 1"; ECW2: "Extremely Cold And Wet 2"; CW: "Cold And Wet"; ECM: "Extremely Cold And Mesic"; CM: "Cold And Mesic"; CTD: "Cool Temperate And Dry"; CTX: "Cool Temperate And Xeric"; CTM: "Cool Temperate and Moist"; WTM: "Warm Temperate And Mesic"; WTX: "Warm Temperate And Xeric"; HM: "Hot And Mesic"; HD: "Hot And Dry"; HA: "Hot And Arid"; EHA: "Extremely Hot And Arid"; EHX: "Extremely Hot And Xeric"; EHM: "Extremely Hot And Moist". The two Arctic environmental zones were discarded from the figure because of missing LSP data.

Significant GSL trends were found in each environmental zone and biome, but there was large variation is the area displaying change as well as in the magnitude of the trends found for each zone and biome. We found the "Boreal/Alpine" zone to contain the largest area of change found by both methods i.e. more than 1/3 of the total area. Within this biome, the "Cold and Mesic" zone – covering a long latitudinal belt around Eurasia and North American continents – stands out for its large area of change (approximately 20% of the total) – regardless of the method. Also, MI and MP methods agreed again on the strong positive GSL trend across this zone (on average, 0.73-0.8 days/year) as well as on the large proportion of this zone displaying significant trends (up to 37% of this zone, Figure 3.5). As such, the "Cold and Mesic" zone appeared as a 'hotspot' zone of GSL change.

Other zones displaying considerable areas of change (>10% of total) were: the "Extremely Cold and Mesic" zone – which showed GS shortening of up to 0.5 days/year across a wide area covering Pan-Arctic lands, and was characterized by an average shortening of the GSL of -0.32 and -0.47 days/year (MP and MI, respectively; Figure 3.5); the "Cool, Temperate and Dry" zone, the "Extremely Hot and Xeric" and the "Extremely Hot and Mesic" zone. All environmental zones mentioned are illustrated in Figure 3A.4 in the Supplementary Information (SI) section.

Figure 3.6 illustrates the variation in mean GSL with time for the "Cold and Mesic" zone as well as for all land areas taken together. The MP and MI methods showed a very similar pattern in inter-annual GSL variation, with R-squared values of 0.82 and 0.91 for the "Cold and Mesic" and global times series (Figure 3.6). The between-method structural difference in global GSL estimates was 7.29±0.73 days, but was only of the order of ~1-2 days for both the "Cold and Mesic" zone (Figure 3.6).

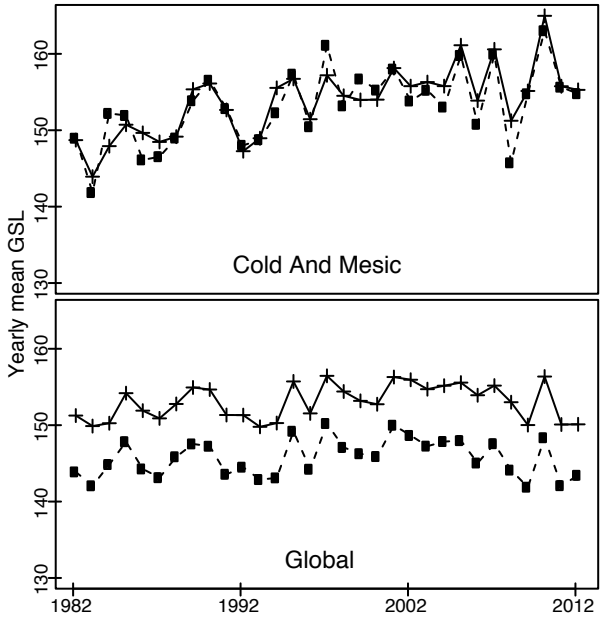

Figure 3.6 Time series of average global $NDVI_{3g}$-derived Growing Season Length (GSL) for 1982-2012, using both MP and MI methods (solid and dashed lined, respectively), for the "Cold and Mesic" zone (top panel) and for all land areas ("Global", bottom panel).

3.3.3 Inter-annual variation and trends in SOS and EOS

Figure 3.7 presents the seasonal and inter-annual variation in global NDVI, SOS and EOS over the study period. Similarly to the overall GSL results (previous section), the year-to-year variations in SOS and EOS at global scale were consistent between MP and MI methods (Figures 3.6), although the MP method led to consistently later SOS than the MI method both in each environmental zone individually and globally (Figure 3.7 and Figure 3A.5 in SI). We found that, when averaged globally, both SOS and EOS underwent significant trends over 1982-2012 (α = 5%, Figure 3.7). The global EOS trend was stronger than the SOS equivalent: the global EOS delay was +0.22 / +0.26 days/year (MI and MP estimates, respectively), compared to -0.02 / -0.08 days/year of SOS change (Table 3.2).

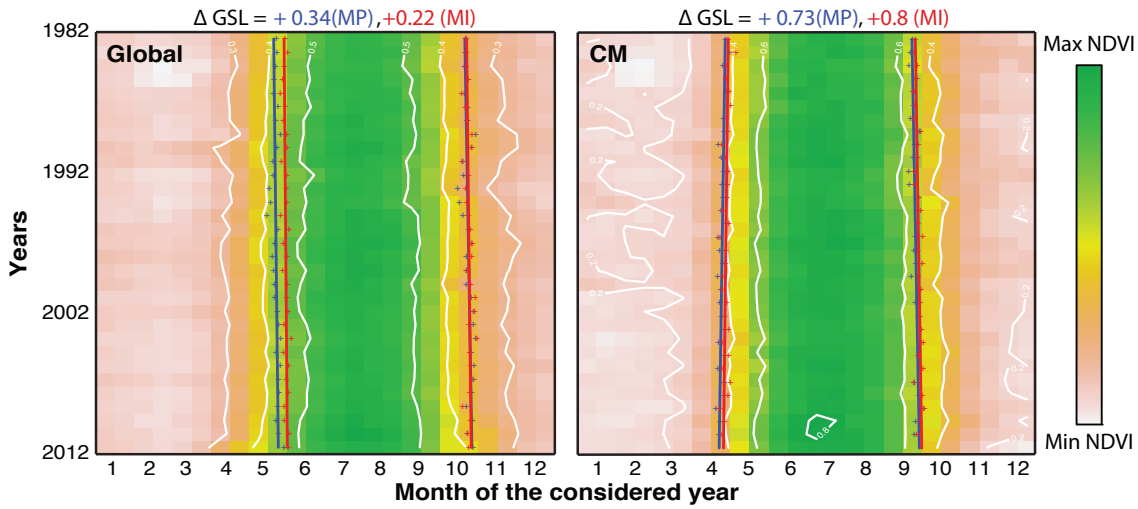

Figure 3.7 Seasonal and inter-annual variability in NDVI, SOS and EOS for global land areas (left panel) and the "Cold and Mesic" zone (CM, right panel). Markers indicate yearly average SOS and EOS values and lines represent trends (significant at 5%), as derived from the MP (blue) and MI (red) methods. Contour lines indicate average NDVI values. Quantitative estimates for the average GSL trend are expressed at the top of each plot in days/year. Calendar years (January-to-June) are used for Northern Hemisphere pixels; June-to-July are used for Southern Hemisphere pixels.

The per-pixel distributions of SOS and EOS trends are presented in Figure 3.8. Regardless of the method used, we found significant advances in SOS over most of the boreal and continental Pan-Europe, parts of central Asia as well as central China (Figure 3.8a). On the other hand, significantly delayed SOS was found over parts of the mid-Western United States and in North-Eastern Argentina. Most of the Pan-Arctic showed an advanced EOS, whereas a delayed EOS was visible over most of the Northern boreal belt – mainly concentrated around the Baltic Sea, Eastern Canada and in the Sudano-Sahelian region (Figure 3.8b). EOS trends covered 13-21% of the land surface (MI and MP estimates, respectively), and were thus more widespread than SOS trends, which covered 9-14% of the land surface (MI and MP methods, respectively).

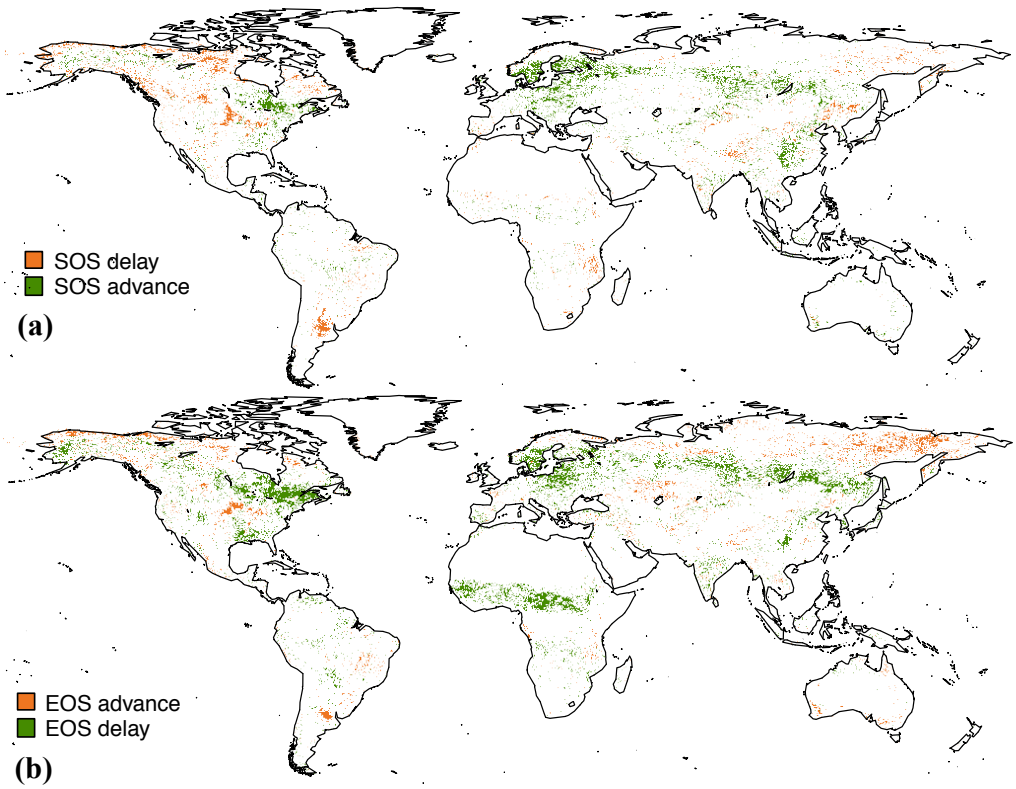

Figure 3.8 Spatial distribution of SOS (a) and EOS (b) trends (significant at $\alpha = 0.05$) contributing to significant GS shortening (orange) and lengthening (green), using the MP method. The corresponding figure as derived from the MI method is presented in the SI section (Figure 3A.5).

3.4 Discussion

Examining the variability in the phenology of land surfaces globally and over the last 30+ years (as derived from $NDVI_{3g}$) reveals substantial spatial variation in GSL, SOS and EOS trends. Over 1/3 of areas with significant GSL change were found over the "Boreal/Alpine" biome. Yet within this biome are two environmental zones with contrasting GSL evolution. In the following discussion we examine more closely our findings and their implications, and highlight key areas for further research.

3.4.1 A global GSL climatology for 1982-2012

Numerous studies in the last decade have revealed a recent increase in carbon uptake by vegetated land areas (Schimel *et al.* 2001; Poulter *et al.* 2014; Sitch *et al.* 2015), in parallel with marked vegetation 'greening' across vast areas of the Earth's surface (de Jong *et al.* 2011). Our global study of LSP trends contributes to this field of research, in that it provides a recent climatology of intra-annual vegetation dynamics, consistently and at global scale. Indeed, the gradients of average GSL seen in Figure 3.3 reflect the spatial variation in the vegetation's seasonal carbon uptake.

We found both dryland and tropical biomes to have high year-to-year variability in GSL estimates throughout the study period (Figure 3.3). In tropical areas, however, the high variability in LSP metrics is unlikely to reflect actual land surface processes. Intense and persistent cloud cover together with dense canopies – where the NDVI signal saturates – are two characteristics of the evergreen tropics that may lead to irregular $NDVI_{3g}$ profiles and thus to the low proportion of LSP metrics successfully extracted over our 31-year-long study analysis (as seen in Figure 3.3). For drylands, however, the high GSL variability is in agreement with the findings of Zhang *et al.* (2014), who relate this to the high year-to-year variation in soil moisture as compared to temperature. Rainfall-driven systems tend to have much more variable phenological cycles (Hein *et al.* 2011), as for instance in Australia, where shifts in peak timing of more than 1 month may be found (Broich *et al.* 2014). High GSL inter-annual variability may thus indicate a moisture limitation of the vegetation.

3.4.2 Shifting global LSP dynamics

Our average GSL change estimates using $NDVI_{3g}$ were comparable with the two other global LSP studies using AVHRR data when considering the same time periods (Julien & Sobrino, 2009; Myneni et al., 1997; Table 3.2). Our GSL trend estimate for 1982-2012 represents a slower GS lengthening than indicated by previous (shorter-spanning) studies (Figures 3.1 and 3A.1, Table 3.2). The multi-decadal differences in average GSL change estimate (Table 3.2) as well as the varying rate of global change

found when performing a 10-year moving-window regression indicate that global GS lengthening has not occurred at a regular pace over the past three decades. In particular, the decreasing rate found in GS lengthening between the 1990s and the 2000s suggests that the 'global growing season' has lengthened, but at a decreasing rate. This indication evokes the slowing-down hypothesis previously put forward by Jeong *et al.* (2011) for SOS in temperate regions of the NH, whereby average GSL change estimates went from +0.56 days/year for 1982-1999 to +0.39 days/year for 2000-2008. Interestingly this appears to contrast with the results from our structural change tests: these qualified most GSL trends as monotonic and are in agreement with a recent study on shifts or abrupt changes in SOS, which also concluded that linear models were best suited to explain trends over most of the NH (Wang *et al.*, 2015). Further analyses at regional scale are needed to ascertain this aspect in view of seemingly contrasting indications from different sources. However, it is likely that the few observations (31 data points) available from the present observational record as well as the considerable year-to-year variability found in GSL estimates (Figure 3.3, Figure 3.6) are important hindrances to the statistical derivation of structural change in our LSP time series.

Understanding the relative contribution of shifting SOS and EOS towards the GSL trends found is a key first step towards the understanding of large-scale drivers of LSP variability. Given varying physical processes driving SOS and EOS, leaf phenology coupled to LSP corresponds better to vegetation greenness during SOS, while greenness is not an optimal predictor for EOS. Our results indicate that the overall GS lengthening for 1982-2012 may increasingly be attributed to an EOS delay. Long-term trends in EOS were both more extensive and stronger globally than those of SOS. This highlights the importance of shifting autumn events in studying large-scale phenological change, despite their being relatively understudied as compared to spring events (Gallinat *et al.* 2015). The between- and within-species asynchrony in leaf senescence, the complex mix of drivers involved and the lack of a precise definition for EOS are some of the challenges involved in studying leaf senescence at large scales (Gallinat *et al.* 2015; Panchen *et al.* 2015). Indeed, amongst the LSP studies reviewed in

Figure 3.1, only two (Julien & Sobrino 2009; Jeong *et al.* 2011) highlighted the important contribution of senescence timing to GSL changes at large scale. At regional or smaller-scale, studies have increasingly put forward the study of autumn leaf phenology as key for better explaining variations in productivity. For instance, a study using eddy covariance measurements reported that changes in autumn leaf phenology better explained the variation in annual net ecosystem productivity at Harvard Forest over 1992-2008 than spring phenology (Wu *et al.* 2013). Following research efforts will examine attribution of LSP change to large-scale drivers at global scale, independently for SOS and EOS.

3.4.3 The "Boreal/Alpine": predominant biome of LSP change (1982-2012)

MP and MI showed good agreement on the spatial distribution of significant LSP trends – albeit with some differences in the average trend estimates (Table 3.2, Figures 3.5 and 3.6). Both methods found more than 1/3 of all trends found within the "Boreal/Alpine" biome of the Northern Hemisphere (NH). This distribution suggests that intra-annual vegetation dynamics are mirroring global warming over this period – which has been twice as fast as the global average in this region (IPCC 2007; Scheffer *et al.* 2012; IPCC 2013). The consequences of these changes for the boreal carbon sink remain to be further studied. Indications are that the boreal (and arctic) carbon-climate feedbacks could be disproportionally large (Schimel *et al.* 2015).

The fact that the "Boreal/Alpine" biome has relatively little anthropogenic presence and hence, direct pressure on vegetated lands (Ellis & Ramankutty 2008) suggests that these LSP changes may be primarily climate-driven. Increased vegetation activity (i.e. greening), increasing air temperatures and reduced snow cover duration (Brown 2000; Dye 2002) have already been associated with a longer GS in these areas (Bogaert *et al.* 2002; Alcaraz-Segura *et al.* 2010). Undoubtedly snow cover duration plays a large role in this biome's LSP dynamics for two main reasons. Firstly, snow cover influences vegetation physiology and phenology through the micro-climate, soil hydrology and geochemistry (Walker *et al.* 2001). Secondly, the reflectance of snow

being very high at optical wavelengths (Pomeroy & Brun 2001), the presence of numerous and repeated snow-affected satellite observations leads to a characteristic sharp rise/drop in NDVI at the first/last snow-free retrieval and make snow presence a major determinant of the land surface seasonality (Dye 2002). For the "Boreal/Alpine" biome, 10% of the raw $NDVI_{3g}$ time series on average (1982-2012) were flagged as "possibly snow". We therefore consider shifts in snow cover duration as a probable main driving factor of LSP change in this biome. This is in agreement with a previous study comparing the spatial and temporal patterns among snow-cover and the NDVI trends in northern Eurasia (1982-1999), and linking the derived "greening" trends both to more favourable conditions for growth (through rising temperatures) and to declining snow-cover effects on NDVI (Dye & Tucker 2003). A promising step forward for the study of vegetation dynamics in this region is the reconstruction of long-term AVHRR NDVI time series that aim to correct for the effect of confounding abiotic factors such as snow or bare soil, such as presented in Zhang (2015). However, the presence of snow within an AVHRR pixel does not rule out that vegetation may be active. It is therefore difficult to exclude snow contamination to some extent, particularly at large spatial scales and in a boreal biome.

Within the boreal biome, the "Cold and Mesic" and the "Extremely Cold and Mesic" environmental zones display the most significant large-scale changes in LSP (Figure 3A.4). Interestingly, these two zones have contrasting average trends in GSL: the "Cold and Mesic" zone is where the most extensive rapid lengthening of the GS has occurred between 1982-2012; and the "Extremely Cold and Mesic" zone has undergone widespread shortening during the same period. On one hand, our results reveal the "Cold and Mesic" zone – covering broadly boreal forest areas at 50-65°N – as a hotspot of LSP change, because it encompasses the largest area of GSL change whilst displaying close agreement in the trend estimates found between methods (Figures 3.5 and 3.6). This has particular relevance in view of examining shifts in large-scale climatic phenological controls over this area, and testing the links between these observed LSP trends and their potential climatic drivers. Both SOS and EOS trends appear to contribute to this GS lengthening found, which we estimated at ~0.7

days/year on average. Trend estimates for this environmental zone relied on a full time series for the three decades i.e. no special flag appeared as illustrated in Figure 3.3, adding confidence to the idea that this region is a global hotspot of LSP change.

On the other hand, the boreal "Extremely Cold and Mesic" zone – showed an opposite overall trend in GSL over the period 1982-2012. Negative GS trends were widespread in this zone (Figure 3.4). However, different processes stand out between North America and Eurasia: whilst both SOS and EOS appear to have contributed to the negative GSL changes in North America, the East Siberian GSL trend appeared to be driven mostly by an earlier senescence (Figure 3.8). A recent small-scale study in Alaska highlighted that the increasingly abundant shrubs are transforming the landscape phenology of many tundra areas, and that these tend to have an earlier onset of senescence compared to evergreen/graminoid canopies (Sweet *et al.* 2015). The "Extremely Cold and Mesic" zone is also where we found two large-scale structural change areas: Canada (in the 1990s) and Eastern Siberia (post-2000). These continental differences contribute to on-going discussions. Browning trends have been identified in boreal North America from a variety of VI datasets (e.g. $GIMMS_g$, $GIMMS_{3g}$, SeaWiFS, SPOT-VGT and MODIS in Guay *et al.* (2014), as well as greening trends in boreal Eurasia including Eastern Siberia (de Jong *et al.* 2011; Dutrieux *et al.* 2012; Guay *et al.* 2014). Chen *et al.* (2014) identified a turning point in the late 1980s in North America, and Buermann *et al.* (2014) found that the accelerated summer warming without an accompanying increase in summer precipitation for the period 1970-2000 in Siberian boreal forest may have led to declining vegetation growth since the mid-1990s. The attribution of the Eastern Siberian GSL trend to an EOS change mostly appears to be in agreement with Barichivich *et al.* (2013), who found that the spring green-up has kept up with the pace of warming in Northern biomes (>45° N), whereas leaf senescence delay has not, because of limiting factors such as light and moisture.

It is unclear whether the (slow but significant) shortening of the GS we identified for the "Extremely Cold and Mesic" is linked to a shift to a negative response of vegetation growth to increasing temperatures from the mid-1990s onward, as

suggested by Buermann *et al.* (2014); or to a cooling trend as identified over the last decade in western North America and Eurasia by both *in situ* and remotely-sensed temperature and sea ice extent data (Bhatt *et al.* 2013); or to large-scale transformation of the landscape because of increasing deciduous shrubs. Overall, a number of co-occurring climatic and vegetation changes appear to be at play over this area and need to be further explored (Urban *et al.* 2014; Park *et al.* 2015). Overall, our results highlight LSP change in an area that is already an important research focus for climate change science. This is not only because of the magnitude of environmental changes occurring in boreal areas (IPCC 2013) but also for the multiple atmosphere-biosphere feedbacks to be considered (Pearson *et al.* 2013). For instance, as thawed soils release greenhouse gases (Parmentier *et al.* 2013) and as the albedo decreases with Arctic greening, studies have pointed to a potential switch of Pan-arctic tundra from a carbon sink to a carbon source.

3.4.4 Limitations and outlook

It is generally agreed that no method is consistently superior for deriving LSP metrics for global applications (Reed *et al.* 2003; Atkinson *et al.* 2012). We chose HANTS based on previous assessments showing its ability to represent the intra-annual variability of GIMMS NDVI data (de Jong *et al.* 2011). An important known limitation to this algorithm is its weaker ability to reproduce abrupt NDVI rise/fall upon snow melt/fall compared to – for instance – a double logistic fit (Beck *et al.* 2006). It is therefore important to state that our choice of a common and consistent approach for the entire globe comes at the cost of it not being equally adapted to all biomes. Given our indication of the "Boreal/Alpine" biome as a major region of LSP change, future studies focusing on this biome should take this limitation into account.

Finally, despite the usefulness of studying LSP trends for understanding phenological patterns consistently and a variety of scales, it is important to reiterate that vegetation phenology and land surface phenology remain related yet distinct. LSP incorporates the effects of soil and snow (Kathuroju *et al.* 2007) as well as

anthropogenic disturbance or fires (White *et al.* 2009). Upscaling ground phenological information to an $NDVI_{3g}$ pixel footprint requires taking into account not only interspecific variation in phenological state – which may be important (Gill *et al.* 2015; Panchen *et al.* 2015), but also the influence of the entire landscape on the NDVI (Fisher *et al.* 2006). That is why establishing a relationship between NDVI-derived metrics and plant-physiological events remains a challenge (D'Odorico *et al.* 2015). Steps forward in this direction are important and on going, particularly through the development of webcam observation networks as well as through the upscaling of field observations to landscape level (Liang & Schwartz 2009; Hufkens *et al.* 2012).

Acknowledgements

The study has been conducted in the framework of the University of Zurich Research Priority Program on 'Global Change and Biodiversity' (URPP GCB). We thank Jim Tucker and the NASA GIMMS team for providing the $NDVI_{3g}$ data for this analysis. We are grateful for the support of the Functional Genomics Center Zurich (FGCZ) of the University of Zurich in processing the data. In particular, we thank M. Hakateyama, H. Rehrauer and K. Shimizu. We are grateful to B. Schmid for discussions on the methodology and the interpretation of our results, and for suggesting useful references for this manuscript. We thank G. Schaepman-Strub for discussions on phenology studies in the Pan-Arctic region.

Supporting Information

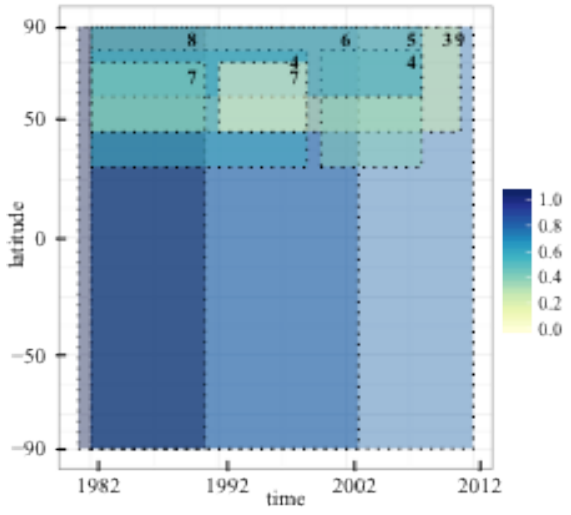

Figure 3A.1: Accompanying figure to Figure 3.1, illustrating the temporal and spatial scope of each study GSL trend estimate, including the present one. *Key*: **3**: Barichivich *et al.*, 2013; **4**: Jeong *et al.*, 2011; **5**: Zeng *et al.*, 2011; **6**: Julien & Sobrino, 2009; **7**: Tucker *et al.*, 2001; **8**: Myneni *et al.*, 1997; **9**: Present study.

Table 3A.1 Reported average trends, the sensor used and the broad type of LSP metric definition for each study of Figure 3.1.

♯	Reference	Sensor	Type of SOS/EOS definition	Period	Region	Reported average change (per year) in		
						SOS	EOS	GSL
1	Wang et al. (2015)	AVHRR, MODIS, SPOT	Derivative-based	1982-2011	30°-75°N	-0.14	×	×
2	Jeganathan et al. (2014)	AVHRR	Derivative-based	1982-2006	>45° N	-0.58	0.64	×
3	Barichivich et al. (2013)	AVHRR	Threshold-based	1982-2011	>45 °N	-0.11	0.09	0.22
4	Jeong *et al.* (2011)	AVHRR	Threshold-based	1982-1999	30-80° N	-0.29	0.24	0.56
				2000-2008		-0.02	0.25	0.39
5	Zeng et al. (2011)	MODIS, AVHRR	Threshold-based	1982-2008	> 60° N	-0.47	0.16	0.63
6	Julien & Sobrino (2009)	AVHRR	Model fitting	1982-2003	Global	-0.38	0.45	0.8
7	Tucker *et al.* (2001)	AVHRR	Model fitting	1982-1991	45°N – 75°N	-0.56	×	0.39
				1992-1999		-0.21	×	0.05
8	Myneni *et al.* (1997)	AVHRR	Threshold-based	1981-1991	Global	-0.73	0.36	1.09

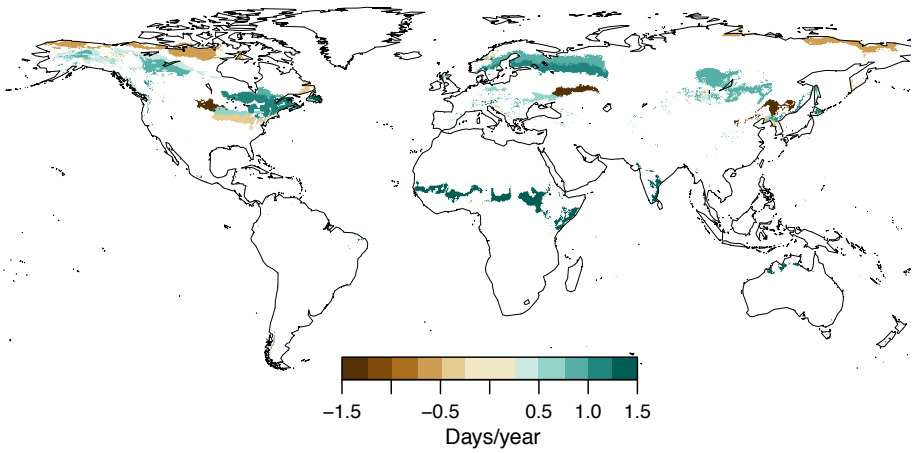

Figure 3A.2 Average linear trends in GSL (in days/year) using the MI method, averaged by environmental stratum. Only significant trends (α = 5%) are considered. Environmental strata for which less than 20% of the area displays significant trends are left white.

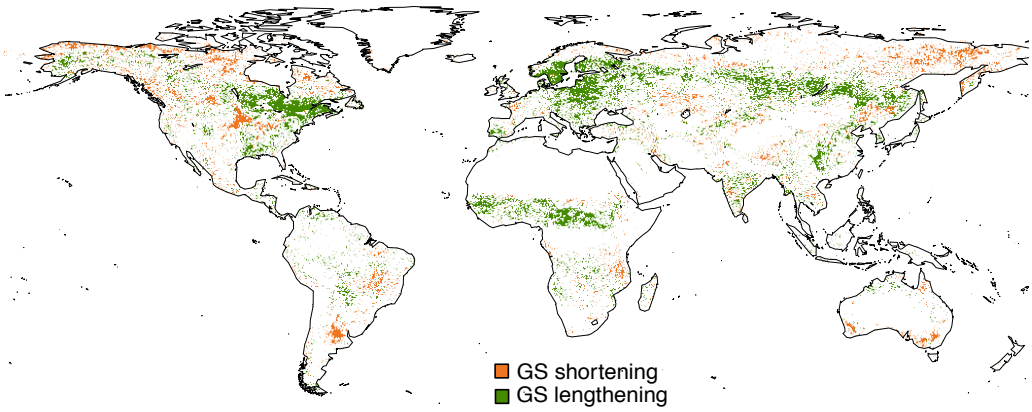

Figure 3A.3 Spatial distribution of significant trends (at 5%) in GSL, on a per-pixel basis as derived from the MI method. Pixels in orange had an overall shortening of the Growing Season (GS), and pixels in green appeared to have undergone lengthening of the GS.

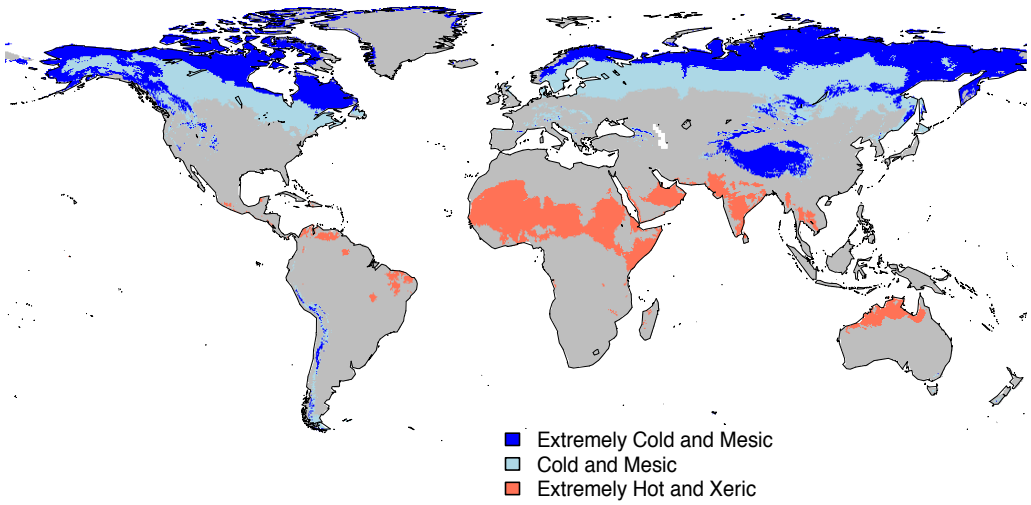

Figure 3A.4 The distribution of the "Extremely Cold and Mesic" (dark blue), the "Cold and Mesic" (light blue) and the "Extremely Hot and Xeric" (orange) environmental zones, according to the Global Environmental Stratification (Metzger *et al.* 2013b).

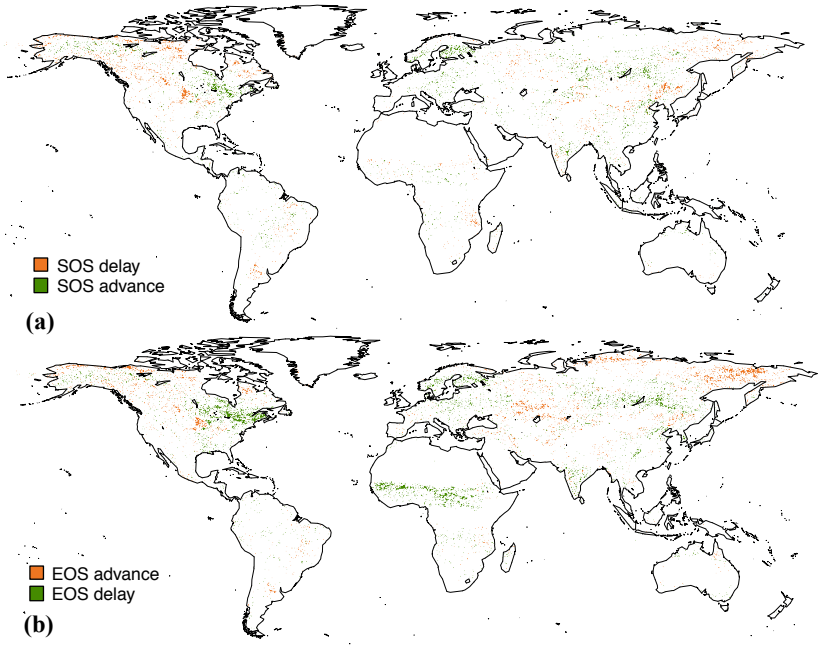

Figure 3A.5 Spatial distribution of SOS (a) and EOS (b) trends (significant at α = 0.05) contributing to significant shortening (orange) and lengthening (green) of the GS, using the MI method.

Chapter

4

Linking land surface phenology and climatic constraints shifts over the past three decades

Garonna, I., de Jong, R., Stöckli, R.,

Schenkel, D., Schimel, D., Schmid, B.

and Schaepman, M.E.

This chapter is based on the article:

"Increasing importance of moisture constraint on land surface phenology over the last 30 years", to be submitted.

It has been modified to list all cited references in the Bibliography chapter.

Abstract

Land-Surface Phenology (LSP) not only responds to climatic factors, but also influences the climate system through various feedback mechanisms, and is thus an important constituent of Terrestrial Biosphere Models (TBMs). Despite LSP being used as a global change indicator, the effects of climatic change on LSP depend on the relative importance of climatic constraints in specific regions and are not well understood globally.

Analysing a global phenology reanalysis in combination with a remotely sensed LAI product, we examined three climatic constraints to canopy greenness at Start- and End-Of-Season (SOS and EOS, respectively) over the last three decades. Specifically, we quantified the photoperiod, evaporative demand and minimum temperature constraints at SOS and EOS globally, and considered their evolution over the 1982-2010 period.

Our analysis revealed significant trends in the relative importance of climatic constraints in the temperate and boreal biomes, ranging from 1 to 8% during the study period. We found a widespread decrease in the influence of minimum temperature at SOS and EOS, with spatially heterogeneous shifts towards moisture and photoperiod constraints. Overall, the relative importance of the moisture constraint increased considerably over the study period, with the strongest signal at EOS and within temperate zones. Furthermore, we discuss key differences in the distribution of climatic constraints between SOS and EOS, which are often not reflected in TBMs.

Authors' contributions (alphabetical order): IG, RdJ designed the study. IG, RdJ, MES developed the methodology. IG, RdJ, RS collected the data. IG, RdJ, DSchenkel, RS performed the analysis. All authors wrote the manuscript.

4.1 Introduction

Vegetation phenology modulates the hydrology and the energy balance of the Earth's surface through for instance changes in evapotranspiration, soil moisture, albedo and surface roughness (Richardson *et al.* 2013; MacBean *et al.* 2015). In turn, vegetation phenology is largely regulated by climatic conditions, and in particular by three main drivers: temperature, moisture and radiation (Cleland *et al.* 2007; Körner & Basler 2010). This strong role in the seasonal atmosphere-biosphere exchanges of energy, carbon and water makes phenology an important component of Terrestrial Biosphere Models (TBMs).

In recent years, remote sensing has greatly contributed to the study of leaf phenology, complementing traditional phenological observations with wall-to-wall information on the phenological status of vegetated land surfaces. This has been done largely through the analysis of time series of Vegetation Indices (VIs), from which metrics such as the timing of Start-, End- and the Length- of the Growing Season (SOS, EOS and GSL, respectively) can be derived at a variety of scales (Reed *et al.* 2003). Various studies reported large-scale shifts in Land Surface Phenology (LSP) metrics, in particular over the Northern Hemisphere boreal and temperate zones (Myneni *et al.* 1997; Julien & Sobrino 2009; Garonna *et al.* 2016). For these regions, *in situ* observations (Parmesan & Yohe 2003; Menzel *et al.* 2006) and remote sensing studies (Myneni *et al.* 1997; Tucker *et al.* 2001) found an advance in spring timing that correlated with increasing temperature. More recently, studies have also found strong shifts in leaf senescence timing over the last three decades and put forward the need for a better understanding of autumn processes (Jeong *et al.* 2011; Estiarte & Peñuelas 2015; Gallinat *et al.* 2015).

Despite the increasing availability of phenological data, it is recognized that the representation of phenology in TBMs needs improvement (Richardson *et al.* 2012; Delpierre *et al.* 2016). A comprehensive evaluation using long-term AmeriFlux and

Fluxnet-Canada measurements reported consistent over-prediction and bias in GSL from a number of models (Richardson *et al.* 2012); leading to a considerable over-estimation of modelled gross ecosystem photosynthesis. Migliavacca *et al.* (2012) found model prediction errors to be predominantly caused by driver uncertainty rather than inaccurate parameterization. Thus, improving our understanding of what climatic factors govern the phenology of the land surface is critical for estimating both the impact of climate change on productivity and the feedback mechanisms of vegetation activity to climate (Zhu & Meng 2014).

In this paper, we examined three climatic constraints on foliar phenology at global scale and tested for temporal trends over the past three decades. We focused on three meteorological drivers on observed phenological variability: incoming radiation, evaporative demand and minimum temperature. Our aim was to elucidate their respective influence on SOS and EOS over 1982-2010 and to answer the following questions: (i) what is the spatial distribution of climatic constraints on SOS and EOS?; (ii) have these constraints decreased or increased over the past 30 years?; and (iii) has the relative importance of each climatic constraint on SOS and EOS changed, and how? Our approach involved the use of a modelled global phenology dataset combined with remotely sensed observations to disentangle the influence of these three climatic constraints. Given the LSP trends identified at global scale in previous studies (Garonna *et al.* 2016), we expected climatic constraints to have significantly shifted over the past three decades, with repercussions on the relative importance of these constraints in many areas of the world and with potential implications for the modelling of phenology at global scale.

4.2 Data and methods

4.2.1 Time series of Leaf Area Index (1982-2010)

Two global Leaf Area Index (LAI) datasets (one remotely sensed, one modelled in response to climate) were used in combination for the period 1982-2010. The first is LAI_{3g} (Zhu *et al.* 2013), which was developed using a neural network based approach on the third generation Normalized Difference Vegetation Index non-stationary dataset (Pinzon & Tucker 2014) and Terra Moderate Resolution Imaging Spectroradiometer (MODIS) fraction of Photosynthetically Active Radiation (fAPAR) and LAI products. LAI_{3g} was used to represent 'observed' (through remote sensing) LSP metrics at global scale for the past 3 decades.

The second LAI dataset is the Global Phenology Reanalysis (Stöckli *et al.* 2011) and is referred to as LAI_{re} in this paper. All details concerning the reanalysis development and assessment are provided in Stöckli *et al.* (2011). To produce LAI_{re}, empirical parameters were used in combination with European Centre for Medium-Range Weather Forecast (ECMWF) ERA-Interim data in a prognostic mode. The empirical parameters were optimized using a data assimilation framework based on an Ensemble Kalman Filter (EnKF) with satellite-based observations from MODIS (Stöckli *et al.* 2011). Various studies already demonstrated the usefulness of such an approach to model seasonal leaf dynamics globally (Stöckli *et al.* 2008; MacBean *et al.* 2015). These data describe leaf development in response to climate and were thus chosen to represent 'climatically-induced' LAI. One advantage of this reanalysis is that, instead of simulating specific events of leaf development, it describes simulated temporal development of canopy greenness through LAI; which is directly comparable to LAI_{3g}.

We aggregated the LAI_{3g} dataset from its native spatial resolution of 1/12 degrees to the LAI_{re} 1/2 degree resolution, using the areal mean and omitting no-data pixels. Additionally, bi-monthly time steps of LAI_{re} were extracted to coincide with the temporal resolution of LAI_{3g}. For both datasets we considered only the overlapping

record i.e. 1982-2010. In a first step, we compared LAI time series from both datasets, finding overall good agreement between them for most areas of the world (Supporting Information Section 4A). This provided us with confidence that the modelled LAI_{re} can reproduce within- and between- year LAI dynamics as observed in the remotely sensed dataset, and that the two datasets can be used in combination in the next steps of our analysis.

4.2.2 Three climatic constraints to phenology

The model predicting LAI in the reanalysis employs the Growing Season Index (GSI), a bioclimatic index summarizing climatic constraints on leaf development (Jolly *et al.* 2005). Daily GSI (iGSI) is calculated as the product of three indices of phenological response to time aggregated climatic states, as follows:

$$iGSI = iT_{Min} \times iVPD \times iPhoto \quad (4.1)$$

where iT_{Min}, iVPD and iPhoto are the daily phenological responses to time aggregated minimum temperature (T_{Min}), vapour pressure deficit (VPD) and photoperiod (Photo) constraints, respectively. These indices are normalized to range between 0 and 1, with lower values signifying a higher limitation to foliar growth (Jolly *et al.* 2005). Combined with structural parameters and embedded in a prognostic LAI state calculation, the GSI drives LAI_{re} intra-annual variations. Stöckli *et al.* (2011) parameterized the light, moisture and temperature requirements of 35 Plant Functional Types (PFTs) by minimizing the cost function of globally predicted versus MODIS-observed LAI. The rationale behind this is that that each PFT has an optimal set of climatic states suitable for photosynthesis. Then, ECMWF ERA-Interim data (Berrisford *et al.* 2009) were used to re-analyse (by use of the prognostic LAI model combined with ensemble data assimilation of MODIS data) LAI on a daily basis for each grid-cell, taking into account the fractional cover of PFTs within the cell (Stöckli *et al.* 2011). Figure 4.1 illustrates a yearly time series of iTmin, iVPD, iPhoto, iGSI and LAI_{re} data for grid cell in Siberia.

We extracted annual GSI time series for all land pixels, and converted these to a simple indicator of the daily constraint imposed by climate on foliar growth. We refer to this metric as Climatic Constraint (CC), calculated on a daily basis as follows:

$$iCC = 1 - iGSI \qquad (4.2)$$

The iCC also ranges from 0 to 1, with 1 indicating no climatological constraint to photosynthesis and 0 representing climatic conditions that are completely constraining to vegetation activity. For each of the three GSI components, we derived the corresponding constraint index. This is calculated as:

$$iCC_{VPD} = 1 - iVPD \qquad (4.3)$$

where iCC_{VPD} is the daily constraint corresponding to iVPD. iGSI and iPhoto were calculated using the same approach.

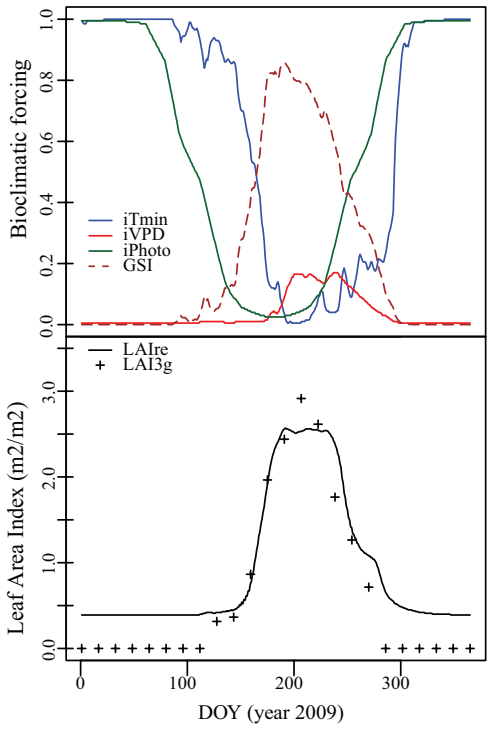

Figure 4.1: Illustration of the reanalysis data for a grid-cell in Siberia (65°N, 84°E). DOY stands for Day-of-Year. Climatic forcing and GSI data are presented in the top panel. The lower panel presents the resulting LAI_{re} and LAI_{3g} observations for the same location, at 0.5 degree spatial resolution.

4.2.3 Extracting SOS and EOS metrics (1982-2010) from LAI3g

We derived Start- and End- of Season metrics (SOS and EOS, respectively) for each year of LAI_{3g} data at native spatial and temporal resolution. We chose LAI_{3g} as a basis for LSP metrics extraction because these data represent observed (albeit through remote sensing) vegetation dynamics. SOS and EOS are both expressed in Day Of Year (DOY). Noise filtering methodology and LSP metric extraction algorithm are the same as described in Garonna *et al.* (2016). We selected the commonly used $Midpoint_{pixel}$ method for defining SOS, whereby SOS is the first day of the year when LAI is greater than its midpoint during the year (i.e. half the annual range) (White *et al.* 2009). Calendar years (January to December) were considered for Northern Hemisphere pixels, and July-to-June years were considered for Southern Hemisphere pixels. In order to restrict our analysis to the most reliable LSP estimates only, we discarded all pixels displaying either very small LAI annual range, more than one growing season during the year or pixels for which the growing seasons straddled two years. The identification of these pixels as well as their geographical distribution are described in Garonna *et al.* (2016).

4.2.4 Quantifying the Climatic Constraint (CC) on SOS and EOS

We quantified CC on SOS and EOS as the sum of daily CC indicators over the pre-season, for each pixel and each year. The pre-season is defined as a period of 21 days before SOS (EOS) day, as derived from LAI_{3g}. In other words, total CC was calculated as:

$$CC_T = \sum_{T-21}^{T} iCC \qquad (4.4)$$

with $T = \{SOS, EOS\}$ as derived from LAI_{3g}. In previous attempts to establish a relationship between SOS (EOS) and climatic factors, a variety of pre-season durations were used, ranging from 1 to 5 months (Liu *et al.* 2016a). Here, we selected a pre-season duration of 21 days based on the mean averaging time for VPD and T_{min} used in Stöckli *et al.* (2011) for all PFTs as well as and given the smoothing window length applied in

Jolly *et al.* (2005). These were themselves selected in order to buffer the GSI and the modelled phenology against short-term meteorological events or changes in environmental conditions. While we acknowledge that the pre-season duration is likely to vary between biome and by climatic constraint considered, we preferred one consistent approach for all situations (more information in SI 4B).

We examined trends in CC_T over the study period for each pixel, in order to test whether climatic constraints over the modelled LAI_{re} increased or decreased during the study period. Where CC_T trends were statistically significant, we considered the sign (not the magnitude) of the linear regression slope as indicative of improved (negative slope / decreasing CC_T) or worsened (positive slope / increasing CC_T) climatic conditions over time. The magnitude of this slope factor was not considered as scientifically meaningful given the nature of the three indicators. We also calculated the Relative Importance (RI) of each climatic indicator (named Z) to the overall constraint on SOS and EOS i.e. irrespective of CC_T. This was calculated as:

$$RI_Z = \frac{1-\sum_{T-21}^{T} 1-iZ}{CC_T} \times 100 \qquad (4.5)$$

with $Z = \{iVPD,\ iT_{Min}, iPhoto\}$ and RI_Z is the percentage of the total constraint (CC) that is due to one of Z. Furthermore, we defined the "predominant" constraint over SOS (EOS) for each year as the indicator with the highest CC over the time period.

4.2.5 Environmental stratification and trend analysis

We stratified our results by environmental zone using the Global Environmental Stratification dataset (GEnZ, Metzger *et al.*, 2013) aggregated at 0.5 degree spatial resolution. GEnZ classifies the global land area in 125 strata and 18 environmental zones based on multi-variate clustering of bio-climatic data (Metzger *et al.* 2013). Pixels dominated by croplands were excluded from our study because we consider their SOS and EOS metrics to be primarily influenced by human intervention rather than climatic conditions. These were pixels with over 50% cropland cover according to the cropland percentage map (Fritz *et al.* 2015).

We analysed trends in CCs for all environmental zones for which our LSP algorithm could obtain sufficient reliable metrics. These were defined with a threshold of a minimum of 50% of the zone's area and a minimum of 500 pixels per zone. Fig. 4.2 presents the remaining 9 (out of the total 18) environmental zones (out of the 18 in total): these cover ~60% of all land areas and encompass the boreal, temperate, sub-tropical and dryland biomes. Hence our study includes the environmental zones that were previously highlighted as hotspot areas of LSP change (Garonna *et al.* 2016). Excluded zones include the artic/alpine and tropical-forest biomes (SI Appendix, Table S1), the latter being also the biome with weakest agreement between LAI_{3g} and LAI_{re}. All trends presented were significant at α=0.1 according to a Student's t-test of a non-zero slope, and all area calculations were performed after projecting data to the equal-area MODIS Sinusoidal projection.

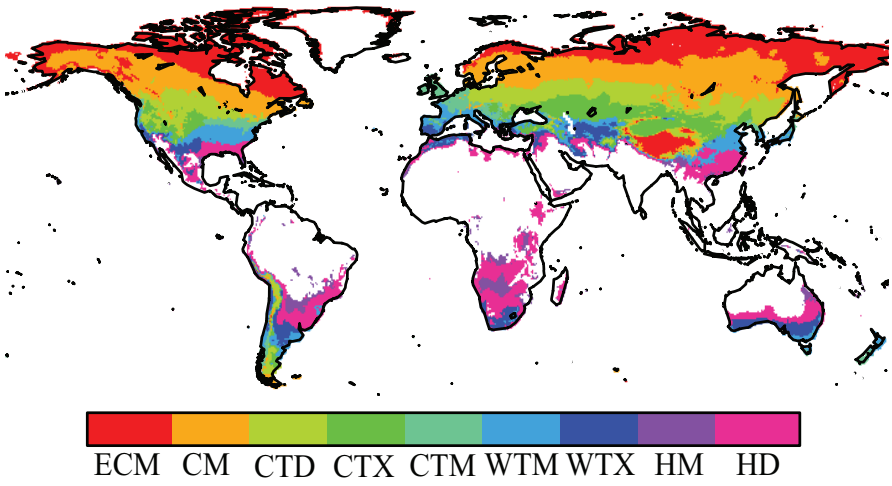

Figure 4.2: Global environmental zones considered for this study. White areas were discarded from the trend analysis. Key: ECM: Extremely Cold and Mesic; CM: Cold and Mesic; CTD: Cool Temperate and Dry; CTX: Cool Temperate and Xeric; CTM: Cool Temperate and Mesic; WTM: Warm Temperate and Mesic; WTX: Warm Temperate and Xeric; HM: Hot and Mesic.

4.3 Results

4.3.1 Distribution of pre-season Climatic Constraints at SOS and EOS

For both SOS and EOS, multiple constraints appeared to simultaneously act on most of the land surface. In particular, large parts of southern South America and Africa see a close combination of the three constraints at SOS (Figure 4.3). At SOS, T_{min} appeared to be largely constraining over most of the Northern Hemisphere, with some influence of photoperiod particularly over western Europe and the eastern United States. Tropical areas displayed a weak overall climatic constraint at both SOS and EOS (Figure 4.3). With the exception of VPD-limited areas, climatic constraints were weaker at EOS than SOS for most areas of the world (Figure 4.3). Indeed, both the magnitude and the mix of constraints varied between SOS and EOS for most areas, except for strongly VPD-constrained ones (e.g. northern America, the Sudano-Sahelian region, southern Africa and Australia), where this constraint appeared consistent between seasons. The area covered by VPD constraint was larger at EOS, including most of central and western North America, as well as in western Europe and central Eurasia. Overall, EOS processes involved a different and more complex mix of climatic constraints.

The T_{Min} constraint is predominant at SOS over approximately 1/3 of areas, and most of the Northern Hemisphere (Figure 4.4a). The remaining 2/3 of areas were fairly equally divided between photoperiod and VPD constraints. This picture was considerably different for EOS: T_{Min} appeared as the predominant constraint in only a small proportion of land areas, mainly around the Arctic sea. Photoperiod and VPD were the most frequent predominant constraints at EOS. These distributions were however not constant through the years, and predominant constraints appeared to be more dynamic at EOS than SOS throughout the study period (Figure 4.4b).

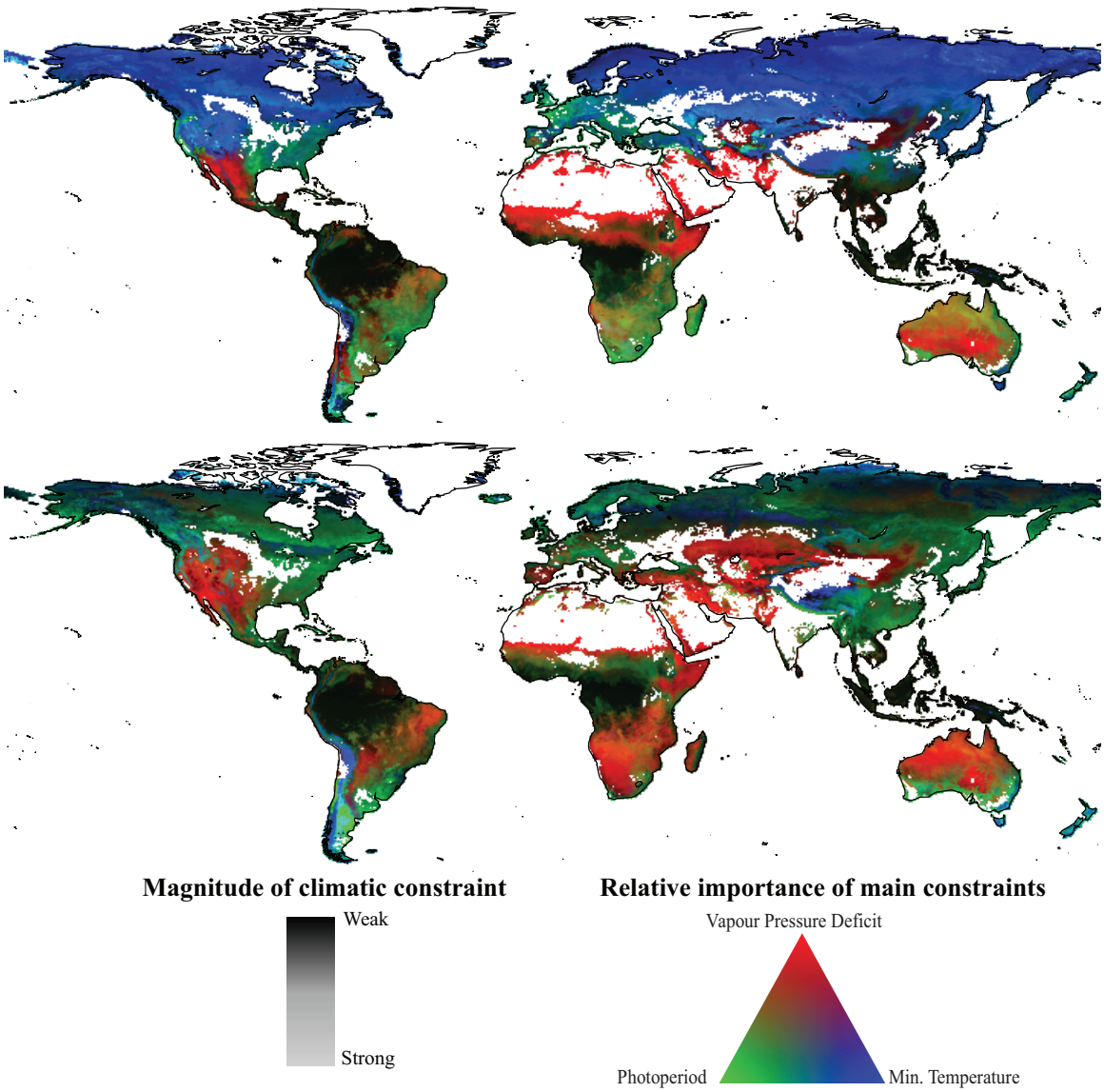

Figure 4.3: Average regional climatic constraints at SOS (top panel) and EOS (bottom panel) pre-seasons for 1982-2010. Light colours indicate strong average CC, and darker colours indicate an absence of CC. White pixels represent discarded pixels.

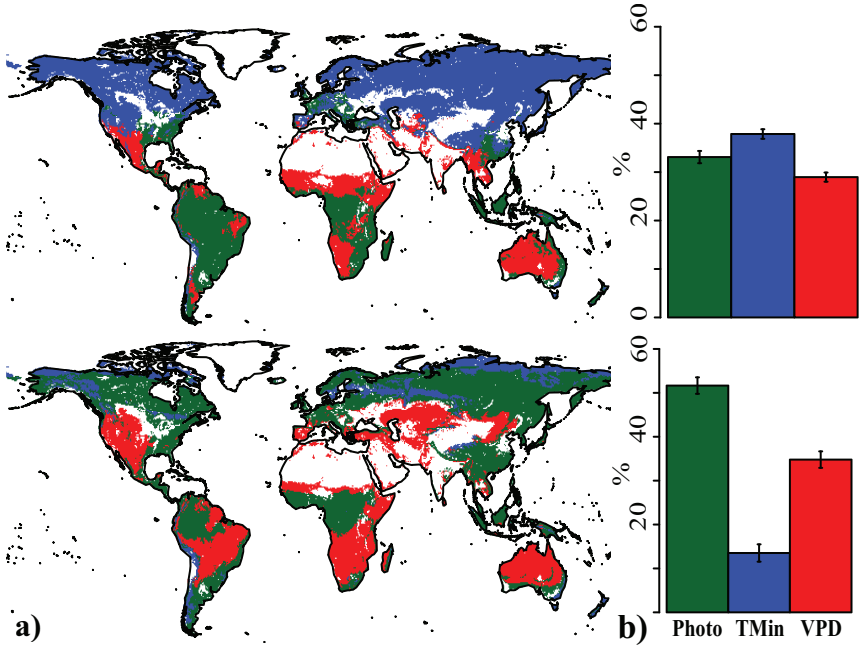

Figure 4.4: Pre-season distribution (a) and frequency (b) of predominant constraints at SOS (top panel) and EOS (bottom panel) pre-seasons over 1982-2010. The error bars represent standard deviation between 1982-2010. White pixels represent discarded areas. 'Predominant constraint' is defined as the most frequently occurring constraint during the study period.

4.3.2 Trends in climatic constraints

Significant trends ($p<0.1$) in modelled Climatic Constraint (CC_T) during the study period were found on 68% of the total area considered (covering 9 global environmental zones). This corresponded to roughly 40% of all land area. Trends varied both spatially and temporally between SOS and EOS (Figure 4.5). At high northern latitudes (>50° N), a significant reduction ('easing') of modelled CC at both SOS and EOS was found across the American and Eurasian continents. On the other hand, increasing climatic constraints were found for both SOS and EOS over parts of western North America and Mexico, central South America and pocket regions such as Fennoscandia in Europe. Contrasting trends between EOS and SOS were mostly present at mid-latitudes, with a shift towards more favourable conditions at either SOS or EOS for instance in pocket areas of central Eurasia.

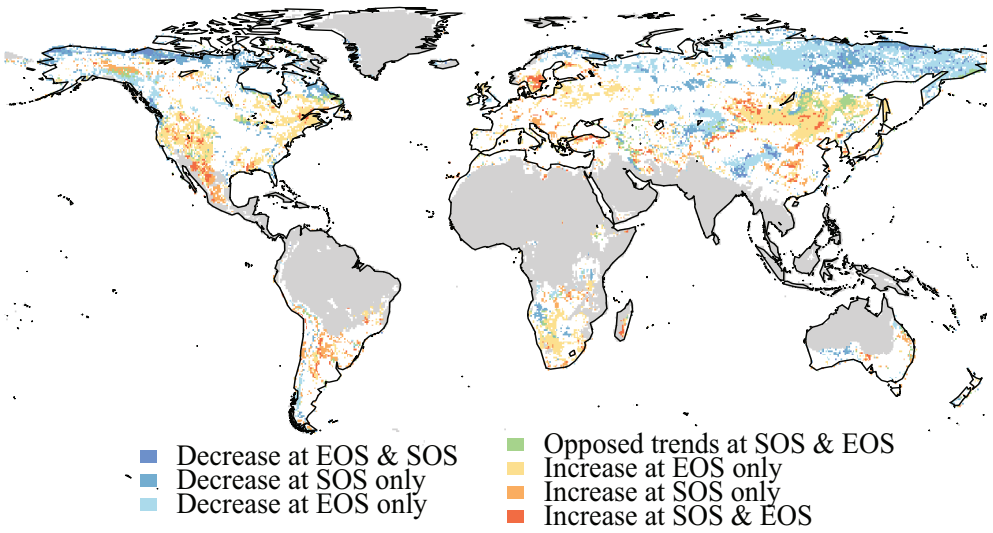

Figure 4.5: Significant (p<0.1) pre-season trends in total CC at SOS and EOS.

Significant (p<0.1) CC_T trends also varied depending on which of the three climatic indicators were considered (Figure 4.6). Photoperiod constraint appeared to have increased both at SOS and EOS, in particular on boreal and continental Europe and parts of North America, whereas T_{Min} constraint decreased over wide areas of the Northern Hemisphere at both SOS and EOS. In the Southern Hemisphere, an increase in T_{Min} constraint at SOS was found in parts of central South America, Southern Africa and Australia. For VPD, we found mostly increasing climatic constraint at SOS over the Southern Amazon, Mexico and pocket areas of central Eurasia, and additionally eastern Pan-Europe and South-eastern Russia at EOS. Overall, significant changes were more widespread at EOS than at SOS, particularly with respect to T_{Min} and VPD indicators (Figure 4.6).

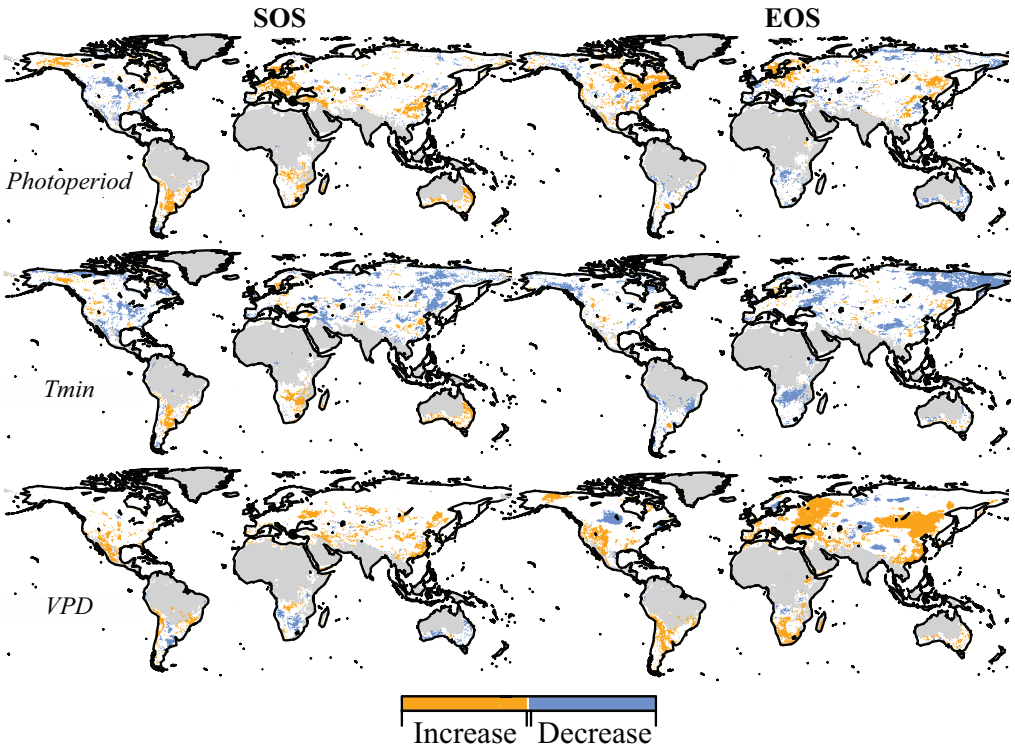

Figure 4.6: Significant (p<0.1) decrease and increase in total CC (in blue and orange, respectively) at SOS (left) and EOS (right) pre-seasons, for each climatic indicator. Grey pixels represent discarded environmental zones; white pixels presented no significant trend.

4.3.3 Shifting relative importance of climatic constraints

The relative importance of T_{Min} (i.e. independent of total CC) on both SOS and EOS decreased in almost all environmental zones considered (Figure 4.7). Interestingly, the resulting change in relative importance of VPD and Photoperiod constraints varied considerably between environmental zones, and between SOS and EOS pre-seasons. At SOS, the decreasing importance of T_{Min} was counterbalanced by both photoperiod and VPD constraints increasing in all boreal and temperate zones. At EOS the decline in T_{Min} constraint was opposed by photoperiod limitation in the boreal biome, and mostly by VPD constraint in the temperate (both cool and warm), sub-tropical and dry biomes. In general, VPD underwent considerable increases in relative importance in all zones except boreal ones at both SOS and EOS – and particularly strongly at EOS (Figure 4.7).

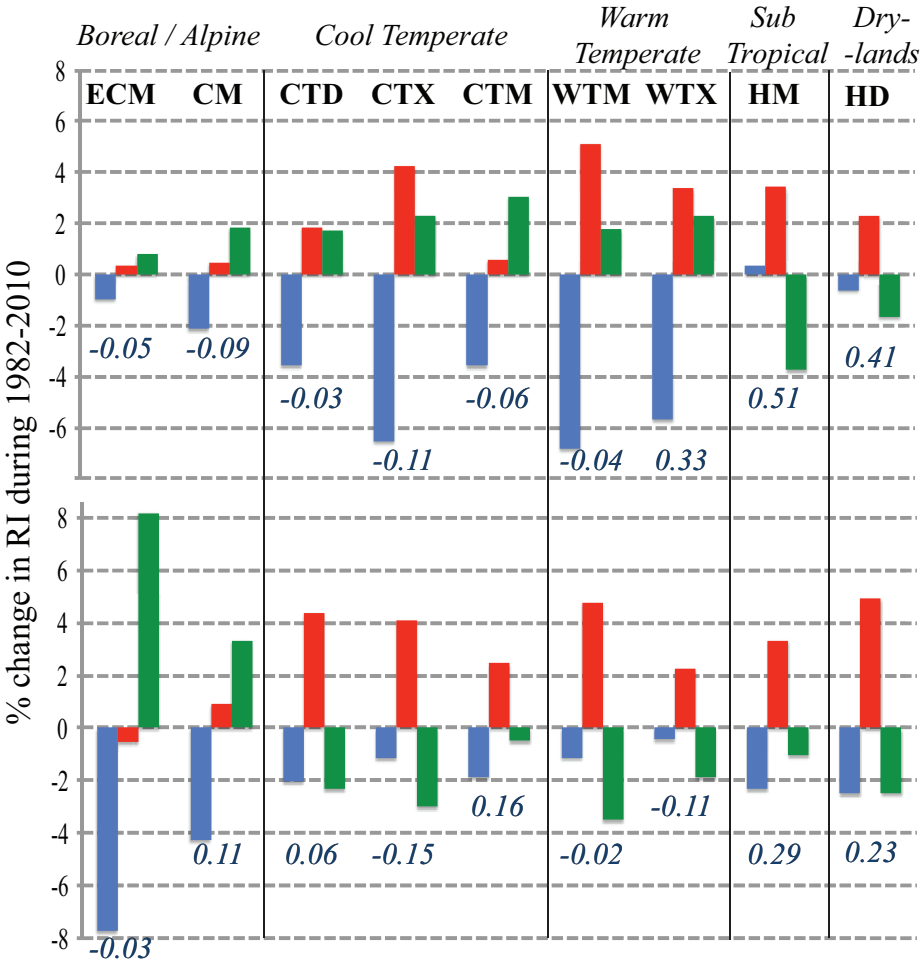

Figure 4.7: Average shift (in %) in the Relative Importance (RI) of each climatic constraint at SOS (top) and EOS (bottom) pre-seasons over the study period, for 8 global environmental zones. Blue, green and red bars represent percentage shift in temperature, light and moisture constraints, respectively. Biomes are labelled in black italics at the top of each bar. The grey numbers represent the average change (days/year) in SOS (top) and EOS (bottom) for each zone as derived from LAI_{3g} records. Key: ECM: Extremely Cold and Mesic; CM: Cold and Mesic; CTD: Cool Temperate and Dry; CTX: Cool Temperate and Xeric; CTM: Cool Temperate and Mesic; WTM: Warm Temperate and Mesic; WTX: Warm Temperate and Xeric; HM: Hot and Mesic; HD: Hot and Dry.

These shifts in relative importance had different repercussions on the predominance of constraints in each zone (Figure 4.8). Globally, the proportion of land areas considered with any given predominance changed through time (Figure 4.8).

Over the time period, the number of pixels with T_{Min} as their predominant constraint for both SOS and EOS decreased, being increasingly replaced by VPD and Photoperiod limitations. Interestingly, while at SOS these two constraints increased by about the same amount, this was not the case at EOS, when VPD predominance increased much more than Photoperiod predominance.

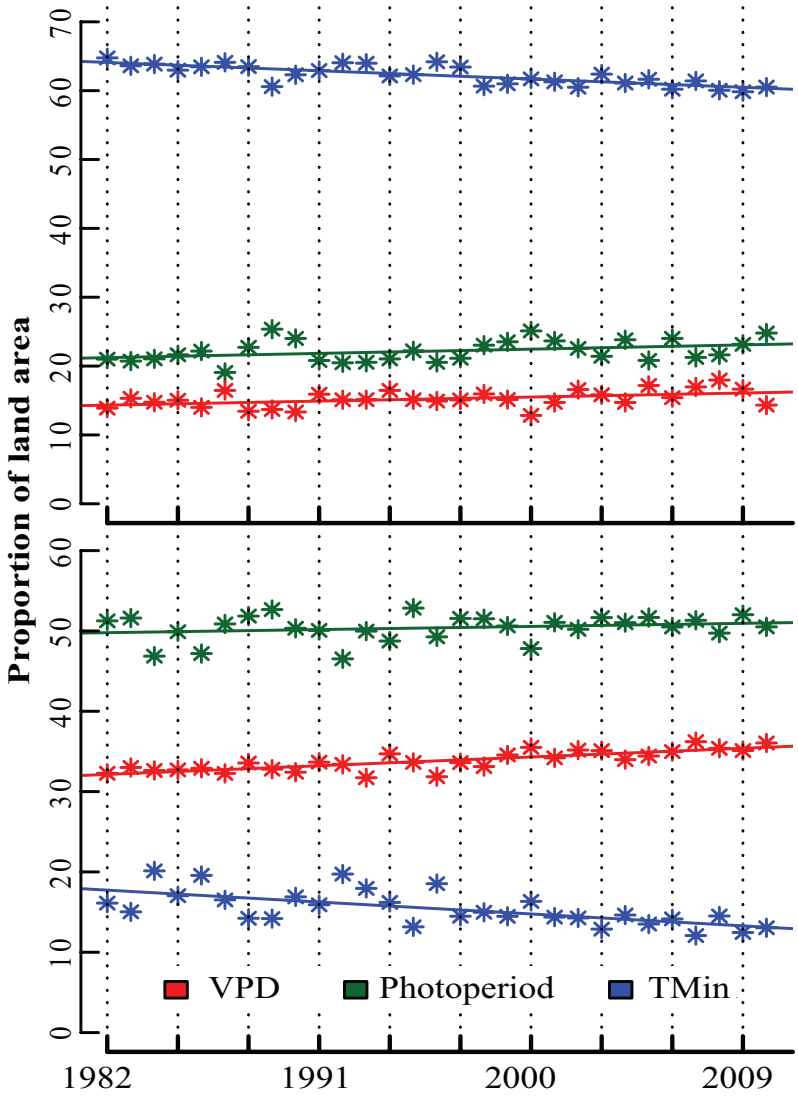

Figure 4.8: Proportion of land area (in %) with predominant constraints on SOS (top) and EOS (bottom) between 1982-2010.

4.4 Discussion

The notion that multiple environmental conditions, rather than single limiting factors, determine phenological variation in most areas of the world has already been recognised in previous literature (Churkina & Running 1998; Nemani *et al.* 2003; Jolly *et al.* 2005). By focusing on SOS and EOS constraints – as opposed to annual constraints such as in Jolly *et al.* (2005), our study corroborates this finding specifically for spring and autumn processes. Despite this, most previous studies have largely focused on the role of single meteorological factors on phenological variability, and most commonly temperature (Chambers *et al.* 2013).

Our analysis highlights the considerable differences in constraints underlying spring and autumn phenological changes (Figure 4.3 and 4.4). These differences are often not reflected in the representation of phenology in Terrestrial Biosphere Models (TBMs). Indeed, the phenology parameter is either prescribed or based on temperature accumulation through Growing Degree Days in most TBMs (Chmielewski & Götz 2016; Delpierre *et al.* 2016). Temperature has long been considered as the main determinant of phenology in many ecosystems (Tanja *et al.* 2003; Barr *et al.* 2009; Liu *et al.* 2016b). In our results, though minimum temperature appeared as the largely dominant constraint over spring phenology, the mix of interacting constraints in autumn appeared much more complex. Hence, our results not only underline the importance of studying how climatic constraints vary in concert to influence large-scale phenological variability (Forkel *et al.* 2015), but also suggest that incorporating more than one forcing climatic parameter in phenology models is key for improving the representation of phenology in TBMs. However, more research is needed to understand how to formulate this knowledge into TBMs.

The prominence of temperature as a phenology indicator in models also reflects the greater attention that spring phenology has received compared to senescence (Gallinat *et al.* 2015). Our characterization of climatic constraints at EOS – namely the

weaker, more variable and more complex mix of climatic constraints as compared to SOS (Figure 4.3 and 4.4) – is in line with the idea that autumnal phenology is more difficult to track and model than spring phenology, as reviewed in Gallinat *et al.* (2015). Recent studies suggested senescence to be controlled by a larger and different suite of environmental cues than spring (Gill *et al.* 2015; Panchen *et al.* 2015; Parmesan & Hanley 2015). Indicators such as frost or wind have been suggested as more strongly related to senescence timing than minimum temperature or light availability (Panchen *et al.* 2015). Understanding what factors may be important for leaf senescence at a variety of scales remains challenging (Estiarte & Peñuelas 2015; Panchen *et al.* 2015; Parmesan & Hanley 2015).

Though they were not the focus of our analysis, tropical areas of South America, Africa and Asia appeared more weakly constrained by the 3 climatic constraints considered. Similarly, Churkina & Running (1998) found no climatic limitation to NPP over 12% of the globe but indicated that other factors such as nutrient availability or biotic stress may be important for defining seasonality in those areas. In our study, the high sensitivity of NDVI to cloud interference as well as the low seasonal LAI variability over tropical areas keep us from drawing conclusions over these areas.

For the 9 environmental zones considered, our results shed light on the dynamic nature of climatic constraints on phenology. We considered two types of shifts: shifts in the magnitude of the climatic constraint (Figure 4.5 and 4.6), and shifts in the relative importance of climatic constraints (Figure 4.7 and 4.8). It is important to state that any shift found may be equally associated to climatic variability as to the variability in timing in SOS and EOS themselves. The influence of the latter is especially clear when considering changes in photoperiod constraint (Figure 4.8 – top panel). Given that photoperiod is mainly determined by a function of latitude and time of year, this parameter does not change from year to year. As a consequence, the changes in CC_{Photo} we report were inevitably due to shifting SOS (EOS) dates (and their corresponding pre-seasons), as well as the relative shift in the other two constraints for RI_{Photo}. That explains why the distribution of areas with significant change in CC_{Photo} (Figure 4.6)

matches well that of LSP change found with $NDVI_{3g}$ in another study e.g. in continental and boreal Europe, north-eastern America, eastern Argentina and Australia (Garonna *et al.* 2016). The fact that these effects were stronger at EOS than SOS is consistent with the asymmetrically strong shifts found at EOS over this time period (Jeong *et al.* 2011).

Interestingly, the boreal and continental areas of Europe, which have undergone growing season lengthening over the last 3 decades (Garonna *et al.* 2014), did not present an easing of climatic constraints in our results, but rather opposing trends between SOS and EOS or even hardening at either SOS or EOS. This could indicate that the drivers of the growing season lengthening in these areas are not solely climatic (Park *et al.* 2015). This is coherent with the fact that Fennoscandia is strongly agricultural (Karlsen *et al.* 2009), and that forest regrowth has followed land abandonment in former Soviet Union Europe (Fuchs *et al.* 2013), thus implying phenological shifts driven by land use/land cover change.

Interestingly, our study revealed shifts in the relative importance of climatic constraints in the temperate and boreal biomes, ranging from 1 to 8% during the study period. As temperature constraints appeared to ease widely across all environmental zones considered, a main finding of our study is the considerable increase in the relative influence of the moisture constraint at both SOS and EOS, which was independent from the LSP trends derived from LAI_{3g} (Figure 4.8). This increase in moisture constraint had repercussions on constraint dominance at EOS – with an increase in 3-4% in moisture-limited areas over the study period (Figure 4.8). This increasing importance of moisture for controlling phenology at large scales, which we reported, goes in the same direction as the findings of Forkel *et al.* (2015), who found water availability to be a co-dominant control for SOS and peak greenness trends over the last 30 years. Another study focusing on tropical areas found the sensitivity of carbon fluxes to inter-annual temperature variations to be regulated by moisture conditions (Wang *et al.* 2014), thus further highlighting the potentially important role of moisture interactions with temperature in controlling terrestrial carbon fluxes.

All in all, while temperature is undoubtedly a major phenological indicator, our results highlight the importance of incorporating moisture and photoperiod effects into phenology models, particularly for autumn timing (Liu *et al.* 2015). This has already been put forward in a number of previous studies. At the global scale, Bauerle *et al.* (2012) found seasonal CO_2 predictions from a global-scale carbon cycle model to improve following the integration of a photoperiodic correction. At the species scale, a study on cherry blossom indicated that models with photoperiod as a forcing factor fared better than models without this parameter (Chmielewski & Götz 2016). Similarly, in a comparison of 35 budburst models for 6 species, better results were found for models with a photoperiod factor during the ecodormancy release phase (Basler 2016).

Finally, our results highlight the usefulness of these reanalysis data in allowing us to quantify the influence of meteorological drivers of leaf onset and senescence at large spatial and temporal scales. It should be noted, however, that by focusing on climatic factors our analysis neglected the important effects of land cover change or disturbance on phenological change. Indeed, annual effects of land use/land cover change and fire have been shown to be considerable at global scale (Forkel *et al.* 2015). Moreover, the reanalysis does not consider the potential effects of nutrient limitation or CO_2 fertilization (Schimel *et al.* 2015). The latter may enhance plants' resistance to several stresses, but also induces greater nutrient deficiency (Niinemets 2010). Nutrient deposition itself may also thoroughly affect the relative influence of environmental controls over productivity (Churkina & Running 1998).

In summary, examining a reanalysed and a remotely sensed LAI time series in combination allowed us to disentangle the climatic constraints underlying large-scale LSP variability of the last three decades, at a scale relevant for TBMs. These results not only reiterate the complex interplay of climatic constraints on phenology, but also the dynamic nature of these constraints. The formulation of these dynamic climatic constraints in models should be further investigated, so as to improve our predictions of phenological change under future climate conditions.

Acknowledgements

We thank Range Myneni & colleagues for the LAI_{3g} dataset and Jorge Pinzon and Compton J. Tucker for the $NDVI_{3g}$ dataset. We are very grateful to the Functional Genomics Center Zurich for facilitating data analysis and providing technical support, in particular to M. Hakateyama, H. Rehrauer and K. Shimizu. This study has been conducted with the support of the University of Zurich Research Priority Program on Global Change and Biodiversity (URPP GCB).

Supporting Information

4A.1. Global comparison of modelled and remotely sensed LAI (LAI_{re} and LAI_{3g}, respectively)

Correlating mean LAI values for all land pixels and for the entire study period 1982-2010 resulted in a Pearson's correlation coefficient of $R=0.92$ ($p<0.01$; Figure 4A.1). Figure 4A.1 presents the Pearson's correlation coefficient for all land pixels and the entire study period of 1982-2010. This figure illustrates a good agreement between the two datasets ($R>0.8$) for most of the Northern Hemisphere. This leads us to believe that the reanalysed LAI reproduces accurately the observed LAI dynamics over these areas and over the past 30 years, and therefore that we may use the model parameters to induce changes in the climatic constraint factors underlying the observed dynamics.

Exceptions to this good correspondence between the two datasets are, firstly, the areas of central North America and southern Europe where the correlations were only moderate ($0.4<R<0.6$). Moreover, very low correspondence between the two datasets ($R<0.2$) is present in areas of the Southern Hemisphere (e.g. Southern and Western Australia) as well as null-to-negative correlations over the Amazon, South East Asia, Namibia and southern Argentina. This weak or negative relationship between the two datasets found over much of the Southern Hemisphere – and particularly over tropical

areas, was not unexpected. Several factors make it particularly challenging both to remotely sense and to model vegetation dynamics over these areas. Firstly, LAI_{3g} is derived from NDVI data – which is known to saturate at high LAI values and to be very sensitive to cloud cover (Huete *et al.* 2002).

An under-estimation of NDVI and thus of LAI would be therefore expected over tropical areas, and is visible in Figure 4A.2, where a distinct outlier group at high LAI values presents higher LAI_{re} than LAI_{3g} values. Secondly, the ECMWF climate data that drive LAI_{re} may be less accurate over Southern Hemisphere areas, where fewer meteorological data are available. Thirdly and finally, low correspondence between a 'climatically-induced LAI' (LAI_{re}) and 'observed' (albeit remotely) LAI (LAI_{3g}) may also reflect the stronger influence climatic factors play over vegetation seasonality in high latitudes than in the tropics.

In our study, the entire Tropical and Arctic biomes were excluded. In doing so, we limited our results to areas where LAI_{re} and LAI_{3g} have a very high correspondence.

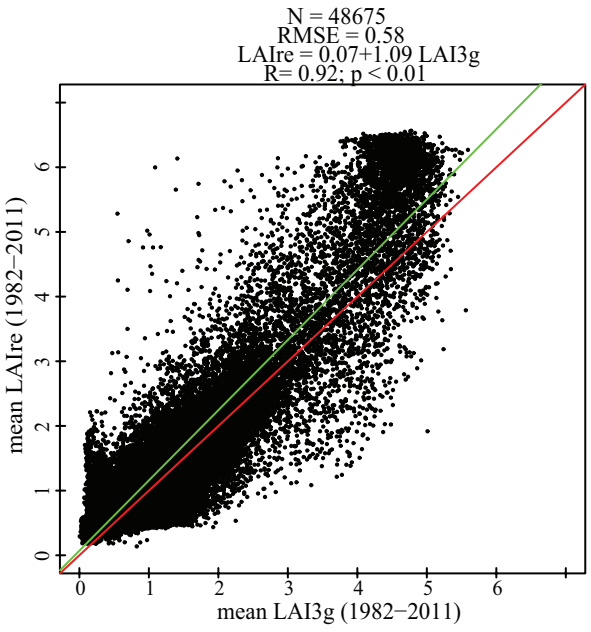

Figure 4A.1: Scatterplot of annual mean LAI_{re} vs LAI_{3g} over 1982-2010 for all land pixels. In red and green are the 1:1 line and the line of best fit, respectively.

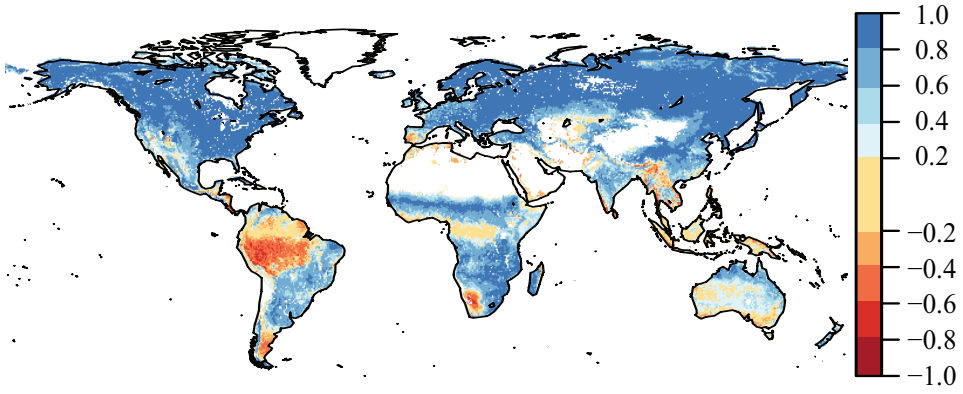

Figure 4A.2: Pearson's Correlation Coefficients for LAI_{3g} vs LAI_{re} (1982-2011)

4A.2. Choice of Pre-Season duration

Our selection of a pre-season duration of 21 days for all three climatic constraints is based on previous literature (Jolly *et al.* 2005; Stöckli *et al.* 2011). Indeed, in their study, Stöckli *et al.* (2011) selected 21 days as a prior averaging parameter, and Jolly *et al.* chose this same number to select the size of the moving window applied to GSI time series.

However, Stöckli *et al.* then constrained this parameter using 10 years of MODIS data (Stöckli *et al.* 2011). The resulting time averaging parameters used in their reanalysis vary by PFT and by climatic factor (see Table 5 in Stöckli *et al.* 2011): on average, they are 16.7±11.8 for T_{Min} and 21.9±2.21 for VPD. In their paper, they also point out that "time averaging needed for temperature and light are likely shorter than 21 days and the time averaging for moisture longer than 21 days"(Stöckli *et al.* 2011).

This highlights the fact that, although we chose one consistent approach in this study, the optimal time window is likely to vary between biome and by climatic constraint considered. A recent study reinforces this idea: Wu *et al.* (2015) investigated the time-lag effects of vegetation responses to different climatic factors at global scale (Wu *et al.* 2015). Over the Northern Hemisphere, their study shows that the time lag at which the maximum correlation between NDVI and climatic factor is found is mostly shorter than 1 month for temperature but well over 1 month for precipitation (see

Figure 2 in Wu *et al.* (2015). Our approach represents a compromise between the findings of previous studies.

4A.3. Environmental stratification and excluded pixels

Table 4A.1: Number of pixels (N) within each environmental zone. Zones in bold were selected for our analysis based on two main criteria: (i) more than 50% of their total area had successfully extracted LSP metrics and (ii) over 500 pixels remained for final zonal statistics, after exclusion of cropland areas.

Global Environmental Zone	Initial N	% of N with LSP metrics	N without croplands
Extremely Cold and Wet 1	143	9	13
Extremely Cold and Wet 2	351	17	59
Cold and Wet	327	71	231
Extremely Cold and Mesic	**4870**	**76**	**3713**
Cold and Mesic	**5336**	**97**	**5150**
Cool Temperate and Dry	**3514**	**93**	**2619**
Cool Temperate and Xeric	**2460**	**78**	**1677**
Cool Temperate and Mesic	**1056**	**97**	**887**
Warm Temperate and Mesic	**2586**	**81**	**1783**
Warm Temperate and Xeric	**2079**	**53**	**994**
Hot and Mesic	**1336**	**58**	**758**
Hot and Dry	**4723**	**58**	**2689**
Hot and Arid	2063	25	511
Extremely Hot and Arid	1603	15	219
Extremely Hot and Xeric	4295	43	1569
Extremely Hot and Mesic	10144	26	2290

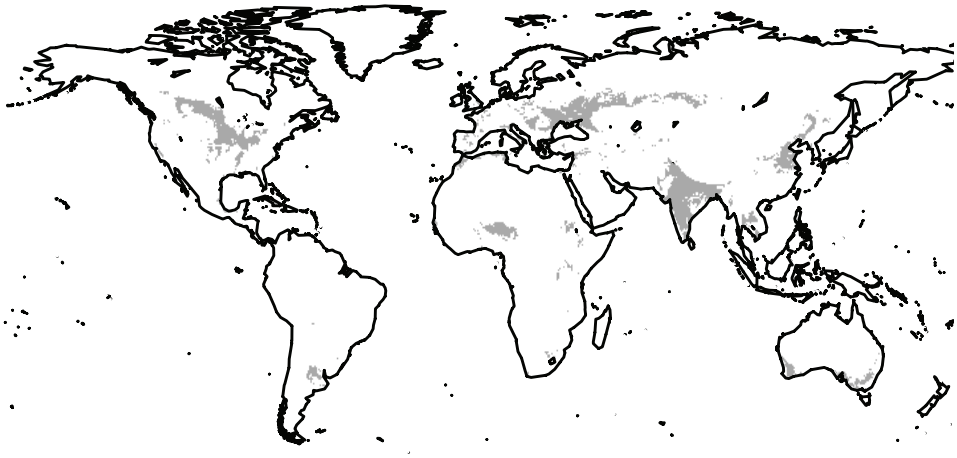

Figure 4A.3: Distribution of predominantly agricultural pixels, which were discarded from our analysis. Grey areas represent pixels with 50% cropland cover or more, according to the IIASA-IFPRI dataset re-gridded to 0.5-degree spatial resolution.

Chapter

5

Synthesis

5.1 Main findings

Recent years have seen vast advances in phenological research at a variety of scales, making phenology a growing – and exciting – research field. The importance of this field of study for global change research is widely recognized: phenology has been described as the "most reported biological indicator of anthropogenic climate change" (Wolkovich & Ettinger 2014) and has been proposed as an Essential Biodiversity Variable (EBV; Pereira *et al.* (2013)).

Using satellite Vegetation Index (VI) records together with modelled data, this thesis provides an assessment of large-scale trends in global Land Surface Phenology (LSP) and advances the characterization of its climatic constraints. Taken together, the previous Chapters contribute to addressing the three Research Questions (RQs) formulated in Chapter 1. These RQs are reassessed and discussed in sequence below, together with the four Hypotheses:

I. that growth constraints have eased over the past 3 decades, resulting in longer growing seasons;
II. that LSP varies differentially in different environmental zones, given the variety of human and environmental pressures that interact on land surfaces;
III. that start and end of season phenology vary differentially because they have differing climatic controls; and
IV. that variation in LSP has repercussions on the relative importance of climatic constraints in many regions.

5.1.1 Can changes in Growing Season Length (GSL) be detected at global scale using VI records, and what do these records of unveil about large-scale phenological shifts?

The analysis of the $NDVI_{3g}$ record allowed the detection, quantification and characterization of large-scale phenological shifts over the past 3 decades at global scale. Chapter 2 presents an approach to consistently derive estimates for Start, End and Length of the Growing Season (SOS, EOS and GSL, respectively), which was applied to the entire $NDVI_{3g}$ time span and to global scale in Chapter 3.

Results indicate considerable variability in large-scale LSP over the past 30 years. This variability is presently ignored by approximately 1/3 of Terrestrial Biosphere Models (TBMs), which prescribe vegetation as a boundary condition (Fisher *et al.* 2014). According to this thesis, GSL has undergone significant change over 18-30% of Pan-Europe and 13-19% of global land areas, with estimates varying with the LSP derivation method chosen. Chapter 3 confirms that the global growing season has on average lengthened over the 1982-2012 period at a rate of 0.22-0.34 days/year (depending on the method used), thus supporting Hypothesis I. These results translate to a global growing season 6.6-10 days longer over three decades, which compare well to previous LSP studies (Section 3.4.1) An illustration of the average NDVI curves for 1982 and 2011, along with the corresponding SOS and EOS dates, is presented in Figure 5.1. The GSL trends found were spatially heterogeneous and varied extensively within and between climatic zones, thus confirming Hypothesis II. The structural analysis of each GSL time series revealed that significant trends found were predominantly linear.

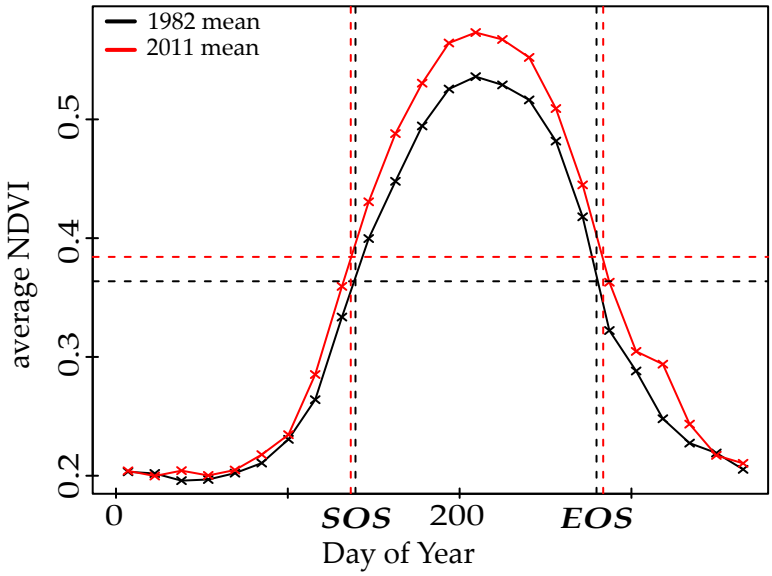

Figure 5.1 Annual $NDVI_{3g}$ curve, averaged over the Northern Hemisphere for 1982 and 2011. The corresponding SOS and EOS dates according to the $Midpoint_{pixel}$ method (Section 2.2.4) are also represented.

Our approach to tackling this RQ boasts two main strong features: firstly, the analysis bases all quantifications on two different indicators rather than a single metric, which had not been done in previous global LSP studies (Julien & Sobrino 2009; Brown *et al.* 2012; Eastman *et al.* 2013) until recently (Buitenwerf *et al.* 2015). Results from the two indicators were compared throughout the thesis. An improvement to the $Midpoint_{pixel}$ method could be the use of a static threshold between years, in order to remove the influence of greening/browning on the SOS/EOS timing. Secondly, our use of environmental stratification schemes such as LANMAP or GEnS (as opposed to commonly used land use/land cover classifications) in Sections 2.2.2 and 3.2.4 avoids circular findings. Indeed, many land cover classifications (e.g. International Geosphere Biosphere Programme (IGBP) classification scheme) are produced using NDVI as a basis. Moreover, in the IGBP as in many land cover classifications, a single vegetation type e.g. woody savannah may exist in both subtropical and boreal biomes (Fu *et al.* 2014a). Given that plants in different regions have different climatic requirements, it makes sense to subdivide vegetation by climatic conditions. Using these environmental

data, we were able to put forward hotspot environmental zones of change, on which Chapter 4 focuses. These were the continental and boreal zones for the European study (Table 2.2 and Section 2.3.3) and the boreal/alpine zone globally (Figure 3.5 and Section 3.4.3). Finally, it is important to note that although the assessment presented in this thesis covered 71% of all land pixels, not all environment zones were equally represented in the global LSP analysis. Indeed, areas with weak seasonal NDVI variation, with frequent NDVI drops or with more than one growing season per year had to be excluded (Section 3.2.2). These areas corresponded mainly to tropical forests or to agricultural areas, where specific approaches or data are necessary and are the focus of other studies (Brown *et al.* 2012; Hilker *et al.* 2014; Guan *et al.* 2015; Girardin *et al.* 2016; Wu *et al.* 2016).

5.1.2 What is the contribution of spring and autumn shifts to overall GSL changes and is there evidence for differing controls underlying spring and autumn phenology at large scale?

In Chapter 2, the relative contribution of SOS and EOS to the overall GSL change observed over the broader European region is quantified using the C-index. Chapter 3 presents the first global LSP assessment to explicitly address this issue (Garonna *et al.* 2016). Both Chapters reveal asymmetric trends in Pan-Europe and globally. The global EOS trend over 1982-2012 was stronger than the SOS equivalent: the average EOS delay was +0.22/0.26 days/year (Maxincrease and $Midpoint_{pixel}$ estimates, respectively), compared to -0.02/-0.08 days/year for SOS change (Section 3.3.3). A study by Jeong *et al.* (2011) substantiates this finding for temperate forests of the Northern Hemisphere for 1982-2009. The global EOS change estimate in Table 3.2 is of the same order of magnitude as that of Liu *et al.* (2016), who report an EOS mean change rate of 0.18 ± 0.38 days across ~70% of the Northern Hemisphere. Although in the boreal zone the spring advance appeared to match delayed senescence trends, the findings of this

thesis support Hypothesis III in that they suggest an uneven contribution of SOS and EOS to large-scale GSL change.

The independent assessment of SOS and EOS in phenological research represents a key first step into exploring large-scale drivers of phenological change. Indeed, these differential trends found in Chapter 3 may be either due to stronger climatic shifts at EOS than SOS (as observed in many habitats in Cohen et al. (2012)) and/or to differential controls underlying SOS and EOS processes. Chapter 4 constitutes a first attempt to examine the distribution of potential climatic constraints on spring and autumn globally. In Figures 4.3 and 4.4, while temperature is the predominant factor underling SOS over the Northern Hemisphere (Figures 4.3 and 4.4), this is not true for EOS – where both photoperiod and moisture appear to play a large role. These results support Hypothesis III by indicating that different controls are at play at these two key phases.

These findings suggest that spring leaf out in the Northern Hemisphere is determined mainly by temperature, while autumn leaf senescence is determined by interactions among multiple factors. In a recent study, Fu *et al.* (2014a) note the poor performance of temperature-driven phenology models in low latitude areas. This is not surprising given that plant phenology appears as largely controlled by moisture patterns in these areas in Figures 4.3 and 4.4. Other studies have highlighted that temperature explains more variation in leaf processes in spring than in autumn, when a larger or different suite of factors appear to be at play than just temperature (Panchen et al. 2015). In Liu *et al.* (2016), the correlation between EOS dates and temperature, precipitation and insolation was also tested: the authors found that both warming and increased insolation were positively associated with EOS date (except in dry regions), and that precipitation sum played a dominant role in arid/semi-arid regions.

Thus, it appears necessary for TBMs to move beyond just temperature in their representation of phenology and particularly of leaf senescence. Indeed, both in the literature (Gallinat *et al.* 2015) and in Chapter 4, the evidence points towards a weaker link between temperature and senescence than with spring. However, many models represent leaf loss using temperature-based indicators (Richardson *et al.* 2012;

Delpierre *et al.* 2016), thus ignoring differences in constraints underlying spring and autumn. Aside from moisture and photoperiod limitations studied here, other potential factors awaiting further study are for instance the North Atlantic Oscillation Index, frost events, wind, disease or a critical GSL (Menzel 2002; Panchen *et al.* 2015). For the latter, both a remote-sensing study (Liu *et al.* 2016) and an experimental study (Fu *et al.* 2014b) put forward a potential influence of SOS date on EOS timing; which was not tested in this work. A 'carryover' effect of SOS on EOS may be explained by traits such as leaf life span, drought caused by an earlier soil water loss at SOS, higher spring frost risk or a limitation in the carbon accumulation in the growing season (Liu *et al.* 2016), and should be investigated in the future.

Overall, the strong contribution of autumnal shifts to overall GSL changes as well as on the differing limiting factors acting at SOS and EOS are novel in the relatively under-studied field of autumn phenology. The slower and arguably more protracted nature of leaf fall as compared to leaf onset or flowering, the challenge posed by defining leaf senescence, as well as the greater complexity of drivers associated with leaf senescence have been put forward as reasons why autumn has been 'neglected' in the past (Gallinat *et al.* 2015). However, this is currently being changing: there has been a doubling of publications dedicated to senescence processes from 2000 to 2015 (data not shown, Scopus, 2016) and a considerable number published in the last year (Estiarte & Peñuelas 2015; Gill *et al.* 2015; Panchen *et al.* 2015; Junker & Ensminger 2016).

5.1.3 What climatic constraints underlie LSP variability and how does their relative importance vary during the study period?

In Chapter 4, a combination of remotely sensed and modelled phenology data were used to disentangle three main climatic constraints driving canopy greenness (photoperiod, moisture availability, temperature) at global scale. This approach allowed the quantification and evaluation of these three constraints during spring and autumn over the past three decades. Results indicate that significant shifts in climatic

constraints underlying LSP variability over the last three decades in the boreal and temperate biomes. These lead to modifications in the relative importance of the three constraints at the start and at the end of the growing season (SOS and EOS, respectively).

More precisely, over the 1982-2012 period, an easing of climatic constraints over the boreal biome was found, thus supporting Hypothesis I for this biome. Although there is not a perfect spatial overlap between the pixels with significant GSL lengthening (Chapter 3) and those with decreasing climatic constraint (Chapter 4), the decreasing temperature constraint at both SOS and EOS is in line with the average lengthening of the growing season found across the boreal biome (Chapter 3). This reduced minimum temperature constraint is counter-balanced by an increasing importance of photoperiod at SOS and EOS. Given that photoperiod does not vary from year to year, this shift suggests a stabilizing influence of photoperiod on SOS and EOS timing.

Overall, the findings of this thesis put forward an intensification of the influence of moisture as a constraint to growth, particularly at EOS and growing with decreasing latitudes. Although minimum temperature remains a predominant constraint on phenology particularly at SOS, the rising influence of the moisture constraint (particularly at EOS as highlighted in Chapter 4) leads to an expansion of predominance of this factor in the temperate biome. This increasing influence of moisture at EOS and over temperate regions is very much in line with a multi-model comparison by Forkel *et al.* (2015), who with a different approach identified moisture limitation as a co-dominant factor in LSP dynamics. Moreover, given the water scarcity projections for future years (Gerten 2013), these results suggest that water limitation is likely to become a central topic in phenology studies.

It is important to note that these results highly rely on the ability of the reanalysed data to reproduce vegetation dynamics, which is not the case in all areas of the world (see Section S4.1). Nevertheless, the modelled LAI dynamics appear to be robust over boreal and temperate regions of the Northern Hemisphere, which were identified in Chapter 3 as hotspot areas of LSP change and are thus key focus areas for

this thesis. Also, the reanalysis assumes fixed thresholds beyond which leaf development is not possible (Chapter 4). These broad thresholds were chosen to reflect differences between broad Plant Functional Types (PFTs). These PFTs were kept static throughout the 30-year-long study period, and also may have strong internal variability, which was not considered given the coarse-scale approach chosen for this thesis.

5.2 General contributions

Given the importance of monitoring phenology for understanding global change and knowing the difficulties associated with field phenological observations at large scales (Section 1.1.1), this work is an example of how the analysis of long-term satellite records of vegetation activity may inform phenological monitoring and understanding. Hence, this thesis showcases the fundamental role of Remote Sensing (RS) as a means to monitor and understand the spatial variability in vegetation dynamics.

The main contributions of this thesis are three-fold. Firstly, this thesis supports expanding the scope of phenological monitoring from the level of an individual plant or forest to the global scale. The development and application of an algorithm to extract LSP metrics from the longest VI record available at global scale demonstrate how long-term VI records are useful tools to detect, quantify and characterize large-scale phenological shifts. Findings reveal significant change in GSL over the past three decades, and quantify long-term and large-scale trends in both SOS and EOS.

Secondly, this thesis allows representing the spatial variability in the phenology of land surfaces in an unprecedented way. This is significant given that many models use fixed vegetation phenology parameters, thus neglecting the dynamic characteristic of vegetated land surfaces (Sellers *et al.* 1996). SOS, EOS and GSL estimates reflect vegetation activity rather than species-level phenology and thus provide a step forward in bridging the scale mismatch between field phenological observations and global models. The global LSP assessment dataset of timing for start, end and

maximum of the growing season over the period 1982-2012 is presently available to the broader scientific community[6]. Aside from its present use for various research projects, this dataset may also serve as a baseline against which to assess present and future LSP observations, for modelling ecological shifts (Schimel *et al.* 2013) or for the calibration of phenology models (Yang *et al.* 2012). Indeed, by calibrating phenology parameters using MODIS-derived metrics, Fu *et al.* (2014a) found significant improvements to the performance of four phenology models that are widely integrated into Dynamic Global Vegetation Models (DGVMs). As data continuity is a prerequisite for separating long-term patterns from inter-year variability, the continued application of the same algorithm on AVHRR-derived NDVI data as they become available is strongly encouraged.

Thirdly, this thesis investigates what climatic factors may be used to model LSP variability. Chapter 4 presents the first characterization of the distribution of climatic constraints on SOS and EOS processes, and proposes that these climatic constraints have shifted over the last three decades over many areas. An increasing importance of moisture constraints at both SOS and EOS in boreal and temperate biomes over the last three decades is also reported. Since the relative importance of climatic constraints to leaf development is key for predicting phenological responses to climatic changes, and their consequent feedback to climate, this thesis constitutes progress towards building a predictive framework for phenology.

5.3 Final considerations and future directions

Together with its main contributions, the findings of this thesis bring forward some considerations not yet discussed in the individual chapters, as well as various research avenues.

[6] Freely available for download at: http://www.zora.uzh.ch/116954/

5.3.1 Open issues

First, the coarse spatial resolution of the $NDVI_{3g}$ data means that this analysis cannot reproduce small-scale patterns and adds to the already-mentioned difficulties associated with comparing LSP metrics to surface-based phenological observations (Section 1.2.2). It is important to remember that each $NDVI_{3g}$ pixel metric comprises mixed phenological signals from multiple biomes, disturbances, urbanization, political changes and agricultural practices as well as climate-driven changes (White et al. 2005). This means that direct correspondence between SOS metrics and field phenological observations cannot be expected (Studer *et al.* 2007; Liang & Schwartz 2009; White *et al.* 2009; Schwartz & Hanes 2010). Nevertheless, the LSP rates of change were compared to those found by field studies in many areas of Europe and the Northern Hemisphere (Menzel 2006) as well by other LSP studies, finding good agreement (Chapter 3).

Other sensors and datasets may be used for LSP trend assessments, at a variety of spatial scales and temporal extents. In order to understand differences and to capitalise on the advantages of each data source, LSP inter-comparisons across sensors and scales are a challenging yet important effort. At a finer resolution, MODIS provides derived phenology metrics globally since 2000 in the Land Cover Dynamics (MCD12Q2) product. MODIS has also the advantage of providing the day of observation within the compositing window. This information is not available for $NDVI_{3g}$ and introduces uncertainty in the SOS/EOS metrics. Studies have also extracted LSP information from passive microwave data with promising results (Jones *et al.* 2011; Alemu & Henebry 2013). Furthermore, the use of proximate RS technologies – in particular through phenocams (Brown *et al.* 2016) – is allowing steps forward in our understanding of spring and autumn processes at regional scale (Melaas *et al.* 2015) as well as in bridging the LSP-vegetation phenology gap.

Secondly, the regular snow cover that mid-to-high latitude forests receive strongly influences the intra-annual VI dynamics. In order to resolve the influence of snow cover on LSP metrics in these key change areas (Chapter 3), Sun-induced Fluorescence (SiF) data may be used. SiF is positively correlated with photosynthetic efficiency and thus provides a closer insight into carbon fluxes associated with

photosynthesis than what is possible through NDVI or EVI (Frankenberg *et al.* 2011; Joiner *et al.* 2014). Although the seasonality of EVI and SiF matches well in temperate deciduous areas, a decoupling exists between SiF- and EVI-derived LSP metrics over high-latitude evergreen needle-leaf forests (Walther *et al.* 2016). In these areas, Walther *et al.* (2016) reported that the SiF-derived photosynthetically active period up to 6 weeks longer than the EVI-indicated one (Walther *et al.* 2016). This may be explained by photosynthesis recovering with spring warming conditions, even when snow is still present on the ground and keeping the EVI values low. However, SiF data from the Global Ozone Monitoring Experiment-2 sensor (GOME-2) are currently only available from 1997 to 2011 at ½ degrees resolution, and thus cannot represent long-term variability of GSL as in this thesis.

5.3.2 Consequences of phenological shifts

The thesis discusses mainly the modelling implications of its findings (Section 4.4 in particular). However, a multi-faceted research avenue arising from these results concerns the potential consequences of the phenological shifts reported: firstly, in terms of global primary productivity and secondly, in species communities. Indeed, the primary productivity impact of longer growing seasons as opposed to, for instance, increased carbon dioxide concentrations, is an interesting topic of investigation (Zhu *et al.* 2016). The extent to which the phenological growing season corresponds to the carbon uptake period is still a matter of uncertainty (Menzel 2002).

Moreover, the shifting climatic constraints in both temperate and boreal biomes identified in this thesis work are likely to lead to changes in species interactions and thus community-level changes, which may have further consequences for ecosystem functioning. For instance, changing spring conditions are likely to disproportionally benefit rapidly-growing, early-flowering species, which tend to show more adaptive ability and gain competitive advantage over later-flowering species (Wolkovich & Cleland 2010; Parmesan & Hanley 2015; Gezon *et al.* 2016). The alterations in the timing of climatic constraints also potentially provide temporal windows of opportunities for species invasion (Wolkovich & Cleland 2010). Thus, phenology may play an important

role in the distribution and abundance of invasive species, which are predicted to increase with climate change in the next decades (IPCC 2007). All these potential consequences of climatic shifts for species distributions and ecosystem functioning are a high research priority and should be studied further.

5.3.3 Exploring the LSP-biodiversity relationship

The scientific community relies only on limited data on key aspects of biodiversity to monitor and support conservation efforts (Jetz *et al.* 2016). That is why a number of networks, groups and partnerships are working towards collecting and integrating data on various biodiversity elements across scales, from *in situ* sampling to airborne and satellite RS (e.g. Group on Earth Observation Biodiversity Observation Network GEO-BON) (Scholes *et al.* 2012). Although it has been pointed out that RS of key variables related to biodiversity is a promising effort (Pereira *et al.* 2013; Turner 2014; Skidmore *et al.* 2015), further research is needed to tie biodiversity metrics to remotely-sensed data at large scales.

As previously mentioned, LSP is a candidate EBV (Pereira *et al.* 2013). Indeed, the larger-scale dynamics of LSP can indirectly inform biodiversity monitoring through models or proxies. For instance, the existence of certain habitats can help estimate potential species ranges, the distribution of ecological communities as well as spatial variation in patterns of biodiversity (Turner 2014). LSP has been used to distinguish between different vegetation types (Yan *et al.* 2015), to map above-ground biomass (Karlson *et al.* 2015) and to model species distributions (Cord *et al.* 2014). Links between floristic and phenological similarity have been established at regional scale (Viña *et al.* 2012; 2016). However, the relationship between LSP and species or functional richness has not been widely explored (Revermann *et al.* 2016), and appears as an important research avenue. In other words, it would be interesting to investigate both how changes in LSP may influence biodiversity, and how differences in species or functional richness may affect a community's ability to fill the available biotope space. For example, given the LSP data presented in this thesis, a next study could evaluate the potential role of biodiversity in providing species with appropriate niches to do so.

One may expect that in highly diverse communities, such species will more likely be included than in species-poor communities.

5.3.4 Integrating phenologies

A vast amount of phenological data is currently and increasingly being collected through satellite imagery, observation networks and citizen science (Beaubien & Hall-Beyer 2003; Studer *et al.* 2007). Yet no agreement currently exists over how these types of data may be combined (Hudson & Keatley 2010; Schwartz & Hanes 2010). Within the field of LSP, for instance, there is often no clear definition of what process is being tracked by a given derived metrics, thus making their ecological interpretation difficult (G. Henebry, *personal communication,* AGU 2015). Some studies have shown the complementary nature of different types of phenological data (Studer *et al.* 2007; Ganguly *et al.* 2010; Schwartz & Hanes 2010). Proposed approaches for integrating data include: the adoption of "multispecies" phenological indices for the ground data that facilitate in the comparison (Studer *et al.* 2005); or the use of landscape phenology (Liang & Schwartz 2009), a holistic method aiming to provide up-scaled phyto-phenology measures at the landscape level, thus integrating multiple scales (Liang & Schwartz 2009).

Overall, the title of Mark Schwartz's book "Phenology: an *integrative* environmental science" (Schwartz 2013) appears as a reminder of the important step – yet to be realized – to integrate phenological data in its various forms in order to reap the benefits of their combined disciplinary perspectives. Thus, exploiting observational networks together with RS and modelling approaches appears as an important avenue for this field (Revermann *et al.* 2016). In order to achieve this, multi-disciplinary thinking and understanding of the various pros and cons of each approach are vital.

Bibliography

Ahas, R, Aasa, R, Menzel, A, *et al.* (2002). "Changes in European spring phenology." International Journal of Climatology **22**(14): 1727-1738.

Alcaraz-Segura, D, Chuvieco, E, Epstein, HE, *et al.* (2010). "Debating the greening vs. browning of the North American boreal forest: differences between satellite datasets." Global Change Biology **16**(2): 760-770.

Alemu, WG and Henebry, GM (2013). "Land surface phenologies and seasonalities using cool earthlight in mid-latitude croplands." Environmental Research Letters **8**(4): 045002.

Andrews, DW and Ploberger, W (1994). "Optimal tests when a nuisance parameter is present only under the alternative." Econometrica: Journal of the Econometric Society **62**(6): 1383-1414.

Andrews, DWK (2003). "Tests for parameter instability and structural change with unknown change point: A corrigendum." Econometrica **71**(1): 395-397.

Aono, Y and Kazui, K (2008). "Phenological data series of cherry tree flowering in Kyoto, Japan, and its application to reconstruction of springtime temperatures since the 9th century." International Journal of Climatology **28**(7): 905-914.

Arora, VK and Boer, GJ (2005). "A parameterization of leaf phenology for the terrestrial ecosystem component of climate models." Global Change Biology **11**(1): 39-59.

Atkinson, PM, Jeganathan, C, Dash, J, *et al.* (2012). "Inter-comparison of four models for smoothing satellite sensor time-series data to estimate vegetation phenology." Remote Sensing of Environment **123**: 400-417.

Atzberger, C, Klisch, A, Mattiuzzi, M, *et al.* (2013). "Phenological Metrics Derived over the European Continent from NDVI3g Data and MODIS Time Series." Remote Sensing **6**(1): 257-284.

Badeck, F-W, Bondeau, A, Böttcher, K, *et al.* (2004). "Responses of Spring Phenology to Climate Change." New Phytologist **162**(2): 295-309.

Bai, J and Perron, P (2003). "Computation and analysis of multiple structural change models." Journal of Applied Econometrics **18**(1): 1-22.

Bailey, RG (2014). Ecoregions: the ecosystem geography of the oceans and continents. New York, Springer-Verlag.

Barichivich, J, Briffa, KR, Myneni, RB, *et al.* (2013). "Large-scale variations in the vegetation growing season and annual cycle of atmospheric CO2 at high northern latitudes from 1950 to 2011." Global Change Biology **19**(10): 3167-3183.

Barr, A, Black, TA and McCaughey, H (2009). Climatic and Phenological Controls of the Carbon and Energy Balances of Three Contrasting Boreal Forest Ecosystems in Western Canada. Phenology of Ecosystem Processes: Applications in Global Change Research. Noormets, A. New York, NY, Springer New York**:** 3-34.

Basler, D (2016). "Evaluating phenological models for the prediction of leaf-out dates in six temperate tree species across central Europe." Agricultural and Forest Meteorology **217**: 10-21.

Bauerle, WL, Oren, R, Way, DA, *et al.* (2012). "Photoperiodic regulation of the seasonal pattern of photosynthetic capacity and the implications for carbon cycling." Proceedings of the National Academy of Sciences **109**(22): 8612-8617.

Beaubien, E and Hall-Beyer, M (2003). "Plant phenology in Western Canada: Trends and links to the view from space." Environmental Monitoring and Assessment **88**(1-3): 419-429.

Beck, PSA, Atzberger, C, H√∏gda, KA, *et al.* (2006). "Improved monitoring of vegetation dynamics at very high latitudes: A new method using MODIS NDVI." Remote Sensing of Environment **100**(3): 321-334.

Berrisford, P, Dee, D, Fielding, K, *et al.* (2009). The ERA-Interim archive. ERA Report Series. Reading, European Centre for Medium-Range Weather Forecasts. **16**.

Bhatt, US, Walker, DA, Raynolds, MK, *et al.* (2013). "Recent declines in warming and vegetation greening trends over pan-Arctic tundra." Remote Sensing **5**(9): 4229-4254.

Bogaert, J, Zhou, L, Tucker, CJ, *et al.* (2002). "Evidence for a persistent and extensive greening trend in Eurasia inferred from satellite vegetation index data." Journal of Geophysical Research D: Atmospheres **107**(11): ACL 4-1 - ACL 4-14.

Botta, A, Viovy, N, Ciais, P, *et al.* (2000). "A global prognostic scheme of leaf onset using satellite data." Global Change Biology **6**(7): 709-725.

Bradley, NL, Leopold, AC, Ross, J, *et al.* (1999). "Phenological changes reflect climate change in Wisconsin." Proceedings of the National Academy of Sciences of the United States of America **96**(17): 9701-9704.

Brearley, FQ, Proctor, J, Nagy, L, *et al.* (2007). "Reproductive phenology over a 10-year period in a lowland evergreen rain forest of central Borneo." Journal of Ecology **95**(4): 828-839.

Broich, M, Huete, A, Tulbure, MG, *et al.* (2014). "Land surface phenological response to decadal climate variability across Australia using satellite remote sensing." Biogeosciences **11**(18): 5181-5198.

Brown, ME, de Beurs, KM and Marshall, M (2012). "Global phenological response to climate change in crop areas using satellite remote sensing of vegetation, humidity and temperature over 26years." Remote Sensing of Environment **126**(0): 174-183.

Brown, RD (2000). "Northern Hemisphere Snow Cover Variability and Change, 1915-1997." Journal of Climate **13**(13): 2339-2355.

Brown, TB, Hultine, KR, Steltzer, H, *et al.* (2016). "Using phenocams to monitor our changing earth: Toward a global phenocam network." Frontiers in Ecology and the Environment **14**(2): 84-93.

Buermann, W, Parida, B, Jung, M, *et al.* (2014). "Recent shift in Eurasian boreal forest greening response may be associated with warmer and drier summers." Geophysical Research Letters **41**(6): 1995-2002.

Buitenwerf, R, Rose, L and Higgins, SI (2015). "Three decades of multi-dimensional change in global leaf phenology." Nature Clim. Change **5**(4): 364-368.

Campbell, JB and Wynne, RH (2011). Introduction to Remote Sensing. New York, London, The Guilford Press.

Cayan, DR, Kammerdiener, SA, Dettinger, MD, *et al.* (2001). "Changes in the Onset of Spring in the Western United States." Bulletin of the American Meteorological Society **82**(3): 399-415.

Chambers, LE, Altwegg, R, Barbraud, C, *et al.* (2013). "Phenological Changes in the Southern Hemisphere." PLoS ONE **8**(10): e75514.

Chen, B, Xu, G, Coops, NC, *et al.* (2014). "Changes in vegetation photosynthetic activity trends across the Asia-Pacific region over the last three decades." Remote Sensing of Environment **144**: 28-41.

Chmielewski, F-M and Götz, K-P (2016). "Performance of models for the beginning of sweet cherry blossom under current and changed climate conditions." Agricultural and Forest Meteorology **218-219**: 85-91.

Chuine, I (2010). "Why does phenology drive species distribution?" Philosophical Transactions of the Royal Society of London B: Biological Sciences **365**(1555): 3149-3160.

Chuine, I, Yiou, P, Viovy, N, *et al.* (2004). "Historical phenology: Grape ripening as a past climate indicator." Nature **432**(7015): 289-290.

Churkina, G and Running, SW (1998). "Contrasting climatic controls on the estimated productivity of global terrestrial biomes." Ecosystems **1**(2): 206-215.

Ciais, P, Schelhaas, MJ, Zaehle, S, *et al.* (2008). "Carbon accumulation in European forests." Nature Geoscience **1**(7): 425-429.

Cleland, EE, Chuine, I, Menzel, A, *et al.* (2007). "Shifting plant phenology in response to global change." Trends in Ecology & Evolution **22**(7): 357-365.

Cohen, JL, Furtado, JC, Barlow, M, *et al.* (2012). "Asymmetric seasonal temperature trends." Geophysical Research Letters **39**(4): L04705.

Coops, NC, Schaepman, ME and Mücher, CA (2013). "What multiscale environmental drivers can best be discriminated from a habitat index derived from a remotely sensed vegetation time series?" Landscape Ecology: 1-15.

Cord, AF, Klein, D, Gernandt, DS, *et al.* (2014). "Remote sensing data can improve predictions of species richness by stacked species distribution models: a case study for Mexican pines." Journal of Biogeography **41**(4): 736-748.

D'Odorico, P, Gonsamo, A, Gough, CM, *et al.* (2015). "The match and mismatch between photosynthesis and land surface phenology of deciduous forests." Agricultural and Forest Meteorology **214-215**: 25-38.

de Beurs, K and Henebry, GM (2010). Spatio-Temporal Statistical Methods for Modelling Land Surface Phenology. Phenological Research: methods for environmental and climate change analysis. Hudson, IL and Keatley, MR. New York, Springer**:** 177-208.

de Beurs, KM and Henebry, GM (2005). "Land surface phenology and temperature variation in the International Geosphere-Biosphere Program high-latitude transects." Global Change Biology **11**(5): 779-790.

de Jong, R, de Bruin, S, de Wit, A, *et al.* (2011). "Analysis of monotonic greening and browning trends from global NDVI time-series." Remote Sensing of Environment **115**(2): 692-702.

de Jong, R, Schaepman, ME, Furrer, R, *et al.* (2013). "Spatial relationship between climatologies and changes in global vegetation activity." Global Change Biology **19**(6): 1953-1964.

de Jong, R, Verbesselt, J, Schaepman, ME, *et al.* (2012). "Trend changes in global greening and browning: contribution of short-term trends to longer-term change." Global Change Biology **18**(2): 642-655.

de Wit, AJW and Su, B (2005). Deriving phenological indicators from SPOT-VGT data using the HANTS algorithm. Proceedings of the 2nd international VEGETATION user conference; 1998-2004: 6 years of operational activities, Luxembourg, EC.

Defila, C and Clot, B (2001). "Phytophenological trends in Switzerland." International Journal of Biometeorology **45**(4): 203-207.

Delpierre, N, Vitasse, Y, Chuine, I, *et al.* (2016). "Temperate and boreal forest tree phenology: from organ-scale processes to terrestrial ecosystem models." Annals of Forest Science **73**(1): 5-25.

Dutrieux, LP, Bartholomeus, H, Herold, M, *et al.* (2012). "Relationships between declining summer sea ice, increasing temperatures and changing vegetation in the Siberian Arctic tundra from MODIS time series (2000-11)." Environmental Research Letters **7**(4): 044028.

Dye, DG (2002). "Variability and trends in the annual snow-cover cycle in Northern Hemisphere land areas, 1972-2000." Hydrological Processes **16**(15): 3065-3077.

Dye, DG and Tucker, CJ (2003). "Seasonality and trends of snow-cover, vegetation index, and temperature in northern Eurasia." Geophysical Research Letters **30**(7): 58-51.

Eastman, J, Sangermano, F, Machado, E, *et al.* (2013). "Global Trends in Seasonality of Normalized Difference Vegetation Index (NDVI), 1982,Äì2011." Remote Sensing **5**(10): 4799-4818.

EEA (2012). Climate change, impacts and vulnerability in Europe: An indicator-based report. Copenhagen, European Environmental Agency. **12/2012**.

Ellis, EC and Ramankutty, N (2008). "Putting people in the map: anthropogenic biomes of the world." Frontiers in Ecology and the Environment **6**(8): 439-447.

Estiarte, M and Peñuelas, J (2015). "Alteration of the phenology of leaf senescence and fall in winter deciduous species by climate change: Effects on nutrient proficiency." Global Change Biology **21**(3): 1005-1017.

Evans, J and Geerken, R (2004). "Discrimination between climate and human-induced dryland degradation." Journal of Arid Environments **57**(4): 535-554.

Field, CB, Randerson, JT and Malmstr√∂m, CM (1995). "Global net primary production: Combining ecology and remote sensing." Remote Sensing of Environment **51**(1): 74-88.

Fisher, JB, Huntzinger, DN, Schwalm, CR, *et al.* (2014). "Modeling the Terrestrial Biosphere." Annual Review of Environment and Resources **39**(1): 91-123.

Fisher, JI, Mustard, JF and Vadeboncoeur, MA (2006). "Green leaf phenology at Landsat resolution: Scaling from the field to the satellite." Remote Sensing of Environment **100**(2): 265-279.

Fitter, AH and Fitter, RSR (2002). "Rapid Changes in Flowering Time in British Plants." Science **296**(5573): 1689-1691.

Forkel, M, Migliavacca, M, Thonicke, K, *et al.* (2015). "Codominant water control on global interannual variability and trends in land surface phenology and greenness." Global Change Biology **21**(9): 3414-3435.

Forrest, J and Miller-Rushing, AJ (2010). "Toward a synthetic understanding of the role of phenology in ecology and evolution." Philosophical Transactions of the Royal Society of London B: Biological Sciences **365**(1555): 3101-3112.

Forsythe, GE, Malcolm, MA and Moler, CB (1977). Computer methods for mathematical computations Englewood Cliffs, Prentice-Hall.

Frankenberg, C, Fisher, JB, Worden, J, *et al.* (2011). "New global observations of the terrestrial carbon cycle from GOSAT: Patterns of plant fluorescence with gross primary productivity." Geophysical Research Letters **38**(17): L17706.

Friedl, M, Henebry, GM, Reed, BC, *et al.* (2006). Land Surface Phenology. A Community White Paper Requested By NASA. NASA.

Fritz, S, See, L, McCallum, I, *et al.* (2015). "Mapping global cropland and field size." Global Change Biology **21**(5): 1980-1992.

Fu, Y, Zhang, H, Dong, W, *et al.* (2014a). "Comparison of Phenology Models for Predicting the Onset of Growing Season over the Northern Hemisphere." PLoS ONE **9**(10): e109544.

Fu, YSH, Campioli, M, Vitasse, Y, *et al.* (2014b). "Variation in leaf flushing date influences autumnal senescence and next year,Äôs flushing date in two temperate tree species." Proceedings of the National Academy of Sciences **111**(20): 7355-7360.

Fuchs, R, Herold, M, Verburg, PH, *et al.* (2013). "A high-resolution and harmonized model approach for reconstructing and analysing historic land changes in Europe." Biogeosciences **10**(3): 1543-1559.

Gallinat, AS, Primack, RB and Wagner, DL (2015). "Autumn, the neglected season in climate change research." Trends in Ecology & Evolution **30**(3): 169-176.

Ganguly, S, Friedl, MA, Tan, B, *et al.* (2010). "Land surface phenology from MODIS: Characterization of the Collection 5 global land cover dynamics product." Remote Sensing of Environment **114**(8): 1805-1816.

Garonna, I, de Jong, R, de Wit, AJW, *et al.* (2014). "Strong contribution of autumn phenology to changes in satellite-derived growing season length estimates across Europe (1982–2011)." Global Change Biology **20**(11): 3457-3470.

Garonna, I, de Jong, R and Schaepman, ME (2016). "Variability and evolution of global land surface phenology over the past three decades (1982–2012)." Global Change Biology **22**(4): 1456-1468.

Gerst, KL, Kellermann, JL, Enquist, CAF, *et al.* (2015). "Estimating the onset of spring from a complex phenology database: trade-offs across geographic scales." International Journal of Biometeorology **60**(3): 391-400.

Gerten, D (2013). "A vital link: water and vegetation in the Anthropocene." Hydrology and Earth System Sciences **17**(10): 3841-3852.

Gezon, ZJ, Inouye, DW and Irwin, RE (2016). "Phenological change in a spring ephemeral: Implications for pollination and plant reproduction." Global Change Biology **22**(5): 1779-1793.

Gill, AL, Gallinat, AS, Sanders-DeMott, R, *et al.* (2015). "Changes in autumn senescence in northern hemisphere deciduous trees: a meta-analysis of autumn phenology studies." Annals of Botany **116**: 875-888.

Girardin, CAJ, Malhi, Y, Doughty, CE, *et al.* (2016). "Seasonal trends of Amazonian rainforest phenology, net primary productivity, and carbon allocation." Global Biogeochemical Cycles: in press.

Goetz, SJ, Bunn, AG, Fiske, GJ, *et al.* (2005). "Satellite-observed photosynthetic trends across boreal North America associated with climate and fire disturbance." Proceedings of the National Academy of Sciences of the United States of America **102**(38): 13521-13525.

Graven, HD, Keeling, RF, Piper, SC, *et al.* (2013). "Enhanced seasonal exchange of CO2 by Northern ecosystems since 1960." Science **341**(6150): 1085-1089.

Gu, Y, Brown, JF, Miura, T, *et al.* (2010). "Phenological classification of the United States: A geographic framework for extending multi-sensor time-series data." Remote Sensing **2**(2): 526-544.

Guan, K, Pan, M, Li, H, *et al.* (2015). "Photosynthetic seasonality of global tropical forests constrained by hydroclimate." Nature Geosci **8**(4): 284-289.

Guay, KC, Beck, PSA, Berner, LT, *et al.* (2014). "Vegetation productivity patterns at high northern latitudes: a multi-sensor satellite data assessment." Global Change Biology **20**(10): 3147-3158.

Hamunyela, E, Verbesselt, J, Roerink, G, *et al.* (2013). "Trends in Spring Phenology of Western European Deciduous Forests." Remote Sensing **5**(12): 6159-6179.

Hansen, BE (2002). "Tests for parameter instability in regreessions with I(1) processes." Journal of Business and Economic Statistics **20**(1): 45-59.

Hazeu, GW, Metzger, MJ, Mücher, CA, *et al.* (2011). "European environmental stratifications and typologies: An overview." Agriculture, Ecosystems and Environment **142**(1-2): 29-39.

Hein, L, De Ridder, N, Hiernaux, P, *et al.* (2011). "Desertification in the Sahel: Towards better accounting for ecosystem dynamics in the interpretation of remote sensing images." Journal of Arid Environments **75**(11): 1164-1172.

Hilker, T, Lyapustin, AI, Tucker, CJ, *et al.* (2014). "Vegetation dynamics and rainfall sensitivity of the Amazon." Proceedings of the National Academy of Sciences of the United States of America **111**(45): 16041-16046.

Høgda, K, Tømmervik, H and Karlsen, S (2013). "Trends in the Start of the Growing Season in Fennoscandia 1982-2011." Remote Sensing **5**(9): 4304-4318.

Holben, BN (1986). "Characteristics of maximum-value composite images from temporal AVHRR data." International Journal of Remote Sensing **7**(11): 1417-1434.

Hudson, IL and Keatley, MR (2010). Phenological research: methods for environmental and climate change analysis, Springer.

Huete, A, Didan, K, Miura, T, *et al.* (2002). "Overview of the radiometric and biophysical performance of the MODIS vegetation indices." Remote Sensing of Environment **83**(1): 195-213.

Hufkens, K, Friedl, M, Sonnentag, O, *et al.* (2012). "Linking near-surface and satellite remote sensing measurements of deciduous broadleaf forest phenology." Remote Sensing of Environment **117**: 307-321.

Huntzinger, DN, Post, WM, Wei, Y, *et al.* (2012). "North American Carbon Program (NACP) regional interim synthesis: Terrestrial biospheric model intercomparison." Ecological Modelling **232**: 144-157.

Ibañez, I, Primack, RB, Miller-Rushing, AJ, *et al.* (2010). "Forecasting phenology under global warming." Philosophical transactions of the Royal Society of London. Series B, Biological sciences **365**(1555): 3247-3260.

IPCC (2007). Fourth Assessment Report (AR4) of the Intergovernmental Panel on Climate Change. Climate Change 2007: Synthesis report. Core Writing Team, P, R.K. and Reisinger, A. (Eds.). IPCC, Geneva, Switzerland**:** 104.

IPCC (2013). Summary for Policymakers. Climate Change 2013: The Physical Science Basis. Contribution of Working Group I to the Fifth Assessment Report of the Intergovernmental Panel on Climate Change, Cambridge University Press.

Jeganathan, C, Dash, J and Atkinson, PM (2014). "Remotely sensed trends in the phenology of northern high latitude terrestrial vegetation, controlling for land cover change and vegetation type." Remote Sensing of Environment **143**: 154-170.

Jensen, JR (2009). Remote Sensing of the Environment: An Earth Resource Perspective 2/e, Pearson Education India.

Jeong, SJ, Ho, CH, Gim, HJ, *et al.* (2011). "Phenology shifts at start vs. end of growing season in temperate vegetation over the Northern Hemisphere for the period 1982-2008." Global Change Biology **17**(7): 2385-2399.

Jetz, W, Cavender-Bares, J, Pavlick, R, *et al.* (2016). "Monitoring plant functional diversity from space." Nature Plants **2**: 16024.

Joiner, J, Yoshida, Y, Vasilkov, AP, *et al.* (2014). "The seasonal cycle of satellite chlorophyll fluorescence observations and its relationship to vegetation phenology and ecosystem atmosphere carbon exchange." Remote Sensing of Environment **152**: 375-391.

Jolly, WM, Nemani, R and Running, SW (2005). "A generalized, bioclimatic index to predict foliar phenology in response to climate." Global Change Biology **11**(4): 619-632.

Jones, HG and Vaughan, RA (2010). Remote Sensing of Vegetation: Principles, Techniques and Applications. Oxford, Oxford University Press.

Jones, MO, Jones, LA, Kimball, JS, *et al.* (2011). "Satellite passive microwave remote sensing for monitoring global land surface phenology." Remote Sensing of Environment **115**(4): 1102-1114.

Julien, Y and Sobrino, J (2009). "Global land surface phenology trends from GIMMS database." International Journal of Remote Sensing **30**(13): 3495-3513.

Julien, Y, Sobrino, JA and Verhoef, W (2006). "Changes in land surface temperatures and NDVI values over Europe between 1982 and 1999." Remote Sensing of Environment **103**(1): 43-55.

Junker, LV and Ensminger, I (2016). "Relationship between leaf optical properties, chlorophyll fluorescence and pigment changes in senescing Acer saccharum leaves." Tree Physiology **00**(1-18).

Karlsen, SR, Høgda, KA, Wielgolaski, FE, *et al.* (2009). "Growing-season trends in Fennoscandia 1982–2006, determined from satellite and phenology data." Climate Research **39**: 275-286.

Karlson, M, Ostwald, M, Reese, H, *et al.* (2015). "Mapping Tree Canopy Cover and Aboveground Biomass in Sudano-Sahelian Woodlands Using Landsat 8 and Random Forest." Remote Sensing **7**(8): 10017.

Kathuroju, N, White, MA, Symanzik, J, *et al.* (2007). "On the use of the advanced very high resolution radiometer for development of prognostic land surface phenology models." Ecological Modelling **201**(2): 144-156.

Keenan, TF (2015). "Phenology: Spring greening in a warming world." Nature **526**(7571): 48-49.

Kimball, S, Angert, AL, Huxman, TE, *et al.* (2010). "Contemporary climate change in the Sonoran Desert favors cold-adapted species." Global Change Biology **16**(5): 1555-1565.

Körner, C and Basler, D (2010). "Phenology under global warming." Science **327**(5972): 1461-1462.

Kucharik, CJ, Barford, CC, Maayar, ME, *et al.* (2006). "A multiyear evaluation of a Dynamic Global Vegetation Model at three AmeriFlux forest sites: Vegetation structure, phenology, soil temperature, and CO2 and H2O vapor exchange." Ecological Modelling **196**(1-2): 1-31.

Kuemmerle, T, Chaskovskyy, O, Knorn, J, *et al.* (2009). "Forest cover change and illegal logging in the Ukrainian Carpathians in the transition period from 1988 to 2007." Remote Sensing of Environment **113**(6): 1194-1207.

Leith, H (1974). Phenology and seasonal modeling. New York, Springer-Verlag.

Liang, L and Schwartz, MD (2009). "Landscape phenology: An integrative approach to seasonal vegetation dynamics." Landscape Ecology **24**(4): 465-472.

Liu, L, Liang, L, Schwartz, MD, *et al.* (2015). "Evaluating the potential of MODIS satellite data to track temporal dynamics of autumn phenology in a temperate mixed forest." Remote Sensing of Environment **160**: 156-165.

Liu, Q, Fu, YH, Zeng, Z, *et al.* (2016a). "Temperature, precipitation, and insolation effects on autumn vegetation phenology in temperate China." Global Change Biology **22**(2): 644-655.

Liu, Q, Fu, YH, Zhu, Z, *et al.* (2016b). "Delayed autumn phenology in the Northern Hemisphere is related to change in both climate and spring phenology." Global Change Biology: n/a-n/a.

Liu, Y, Wu, C, Peng, D, *et al.* (2016c). "Improved modeling of land surface phenology using MODIS land surface reflectance and temperature at evergreen needleleaf forests of central North America." Remote Sensing of Environment **176**: 152-162.

Lobell, DB, Schlenker, W and Costa-Roberts, J (2011). "Climate Trends and Global Crop Production Since 1980." Science **333**(6042): 616-620.

MacBean, N, Maignan, F, Peylin, P, *et al.* (2015). "Using satellite data to improve the leaf phenology of a global terrestrial biosphere model." Biogeosciences **12**(23): 7185-7208.

Marchetti, M (2002). "Environmental changes in the central Po Plain (northern Italy) due to fluvial modifications and anthropogenic activities." Geomorphology **44**(3-4): 361-373.

Marshall, M, Okuto, E, Kang, Y, *et al.* (2016). "Global assessment of Vegetation Index and Phenology Lab (VIP) and Global Inventory Modeling and Mapping Studies (GIMMS) version 3 products." Biogeosciences **13**(3): 625-639.

Marsham, R (1789). "Indications of Spring, Observed by Robert Marsham, Esduire, F. R. S. of Stratton in Norfolk." Philosophical Transactions of the Royal Society of London **79**: 154-156.

Mason, P and Reading, B (2005). Implementation plan for the global observing systems for climate in support of the UNFCCC. 21st international conference on interactive information processing systems for meteorology, oceanography, and hydrology. San Diego.

Meeus, JHA (1995). "Pan-European landscapes." Landscape and Urban Planning **31**(1-3): 57-79.

Melaas, EK, Friedl, MA and Richardson, AD (2015). "Multi-scale modeling of spring phenology across Deciduous Forests in the Eastern United States." Global Change Biology **22**(2): 792-805.

Menzel, A (2000). "Trends in phenological phases in Europe between 1951 and 1996." International Journal of Biometeorology **44**(2): 76-81.

Menzel, A (2002). "Phenology: Its Importance to the Global Change Community." Climatic Change **54**(4): 379-385.

Menzel, A (2006). Temperature and plant development: phenology and seasonality. Plant Growth and Climate Change. Morison, J and Morecroft, MD. Oxford, Blackwell Publishing**:** 70-95.

Menzel, A and Fabian, P (1999). "Growing season extended in Europe." Nature **397**(6721): 659.

Menzel, A, Sparks, TH, Estrella, N, *et al.* (2006). "European phenological response to climate change matches the warming pattern." Global Change Biology **12**(10): 1969-1976.

MeteoSwiss. (2016, 17.03.2016). "Long-term series of phenological observations." Retrieved 14.04, 2016, from http://www.meteoswiss.admin.ch/home/climate/present-day/phenology-and-pollen.

Metzger, MJ, Brus, DJ, Bunce, RGH, *et al.* (2013a). "Environmental stratifications as the basis for national, European and global ecological monitoring." Ecological Indicators **33**: 26-35.

Metzger, MJ, Bunce, RGH, Jongman, RHG, *et al.* (2005). "A climatic stratification of the environment of Europe." Global Ecology and Biogeography **14**(6): 549-563.

Metzger, MJ, Bunce, RGH, Jongman, RHG, *et al.* (2013b). "A high-resolution bioclimate map of the world: A unifying framework for global biodiversity research and monitoring." Global Ecology and Biogeography **22**(5): 630-638.

Metzger, MJ, Bunce, RGH, Leemans, R, *et al.* (2008). "Projected environmental shifts under climate change: European trends and regional impacts." Environmental Conservation **35**(1): 64-75.

Metzger, MJ, Rounsevell, MDA, Acosta-Michlik, L, *et al.* (2006). "The vulnerability of ecosystem services to land use change." Agriculture, Ecosystems & Environment **114**(1): 69-85.

Migliavacca, M, Sonnentag, O, Keenan, TF, *et al.* (2012). "On the uncertainty of phenological responses to climate change, and implications for a terrestrial biosphere model." Biogeosciences **9**(6): 2063-2083.

Moody, A and Johnson, DM (2001). "Land-surface phenologies from AVHRR using the discrete fourier transform." Remote Sensing of Environment **75**(3): 305-323.

Morisette, JT, Richardson, AD, Knapp, AK, *et al.* (2009). "Tracking the rhythm of the seasons in the face of global change: Phenological research in the 21 st century." Frontiers in Ecology and the Environment **7**(5): 253-260.

Morison, JI and Morecroft, MD (2008). "Plant growth and climate change."

Mücher, CA, Klijn, JA, Wascher, DM, *et al.* (2010). "A new European Landscape Classification (LANMAP): A transparent, flexible and user-oriented methodology to distinguish landscapes." Ecological Indicators **10**(1): 87-103.

Myneni, RB, Keeling, CD, Tucker, CJ, *et al.* (1997). "Increased plant growth in the northern high latitudes from 1981 to 1991." Nature **386**(6626): 698-702.

Neigh, CSR, Tucker, CJ and Townshend, JRG (2008). "North American vegetation dynamics observed with multi-resolution satellite data." Remote Sensing of Environment **112**(4): 1749-1772.

Nemani, RR, Keeling, CD, Hashimoto, H, *et al.* (2003). "Climate-driven increases in global terrestrial net primary production from 1982 to 1999." Science **300**(5625): 1560-1563.

Niinemets, Ü (2010). "Responses of forest trees to single and multiple environmental stresses from seedlings to mature plants: Past stress history, stress interactions, tolerance and acclimation." Forest Ecology and Management **260**(10): 1623-1639.

Noormets, A (2009). Phenology of ecosystem processes: applications in global change research, Springer.

O'Brien, MJ, Philipson, CD, Tay, J, *et al.* (2013). "The Influence of Variable Rainfall Frequency on Germination and Early Growth of Shade-Tolerant Dipterocarp Seedlings in Borneo." PLoS ONE **8**(7): e70287.

Panchen, ZA, Primack, RB, Gallinat, AS, *et al.* (2015). "Substantial variation in leaf senescence times among 1360 temperate woody plant species: implications for phenology and ecosystem processes." Annals of Botany **116**: 865-873.

Park, H, Jeong, S-J, Ho, C-H, *et al.* (2015). "Nonlinear response of vegetation green-up to local temperature variations in temperate and boreal forests in the Northern Hemisphere." Remote Sensing of Environment **165**(0): 100-108.

Parmentier, FJW, Christensen, TR, Sørensen, LL, *et al.* (2013). "The impact of lower sea-ice extent on Arctic greenhouse-gas exchange." Nature Climate Change **3**(3): 195-202.

Parmesan, C (2007). "Influences of species, latitudes and methodologies on estimates of phenological response to global warming." Global Change Biology **13**(9): 1860-1872.

Parmesan, C and Hanley, ME (2015). "Plants and climate change: Complexities and surprises." Annals of Botany **116**(6): 849-864.

Parmesan, C and Yohe, G (2003). "A globally coherent fingerprint of climate change impacts across natural systems." Nature **421**(6918): 37-42.

Pau, S, Wolkovich, EM, Cook, BI, *et al.* (2011). "Predicting phenology by integrating ecology, evolution and climate science." Global Change Biology **17**(12): 3633-3643.

Pearson, RG, Phillips, SJ, Loranty, MM, *et al.* (2013). "Shifts in Arctic vegetation and associated feedbacks under climate change." Nature Clim. Change **3**(7): 673-677.

Peñuelas, J, Rutishauser, T and Filella, I (2009). "Phenology feedbacks on climate change." Science **324**(5929): 887-888.

Pereira, HM, Ferrier, S, Walters, M, *et al.* (2013). "Essential biodiversity variables." Science **339**(6117): 277-278.

Pettorelli, N, Vik, JO, Mysterud, A, *et al.* (2005). "Using the satellite-derived NDVI to assess ecological responses to environmental change." Trends in Ecology and Evolution **20**(9): 503-510.

Pinzon, J, Brown, ME and Tucker, CJ (2005). Satellite time series correction of orbital drift artifacts using empirical mode decomposition. Hilbert-Hunang Transform: Introduction and Applications. Huang, N**:** 167-186.

Pinzon, J and Tucker, C (2014). "A Non-Stationary 1981-2012 AVHRR NDVI3g Time Series." Remote Sensing **6**(8): 6929-6960.

Polgar, CA and Primack, RB (2011). "Leaf-out phenology of temperate woody plants: From trees to ecosystems." New Phytologist **191**(4): 926-941.

Poloczanska, ES, Brown, CJ, Sydeman, WJ, *et al.* (2013). "Global imprint of climate change on marine life." Nature Clim. Change **3**(10): 919-925.

Pomeroy, J and Brun, E (2001). Physical properties of snow. Snow ecology: An Interdisciplinary Ecamination of Snow-Covered Ecosystems. Jones, H, Hoham, R, Pomeroy, J and Walker, D. Cambridge, Cambridge University Press**:** 45-126.

Poulter, B, Frank, D, Ciais, P, *et al.* (2014). "Contribution of semi-arid ecosystems to interannual variability of the global carbon cycle." Nature **509**(7502): 600-603.

Primack, RB and Miller-Rushing, AJ (2011). "Broadening the study of phenology and climate change." New Phytologist **191**(2): 307-309.

Puppi, G (2007). "Origin and development of phenology as a science." Ital J Agrometeorol **3**: 24-29.

Rathcke, B and Lacey, EP (1985). "Phenological Patterns of Terrestrial Plants." Annual Review of Ecology and Systematics **16**(1): 179-214.

Reed, BC, Brown, JF, VanderZee, D, *et al.* (1994). "Measuring phenological variability from satellite imagery." Journal of Vegetation Science **5**(5): 703-714.

Reed, BC, White, M and Brown, JF (2003). Remote sensing phenology. Phenology: An Integrative Environmental Science. Schwartz, DM, Springer Netherlands**:** 365-381.

Revermann, R, Finckh, M, Stellmes, M, *et al.* (2016). "Linking Land Surface Phenology and Vegetation-Plot Databases to Model Terrestrial Plant Alpha-Diversity of the Okavango Basin." Remote Sensing **8**(5): 370.

Richardson, AD, Anderson, RS, Arain, MA, *et al.* (2012). "Terrestrial biosphere models need better representation of vegetation phenology: results from the North American Carbon Program Site Synthesis." Global Change Biology **18**(2): 566-584.

Richardson, AD, Braswell, BH, Hollinger, DY, *et al.* (2009). "Near-surface remote sensing of spatial and temporal variation in canopy phenology." Ecological Applications **19**(6): 1417-1428.

Richardson, AD, Keenan, TF, Migliavacca, M, *et al.* (2013). "Climate change, phenology, and phenological control of vegetation feedbacks to the climate system." Agricultural and Forest Meteorology **169**(0): 156-173.

Rockström, J, Steffen, W, Noone, K, *et al.* (2009). "A safe operating space for humanity." Nature **461**(7263): 472-475.

Roerink, G, Menenti, M, Soepboer, W, *et al.* (2003). "Assessment of climate impact on vegetation dynamics by using remote sensing." Physics and Chemistry of the Earth, Parts A/B/C **28**(1): 103-109.

Roerink, G, Menenti, M and Verhoef, W (2000). "Reconstructing cloudfree NDVI composites using Fourier analysis of time series." International Journal of Remote Sensing **21**(9): 1911-1917.

Root, TL, Price, JT, Hall, KR, *et al.* (2003). "Fingerprints of global warming on wild animals and plants." Nature **421**(6918): 57-60.

Rosenzweig, C, Casassa, G, Karoly, DJ, *et al.* (2007). Assessment of observed changes and responses in natural and managed systems. Climate Change 2007: Impacts, Adaptation and Vulnerability. Contribution of Working Group II to the Fourth Assessment Report of the Intergovernmental Panel on Climate Change. Parry, ML, Canziani, OF, Palutikof, JP, van der Linden, PJ and Hanson, CE. Cambridge, UK, Cambridge University Press**:** 79-131.

Rouse, JW, Haas, RH, Deering, DW, *et al.* (1974). Monitoring the vernal advancement and retrogradation (green wave effect) of natural vegetation. NASA Technical Reports Texas A & M University, College Station TX, NASA**:** 8.

Running, SW (2012). "A Measurable Planetary Boundary for the Biosphere." Science **337**(6101): 1458-1459.

Running, SW, Nemani, RR, Heinsch, FA, *et al.* (2004). "A Continuous Satellite-Derived Measure of Global Terrestrial Primary Production." BioScience **54**(6): 547-560.

Schaefer, K, Schwalm, CR, Williams, C, *et al.* (2012). "A model-data comparison of gross primary productivity: Results from the north American carbon program site synthesis." Journal of Geophysical Research: Biogeosciences **117**(3): G03010.

Scheffer, M, Hirota, M, Holmgren, M, *et al.* (2012). "Thresholds for boreal biome transitions." Proceedings of the National Academy of Sciences of the United States of America **109**(52): 21384-21389.

Schimel, D, Pavlick, R, Fisher, JB, *et al.* (2015a). "Observing terrestrial ecosystems and the carbon cycle from space." Global Change Biology **21**(5): 1762-1776.

Schimel, D, Stephens, BB and Fisher, JB (2015b). "Effect of increasing CO2 on the terrestrial carbon cycle." Proceedings of the National Academy of Sciences **112**(2): 436-441.

Schimel, DS, Asner, GP and Moorcroft, P (2013). "Observing changing ecological diversity in the Anthropocene." Frontiers in Ecology and the Environment **11**(3): 129-137.

Schimel, DS, House, JI, Hibbard, KA, *et al.* (2001). "Recent patterns and mechanisms of carbon exchange by terrestrial ecosystems." Nature **414**(6860): 169-172.

Scholes, RJ, Walters, M, Turak, E, *et al.* (2012). "Building a global observing system for biodiversity." Current Opinion in Environmental Sustainability **4**(1): 139-146.

Schwalm, CR, Williams, CA, Schaefer, K, *et al.* (2010). "A model-data intercomparison of CO2 exchange across North America: Results from the North American Carbon Program site synthesis." Journal of Geophysical Research: Biogeosciences **115**(G3): G00H05.

Schwartz, MD (1998). "Green-wave phenology." Nature **394**(6696): 839-840.

Schwartz, MD (2013). Phenology: an integrative environmental science, Springer Netherlands.

Schwartz, MD, Betancourt, JL and Weltzin, JF (2012). "From Caprio's lilacs to the USA National Phenology Network." Frontiers in Ecology and the Environment **10**(6): 324-327.

Schwartz, MD and Hanes, JM (2010). "Intercomparing multiple measures of the onset of spring in eastern North America." International Journal of Climatology **30**(11): 1614-1626.

Schwartz, MD and Reiter, BE (2000). "Changes in North American spring." International Journal of Climatology **20**(8): 929-932.

Sellers, PJ, Los, SO, Tucker, CJ, *et al.* (1996). "A revised land surface parameterization (SiB2) for atmospheric GCMs. Part II: The generation of global fields of terrestrial biophysical parameters from satellite data." Journal of Climate **9**(4): 706-737.

Sitch, S, Friedlingstein, P, Gruber, N, *et al.* (2015). "Recent trends and drivers of regional sources and sinks of carbon dioxide." Biogeosciences **12**(3): 653-679.

Skidmore, AK, Pettorelli, N, Coops, NC, *et al.* (2015). "Environmental science: agree on biodiversity metrics to track from space." Nature **523**: 403-405.

Sobrino, JA, Julien, Y, Atitar, M, *et al.* (2008). "NOAA-AVHRR Orbital Drift Correction From Solar Zenithal Angle Data." Geoscience and Remote Sensing, IEEE Transactions on **46**(12): 4014-4019.

Stöckli, R, Rutishauser, T, Baker, I, *et al.* (2011). "A global reanalysis of vegetation phenology." J. Geophys. Res **116**: G03020.

Stöckli, R, Rutishauser, T, Dragoni, D, *et al.* (2008). "Remote sensing data assimilation for a prognostic phenology model." J. Geophys. Res **113**(G04021): G04021.

Stöckli, R and Vidale, PL (2004). "European plant phenology and climate as seen in a 20-year AVHRR land-surface parameter dataset." International Journal of Remote Sensing **25**(17): 3303-3330.

Studer, S, Appenzeller, C and Defila, C (2005). "Inter-annual variability and decadal trends in alpine spring phenology: A multivariate analysis approach." Climatic Change **73**(3): 395-414.

Studer, S, Stöckli, R, Appenzeller, C, *et al.* (2007). "A comparative study of satellite and ground-based phenology." International Journal of Biometeorology **51**(5): 405-414.

Sweet, SK, Griffin, KL, Steltzer, H, *et al.* (2015). "Greater deciduous shrub abundance extends tundra peak season and increases modeled net CO2 uptake." Global Change Biology **21**(6): 2394-2409.

Tanja, S, Berninger, F, Vesala, T, *et al.* (2003). "Air temperature triggers the recovery of evergreen boreal forest photosynthesis in spring." Global Change Biology **9**(10): 1410-1426.

Tucker, CJ (1979). "Red and photographic infrared linear combinations for monitoring vegetation." Remote Sensing of Environment **8**(2): 127-150.

Tucker, CJ, Pinzon, JE, Brown, ME, *et al.* (2005). "An extended AVHRR 8-km NDVI dataset compatible with MODIS and SPOT vegetation NDVI data." International Journal of Remote Sensing **26**(20): 4485-4498.

Tucker, CJ, Slayback, DA, Pinzon, JE, *et al.* (2001). "Higher northern latitude normalized difference vegetation index and growing season trends from 1982 to 1999." International Journal of Biometeorology **45**(4): 184-190.

Turner Ii, BL, Lambin, EF and Reenberg, A (2007). "The emergence of land change science for global environmental change and sustainability." Proceedings of the National Academy of Sciences of the United States of America **104**(52): 20666-20671.

Turner, W (2014). "Sensing biodiversity." Science **346**(6207): 301-302.

Urban, M, Forkel, M, Eberle, J, *et al.* (2014). "Pan-Arctic Climate and Land Cover Trends Derived from Multi-Variate and Multi-Scale Analyses (1981-2012)." Remote Sensing **6**(3): 2296-2316.

Verbesselt, J, Hyndman, R, Newnham, G, *et al.* (2010). "Detecting trend and seasonal changes in satellite image time series." Remote Sensing of Environment **114**(1): 106-115.

Verburg, PH, Neumann, K and Nol, L (2011). "Challenges in using land use and land cover data for global change studies." Global Change Biology **17**(2): 974-989.

Viña, A, Liu, W, Zhou, S, *et al.* (2016). "Land surface phenology as an indicator of biodiversity patterns." Ecological Indicators **64**: 281-288.

Viña, A, Tuanmu, M-N, Xu, W, *et al.* (2012). "Relationship between floristic similarity and vegetated land surface phenology: Implications for the synoptic monitoring of species diversity at broad geographic regions." Remote Sensing of Environment **121**: 488-496.

Walker, D, Billings, W and De Molenaar, J (2001). Snow-vegetation interactions in tundra environments. Snow Ecology: An Interdisciplinary Examination of Snow-Covered Ecosystems. Jones, H, Hoham, R, Pomeroy, J and Walker, D, Cambridge University Press**:** 266-324.

Walther, G-R, Post, E, Convey, P, *et al.* (2002). "Ecological responses to recent climate change." Nature **416**(6879): 389-395.

Walther, S, Voigt, M, Thum, T, *et al.* (2016). "Satellite chlorophyll fluorescence measurements reveal large-scale decoupling of photosynthesis and greenness dynamics in boreal evergreen forests." Global Change Biology: **22**(1): 2979-2996.

Wang, X, Piao, S, Ciais, P, *et al.* (2014). "A two-fold increase of carbon cycle sensitivity to tropical temperature variations." Nature **506**(7487): 212-215.

Wang, X, Piao, S, Xu, X, *et al.* (2015). "Has the advancing onset of spring vegetation green-up slowed down or changed abruptly over the last three decades?" Global Ecology and Biogeography **24**(6): 621-631.

White, MA, de Beurs, KM, Didan, K, *et al.* (2009a). "Intercomparison, interpretation, and assessment of spring phenology in North America estimated from remote sensing for 1982–2006." Global Change Biology **15**(10): 2335-2359.

White, MA, de Beurs, KM, Didan, K, *et al.* (2009b). "Intercomparison, interpretation, and assessment of spring phenology in North America estimated from remote sensing for 1982-2006." Global Change Biology **15**(10): 2335-2359.

White, MA, Hoffman, F, Hargrove, WW, *et al.* (2005). "A global framework for monitoring phenological responses to climate change." Geophysical Research Letters **32**(4): L04705.

White, MA and Nemani, RR (2006). "Real-time monitoring and short-term forecasting of land surface phenology." Remote Sensing of Environment **104**(1): 43-49.

White, MA, Thornton, PE and Running, SW (1997). "A continental phenology model for monitoring vegetation responses to interannual climatic variability." Global Biogeochemical Cycles **11**(2): 217-234.

Whitfield, J (2001). "The budding amateurs." Nature **414**(6864): 578-579.

Wilczek, AM, Burghardt, LT, Cobb, AR, *et al.* (2010). "Genetic and physiological bases for phenological responses to current and predicted climates." Philosophical Transactions of the Royal Society of London B: Biological Sciences **365**(1555): 3129-3147.

Wolkovich, EM and Cleland, EE (2010). "The phenology of plant invasions: a community ecology perspective." Frontiers in Ecology and the Environment **9**(5): 287-294.

Wolkovich, EM and Ettinger, AK (2014). "Back to the future for plant phenology research." New Phytologist **203**(4): 1021-1024.

Wu, C, Gough, CM, Chen, JM, *et al.* (2013). "Evidence of autumn phenology control on annual net ecosystem productivity in two temperate deciduous forests." Ecological Engineering **60**: 88-95.

Wu, J, Albert, LP, Lopes, AP, *et al.* (2016). "Leaf development and demography explain photosynthetic seasonality in Amazon evergreen forests." Science **351**(6276): 972-976.

Yan, E, Wang, G, Lin, H, *et al.* (2015). "Phenology-based classification of vegetation cover types in Northeast China using MODIS NDVI and EVI time series." International Journal of Remote Sensing **36**(2): 489-512.

Yang, X, Mustard, JF, Tang, J, *et al.* (2012). "Regional-scale phenology modeling based on meteorological records and remote sensing observations." Journal of Geophysical Research: Biogeosciences **117**(G3): G03029.

Yengoh, GT, Dent, D, Olsson, L, *et al.* (2015). Use of the Normalized Difference Vegetation Index (NDVI) to Assess Land Degradation at Multiple Scales: Current Status, Future Trends, and Practical Considerations, Springer.

Yin, H, Udelhoven, T, Fensholt, R, *et al.* (2012). "How normalized difference vegetation index (NDVI) trends from advanced very high resolution radiometer (AVHRR) and système probatoire d'observation de la terre vegetation (SPOT VGT) time series differ in agricultural areas: An inner mongolian case study." Remote Sensing **4**(11): 3364-3389.

Zeileis, A, Kleiber, C, Krämer, W, *et al.* (2003). "Testing and dating of structural changes in practice." Computational Statistics & Data Analysis **44**: 109-123.

Zeng, F-W, Collatz, G, Pinzon, J, *et al.* (2013a). "Evaluating and Quantifying the Climate-Driven Interannual Variability in Global Inventory Modeling and Mapping Studies (GIMMS) Normalized Difference Vegetation Index (NDVI3g) at Global Scales." Remote Sensing **5**(8): 3918-3950.

Zeng, H, Jia, G and Epstein, H (2011). "Recent changes in phenology over the northern high latitudes detected from multi-satellite data." Environmental Research Letters **6**(4): 045508.

Zeng, H, Jia, G and Forbes, B (2013b). "Shifts in Arctic phenology in response to climate and anthropogenic factors as detected from multiple satellite time series." Environmental Research Letters **8**(3): 035036.

Zhang, X (2015). "Reconstruction of a complete global time series of daily vegetation index trajectory from long-term AVHRR data." Remote Sensing of Environment **156**(0): 457-472.

Zhang, X, Friedl, MA and Schaaf, CB (2009). "Sensitivity of vegetation phenology detection to the temporal resolution of satellite data." International Journal of Remote Sensing **30**(8): 2061-2074.

Zhang, X, Friedl, MA, Schaaf, CB, *et al.* (2003). "Monitoring vegetation phenology using MODIS." Remote Sensing of Environment **84**(3): 471-475.

Zhang, X, Tan, B and Yu, Y (2014). "Interannual variations and trends in global land surface phenology derived from enhanced vegetation index during 1982-2010." International Journal of Biometeorology **58**(4): 547-564.

Zhao, J, Wang, Y, Hashimoto, H, *et al.* (2012). "The Variation of Land Surface Phenology From 1982 to 2006 Along the Appalachian Trail." IEEE Transactions on Geoscience and Remote Sensing **51**(4): 2087-2095.

Zhao, M, Peng, C, Xiang, W, *et al.* (2013). "Plant phenological modeling and its application in global climate change research: Overview and future challenges." Environmental Reviews **21**(1): 1-14.

Zhao, M and Running, SW (2010). "Drought-Induced Reduction in Global Terrestrial Net Primary Production from 2000 Through 2009." Science **329**(5994): 940-943.

Zhou, L, Tucker, C, Kaufmann, RK, *et al.* (2001). "Variations in northern vegetation activity inferred from satellite data of vegetation index during 1981 to 1999." Journal of Geophysical Research **106**(D17): 20069-20083.

Zhu, L and Meng, J (2014). "Determining the relative importance of climatic drivers on spring phenology in grassland ecosystems of semi-arid areas." International Journal of Biometeorology: 1-12.

Zhu, W, Tian, H, Xu, X, *et al.* (2012). "Extension of the growing season due to delayed autumn over mid and high latitudes in North America during 1982-2006." Global Ecology and Biogeography **21**(2): 260-271.

Zhu, Z, Bi, J, Pan, Y, *et al.* (2013). "Global Data Sets of Vegetation Leaf Area Index (LAI)3g and Fraction of Photosynthetically Active Radiation (FPAR)3g Derived from Global Inventory Modeling and Mapping Studies (GIMMS) Normalized Difference Vegetation Index (NDVI3g) for the Period 1981 to 2011." Remote Sensing **5**(2): 927-948.

Zhu, Z, Piao, S, Myneni, RB, *et al.* (2016). "Greening of the Earth and its drivers." Nature Clim. Change **in press**.

Curriculum vitae

IRENE GARONNA

Education

2012-2016 Ph.D. candidate in Earth Observation, Department of Geography, Remote Sensing Laboratories, University of Zurich (CH).

2009-2010 M.Sc. in Environmental Change and Management, School of Geography and the Environment, University of Oxford (UK).

Thesis (with Distinction) carried out at Jet Propulsion Laboratory, California Institute of Technology (USA), supervised by Dr. J.B. Fisher. Title: *Land Surface Temperature Model Inter-Comparison and Validation with Fluxnet.*

2006-2009 B.Sc. (*Hons*) in Environmental Biology, Department of Genetics, Evolution and the Environment, University College London (UK).

Dissertation (won the Heaysman Prize) carried out at the Zoological Society of London, supervised by Dr. N. Pettorelli. Title: *Changes in Primary Productivity in Kahua, Solomon Islands.*

Previous research experience

2011-2012 United Nations Environment Programme Global Resource Information Database (UNEP-GRID) and Land Registry Office, Geneva (CH).

2010-2011 Soil Moisture Active Passive team, NASA Jet Propulsion Laboratory, California Institute of Technology (USA).

Teaching and supervision

2012-2015 Teaching assistant for various courses within the Department of Geography, University of Zurich. Namely: GEO371 Methods in Remote Sensing; GEO442 Spectroscopy of the Earth System; GEO229 Small Group Teaching in Geography.

2014-2015 M.Sc. co-supervision, David Schenkel. Title: *Impact of Climatic Controls on Global Changes in Land Surface Phenology.*

Graduate courses and training

- European Space Agency Earth Observation Summer School (ESRIN, August 2012)
- Land-Climate Interactions (ETH Institute for Atmospheric and Climate Sciences)
- PhD Seminars I & II
- Principles and Theory in Geography
- Graduate School Retreat Seminars (I and II)
- Scientific writing
- Project management
- Voice training and presentation skills
- Data analysis with R; R for spatial data analysis and visualization

Peer-reviewed publications

Garonna, I. *et al.* (**2016**) Variability and evolution of global land surface phenology over the past three decades. *Global Change Biology,* Vol. 22, pp. 1456-1468.

Garonna, I. *et al.* (**2014**) Strong contribution of autumn phenology to changes in satellite-derived growing season length estimates across Europe. *Global Change Biology,* Vol. 20, 3457-3470.

Allenbach, K., **Garonna, I.**, *et al.* (**2014**) Black Sea sandy coastline vulnerability to sea level rise. *Environmental Science and Policy,* Vol. 46, pp. 95-109.

Garonna, I., *et al.* (**2009**) Rapid primary productivity change in one of the last coastal rainforests: The case of Kahua, Solomon Islands. *Environmental Conservation*, Vol. 36, pp. 253-260.

Conference contributions (selected)

2016 Colloquium on Remote Sensing, University of Zurich (UZH): *Studying seasons from space.*

2015 American Geophysical Union (AGU) Fall Meeting, San Francisco (USA): *Linking Land Surface Phenology (LSP) and growth limiting factor shifts over the past 30 years.*

2015 Phenology Conference, Kusadasi (TK): *Evaluating shifting LSP and its climatic drivers at global scale.*

2014 ForestSAT Conference, Riva del Garda (IT). *Variability in phenology using* $NDVI_{3g}$.

2013 Swiss Geoscience Meeting, Lausanne (CH). *Pan-European assessment of phenology trends.*

2013 AGU Fall Meeting, San Francisco (USA) *Asymmetric trends in LSP*

Acknowledgements

First and foremost, I would like to thank my advisors in the PhD committee for sharing their enthusiasm and for guiding me. I always came out of meetings with them feeling motivated and eager for the next steps. I am thankful to my supervisor Dr. Rogier de Jong for his constant support, patience and precious coaching, which helped me at each step of the way. The work together has been inspiring and stimulating, and I feel fortunate to have been his first PhD student. I am very grateful to Prof. Michael Schaepman for his leadership and his scientific guidance, which pushed me to give my best and to enjoy research. Thank you to Prof. Bernhard Schmid for his contagious passion and invaluable feedback.

I am indebted to David Schenkel, Dr. Allard de Wit, Dr. Sander Mücher and Dr. David Schimel for their contributions to the manuscript at various stages, and in particular to Dr. Reto Stöckli for the constructive collaboration and interesting discussions. The Functional Genomics Center Zurich has greatly facilitated data analysis and provided technical support, in particular Masa Hakateyama and Hubert Rehrauer.

I have very much appreciated interacting with the whole URPP Global Change and Biodiversity team. Prof. Kentaro Shimizu, Dr. Gabriela Schaepman-Strub, Dr. Pascal Niklaus and Dr. Samuel Abiven provided helpful inputs and mentoring. The RSL environment has offered me all the comfort, coziness and values of a 'home' for the PhD labour. In particular, my fellow PhDs on the J-floor and in the URPP have always been collaborative and fun to be with. Inge Juszak, Jennifer Bartmess, Johann Müller, Benjamin Kellenberger and Daniel Henke proof-read sections of this thesis and offered practical advice. At key times of my journey, Fabian Schneider, Sanne Diek, Daniela Braun, Reik Leiterer and Gillian Milani provided crucial help. At the beginning of my work, I benefited from the support of Karin Allenbach and Prof. Jean-Michel Jaquet.

My gratitude goes also to Laurent Grand-Dufay for being by my side and sharing this adventure, and to my Geneva friends for providing constructive distractions. Lastly, I am grateful to my family, in particular Paolo, Adriano and Elena, who triggered and nurtured my wish to pursue a PhD, and to whom this work is dedicated.

ISBN Nr. 978-3-906894-01-0